DESIGN AND SIMULATION OF A TORQUE SENSING GOVERNOR FOR AN INTERNAL COMBUSTION ENGINE

by

Francis Morgan Donovan, Jr.

Thesis submitted to the Graduate Faculty of the
Virginia Polytechnic Institute
in candidacy for the degree of

MASTER OF SCIENCE
in
MECHANICAL ENGINEERING

July 1962
Blacksburg, Virginia

TABLE OF CONTENTS

LIST OF FIGURES

Figure Page

LIST OF TABLES

NOMENCLATURE

A - Input elements

B - Feedback signal

C - Controlled variable

E - Error signal

G_1 - Control elements

G_2 - Controlled system

H - Feedback elements

k_c - Proportional sensitivity

k_t - Torque sensor sensitivity

L - Load system

M - Control signal

Meg - Megohm

N - Engine speed in rpm

N_{nl} - No Load engine speed in rpm

P - Set point

R - Reference signal

t - Time

T - Torque sensor output in volts

Ta - Decrease in torque sensor output in volts due to engine acceleration

T_d - Derivative time

T_I - Integral time

T.S. - Steady state torque sensor output in volts

U - Load variable

V - Throttle signal in volts

α - Engine acceleration in rpm/sec

I. INTRODUCTION

"The first use of automatic control seems to have been the flyball governor on Watt's steam engine in about 1775. This device was employed to regulate the speed of the engine by manipulating the steam flow by means of a valve... .

"The first analysis of automatic control is the mathematical discussion of the flyball governor by James Clerk Maxwell in 1868. ...Further application of the governor techniques to other engines and turbines was made, and in the early 1900's the application to process control began. At the same time regulators and servomechanisms were being studied for their application to steam-power regulators and ship steering.

"The general application of process control did not begin until the 1930's. The usefulness of control techniques quickly established their value, so that by the 1940's rather complex control networks were in common use."[1]

Today automatic controllers are used to regulate the speed of prime movers in practically every application where close speed regulation over an extended period of time is necessary. As the performance demands become more exacting, the sensitivity of control must be increased.

Because of the increased sensitivity demanded, it is often necessary to use a combination of several different types of controllers to maintain stability.

The best controllers used at the present time for constant speed governing of prime movers consist of a combination of proportional, integral, derivative, and sometimes power sensing controllers. The power sensing governors are generally better than the normal proportional-integral-derivative governors, but they can be easily applied only in cases where the load is electrical rather than mechanical. It appears that there is a need for some type of simple load sensing governor which can be used with mechanical loads, such as a torque sensing governor.

It is the intent of this investigation to present the design of a practical torque measuring device which can be used with any type of load, and to show that the use of such a device with a constant speed governor will produce less error for less time than the conventional proportional-integral-derivative constant speed governor when used on an internal combustion engine.

II. REVIEW OF LITERATURE

Types of Controllers[3]

Eckman[2] defines automatic control as "the maintenance of a desired value of a quantity or condition by measuring the existing value, comparing it to the desired value, and employing the difference to initiate action for reducing this difference." (See Figure 7.)

An automatic controller then must consist of a means of measuring the desired variable, a means of comparing the measured variable to a desired value or set point, a means of sensing an error between the desired variable and the set point, and a means of making the changes necessary to correct this error.

In the case of a speed controller the measuring means is a device which senses the speed and produces a signal which can be interpreted by the controller. An electric tachometer, for example, would be a measuring device which senses the speed of a rotating shaft and produces a proportional voltage.

The measured variable, which is the signal received from the measuring means, is compared to the set point by a simple subtraction such as $E = R - B$, where E is the error, R is the set point or reference signal, and B is

the signal received from the measuring means. The signal B is called the feedback signal.

The means of making changes necessary to correct the error in the desired variable is a device called the controlling means, which senses the error E and changes some variable, such as the throttle setting, according to a transfer function which is built into the controlling means. The transfer function is usually such that the controlling means produces proportional control, integral control, derivative control, or any combination of these controls.

Proportional Control

Proportional control is a type of control in which there is a continuous linear relation between the error E and the manipulated variable M. The transfer function for proportional control is

$$M = k_c E$$

where k_c is called the proportional sensitivity and is usually adjustable to allow greater flexibility of the controller.

Integral Control

Integral control is a type of control in which the value of the manipulated variable is changed at a rate proportional to the error. The transfer function for integral control is

$$\frac{dM}{dt} = \frac{E}{T_i} \quad \text{or} \quad M = \frac{1}{T_i} \int E dt + C$$

where T_i is called the integral time. C is a constant of integration.

Derivative Control

Derivative control is a type of control in which the magnitude of the manipulated variable is proportional to the rate of change of the error. The transfer function for a derivative control is

$$M = T_d \frac{dE}{dt} .$$

T_d is called the derivative time.

The transfer function of a combination control is found by adding the transfer functions of the component controllers. The transfer function for combined proportional-integral control is

$$M = k_c E + \frac{1}{T_i} \int E dt$$

or in operator form,

$$M = (k_c + \frac{1}{T_i D}) E.$$

Similarly the transfer function for combined proportional-integral-derivative control is

$$M = (k_c + \frac{1}{T_i D} + T_d D) E$$

in operator form.

The effect of the different types of control on a system can be illustrated by considering the typical effect of a controller on a single capacitance process, such as the effect of a speed controller on an internal combustion engine.

Figure 1 shows the typical response of proportional control on an engine having a step increase in load. It can be seen from Figure 1, that increasing k_c has the effect of decreasing the offset, but if k_c is made too large the system becomes unstable and begins to oscillate.

Figure 2 shows the typical response of integral control on an engine having a step increase in load. Integral control has no offset. It can be seen from Figure 2 that decreasing T_i has the effect of decreasing the time it takes to return to the set point, but if T_i is made too small the system becomes unstable and begins to oscillate.

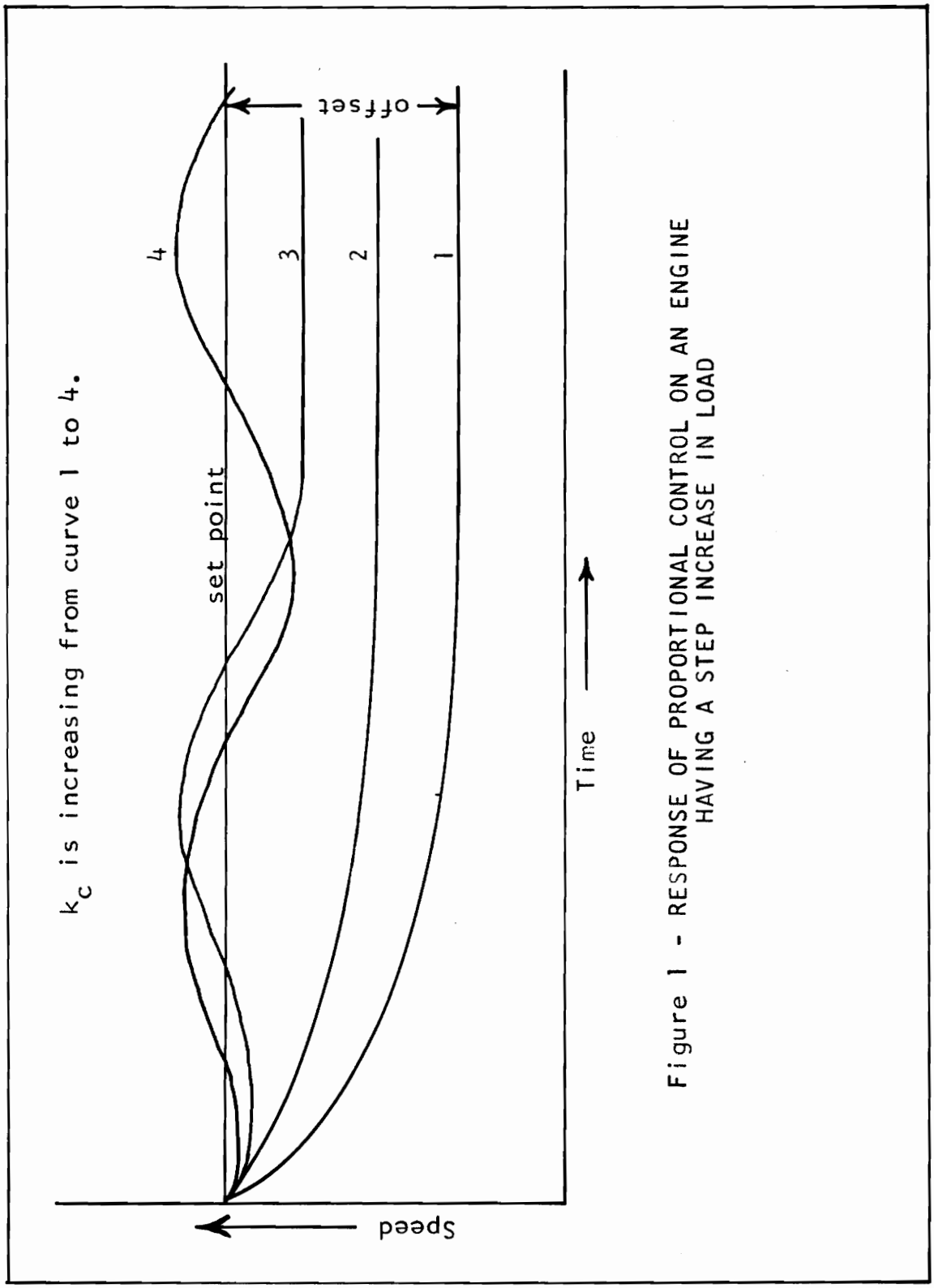

Figure 1 - RESPONSE OF PROPORTIONAL CONTROL ON AN ENGINE HAVING A STEP INCREASE IN LOAD

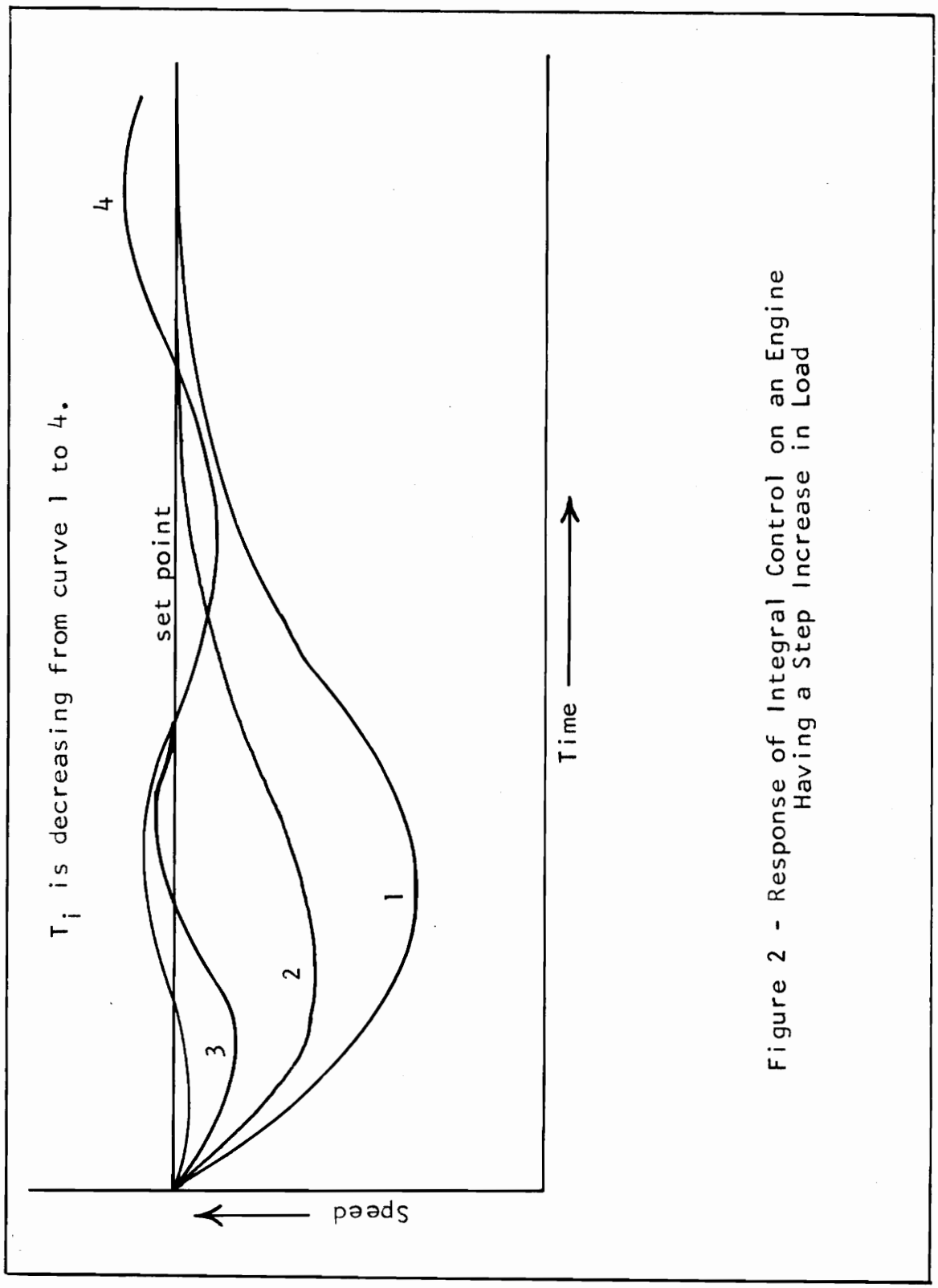

Figure 2 - Response of Integral Control on an Engine Having a Step Increase in Load

Since derivative control is usually never used alone, its effect on a system will be shown by considering derivative control combined with proportional control. Figure 3 shows the typical effect of adding derivative control to proportional control. It can be seen from Figure 3 that the addition of derivative control to proportional control decreases the maximum error as long as T_d is not too large. If T_d is made too large, the error near zero time may actually go in the opposite direction from the load change, and if T_d is large enough the system may become unstable. Derivative control has effect only when there is a change occurring in the error E, which means that the final offset is unaffected by the addition of derivative control. Derivative control has a similar effect on integral control.

Figure 4 shows the typical effect of adding integral control to proportional control. It can be seen from Figure 4 that the addition of integral control reduces the offset to zero. If T_i is very small compared to k_c, the control will behave very nearly as a straight integral control. If T_i is very large compared to k_c, the control will behave very nearly as a straight proportional control, but the error will eventually be zero, unless $T_i = \infty$.

Figure 5 shows the typical effect of adding derivative control to proportional-integral control. As is shown in

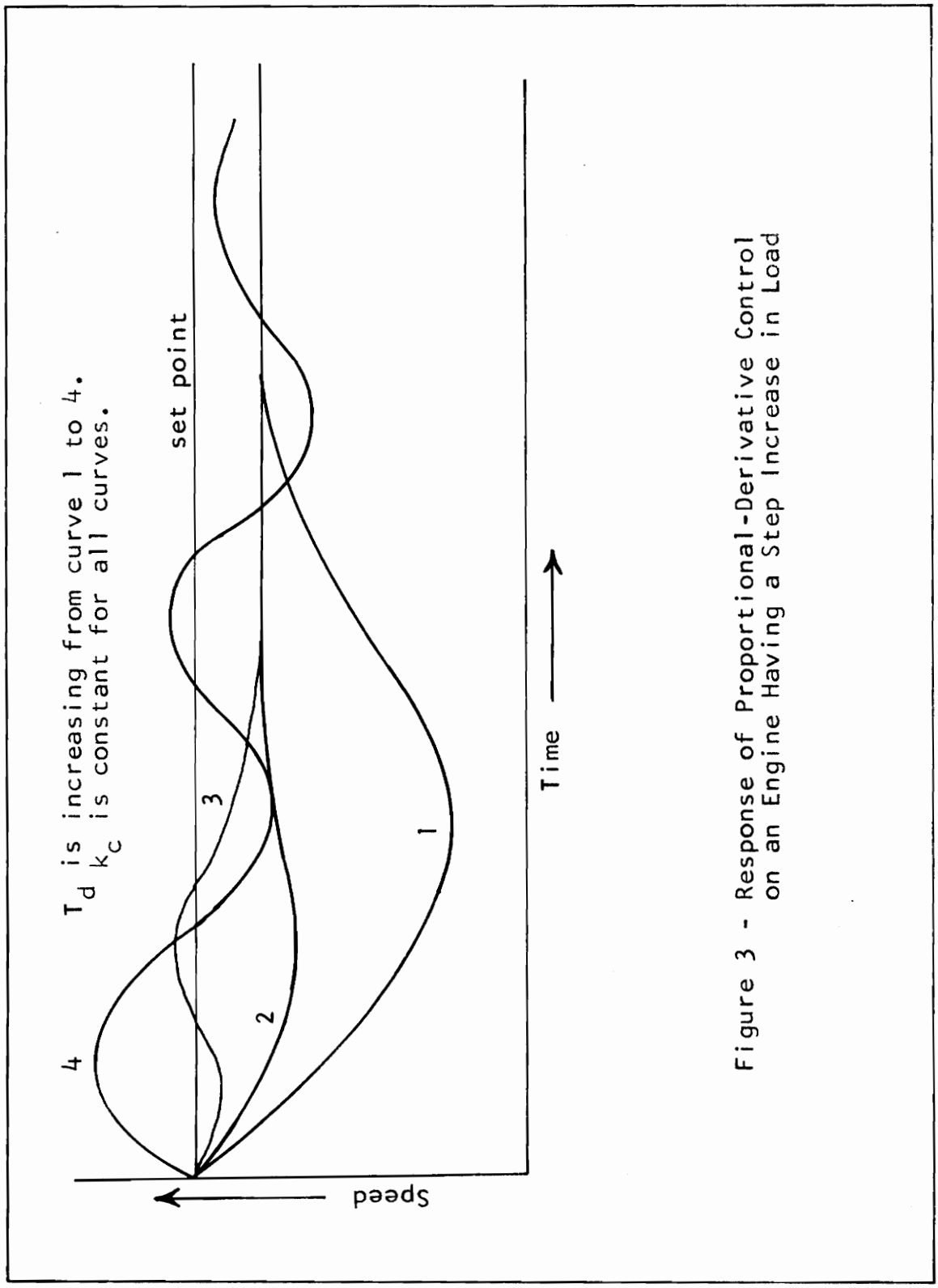

Figure 3 - Response of Proportional-Derivative Control on an Engine Having a Step Increase in Load

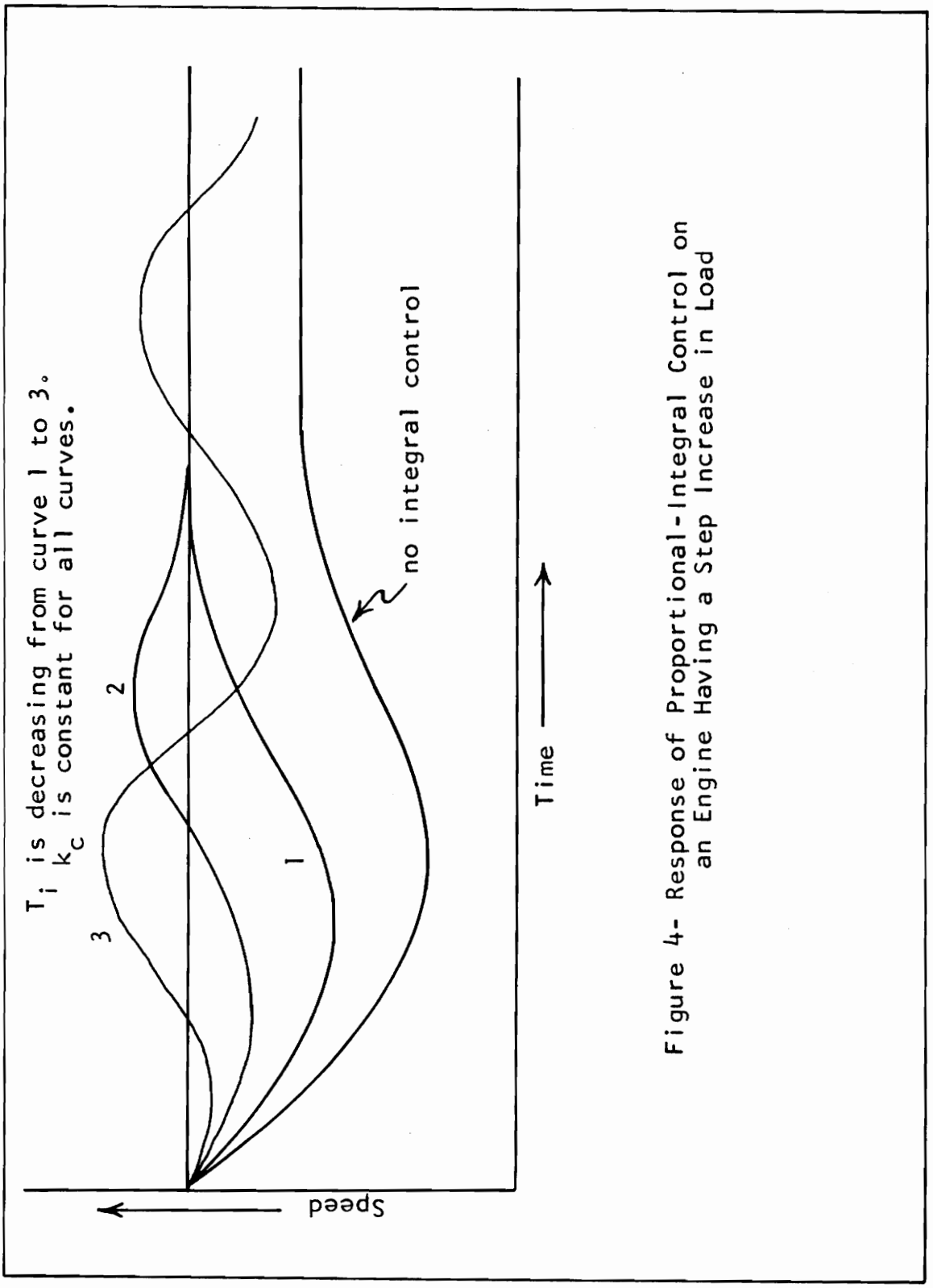

Figure 4- Response of Proportional-Integral Control on an Engine Having a Step Increase in Load

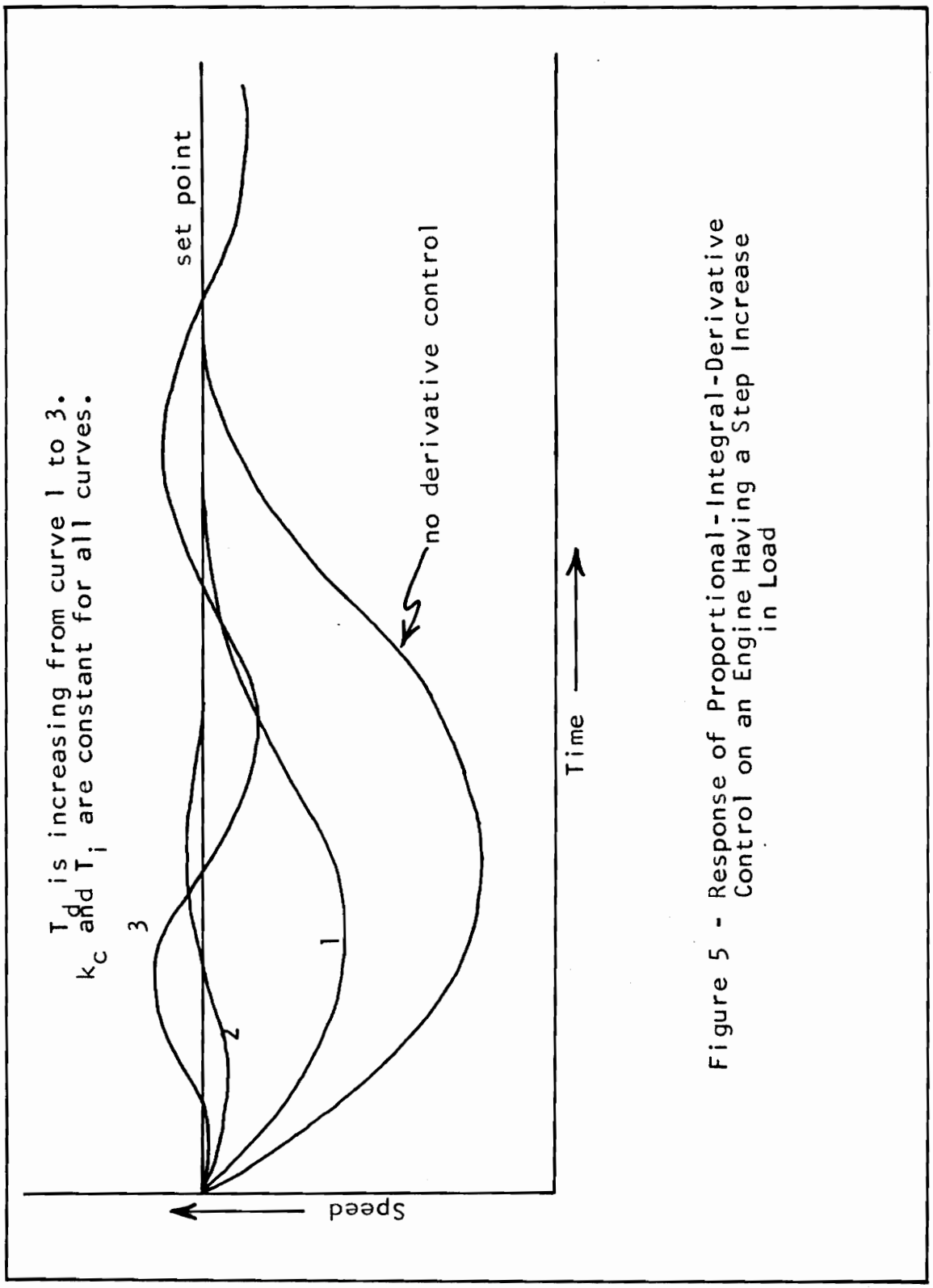

Figure 5 - Response of Proportional-Integral-Derivative Control on an Engine Having a Step Increase in Load

Figure 5, the addition of derivative control causes the error near zero time to decrease, but if T_d is made too large the system may become unstable.

Figure 6, reproduced from reference (4), shows a comparison of proportional, integral, proportional-derivative, proportional-integral, and proportional-integral-derivative control.

"Proportional-derivative control [1] provides the smallest maximum error because the derivative part of the response allows the proportional sensitivity to be increased to a high value. The stabilization time is the smallest because of the derivative action. Offset is allowed but is only half that experienced without derivative action.

"Proportional-integral-derivative control [2] has the next smallest maximum deviation and offset is eliminated because of the integral action. Notice, however, that the addition of integral action markedly increases the stabilization time.

"Proportional control [3] has a larger maximum deviation than controllers with derivative action because of the absence of this stabilizing influence. Offset is also larger.

"Proportional-integral control [4] has no offset because of the integral action. The unstabilizing influence

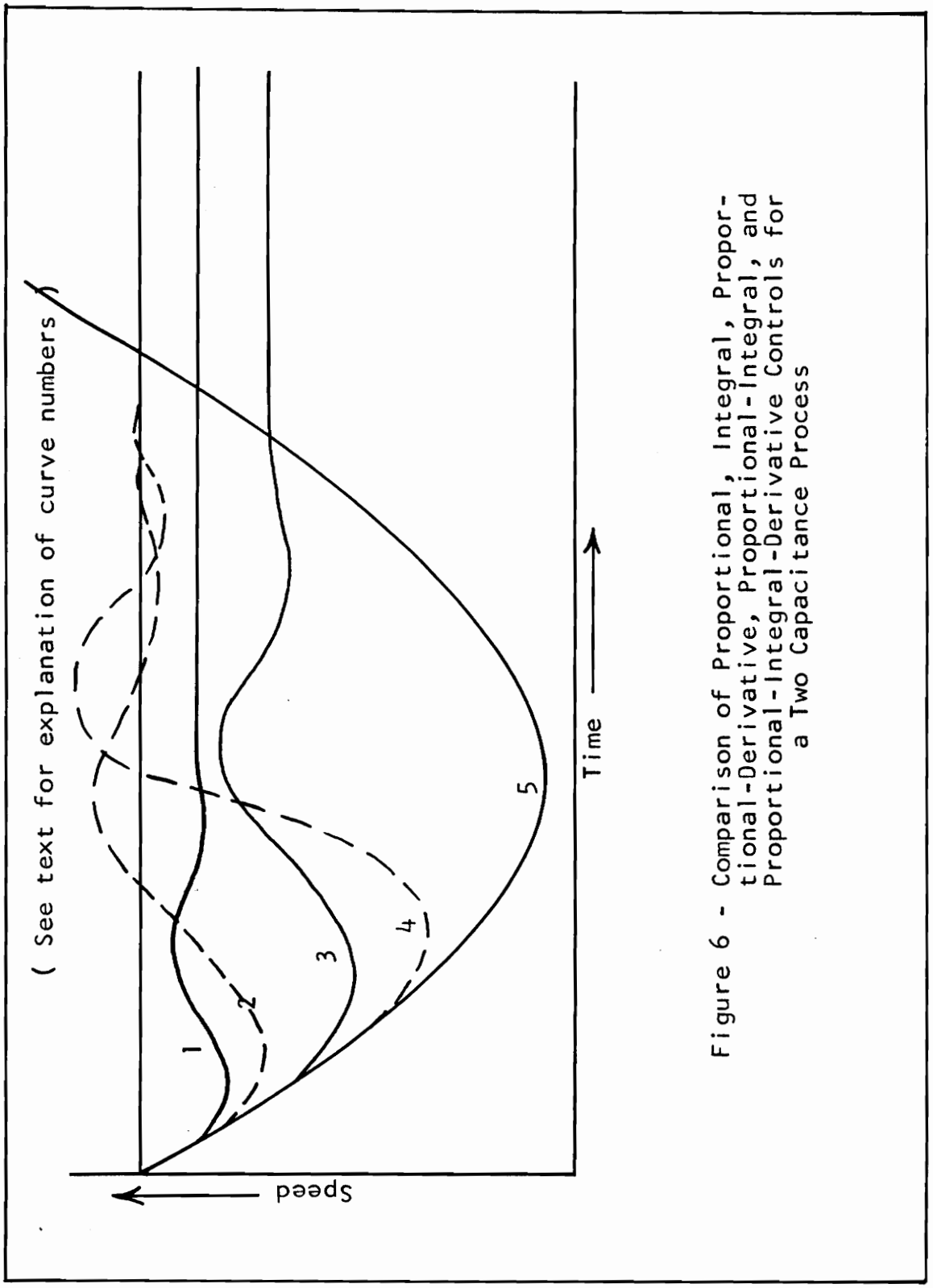

Figure 6 - Comparison of Proportional, Integral, Proportional-Derivative, Proportional-Integral, and Proportional-Integral-Derivative Controls for a Two Capacitance Process

of integral response is reflected in the large maximum deviation and the persisting deviation.

"Integral control [5] is best suited for the control of processes having little or no energy storage and the results of the comparison are not representative of all integral control. However, on this process, the results indicate a large maximum deviation and a long stabilization time."[4]

Figure 6 shows that if it is desired that a process have the least error for the least time, then the proportional-integral-derivative control is the best control to use.

Stability of Controllers

"A feedback control loop is said to be stable when at such a condition that, following a disturbance, its controlled variable will come eventually to a steady, noncyclic value."[5]

"Automatic control consists of a chain of energy exchanges—measurement, comparison, correction, reaction—going round and round in a closed loop, through the control system and through the process. Both the process and the control system can retard and delay these energy exchanges. The simplest explanation of control-loop stability is in

terms of the time retardations and energy loss or gain around the loop.... A signal (energy) from a process output is fed back by the control system into an input to the process.

"Corrections to process input must be opposed to changes in process output if these corrections are to restore the desired value of output.... In other words, the signal (energy) fed back must be in such direction as to change the process input negatively with respect to the change in process output. Thus, control systems are made with built-in 180 - angular degree phase lag or shift (-180^{o}), that is, negative feedback.

"...it is known that the process capacity, resistance, and transportation cause lags or negative phase shifts between changes to process input and resultant changes in output. It has been pointed out, too, that these same properties cause negative phase shifts in the control system itself. These process and control system phase shifts add to the negative 180^{o} phase shift built into the controller, and, if these several phase shifts are large enough, the result can be a total phase shift around the control loop that approaches 360 angular degrees, that is, positive feedback.... Under this condition, the controller corrections will actually increase output changes instead of opposing them.

"...This tendency to self-sustaining oscillation is the greatest limitation to feedback control."[5]

Mathematical Theory of Stability[6]

The mathematical theory of stability can be explained by a consideration of the system shown in Figure 7. The symbols A, G_1, G_2, L, and H represent the LaPlace transforms of the transfer functions.

If the system is considered with a fixed set point and a varying load then

$$C = \frac{L\ U}{1 + H\ G_1\ G_2} .$$

Since A, G_1, G_2, H, and U are LaPlace transforms, they are all functions of the complex variable s, so that C can be defined by the equation

$$C = \frac{a_m s^m + a_{m-1} s^{m-1} + \dots a_1 s + a_o}{b_n s^n + b_{n-1} s^{n-1} + \dots b_1 s + b_o}$$

where a_m and b_n are constants. For any real physical system $n \geq m$. The inversion of the above transform can only yield terms like

$$C = f(A,\ e^{+r_n t},\ t^k\ e^{+r_n t})$$

where r_n are roots of the denominator polynomial, A is a constant, and k is a constant. The time constant terms

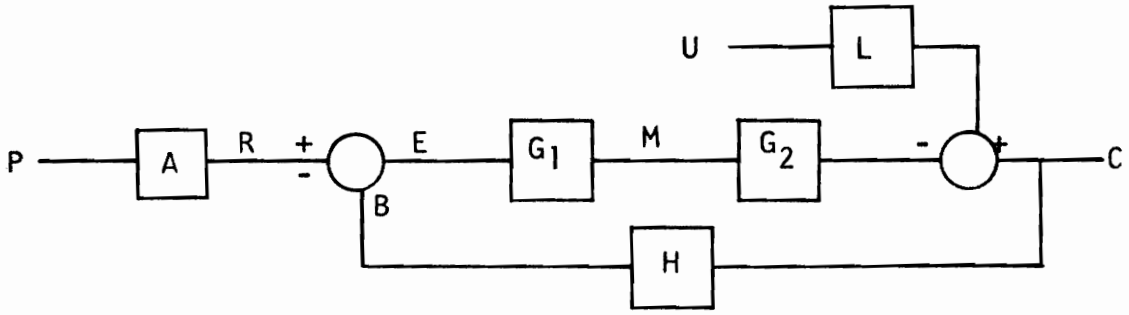

P = Set point
A== Input element
R = Reference signal = PA
B = Feedback signal = CH
E = Error signal = R-B = PA-CH
G_1 = Control elements
M^1 = Control signal = $EG_1 = G_1(PA-CH)$
G_2 = Controlled system
U^2 = Load variable
L = Load system
H = Feedback elements
C = Controlled variable

$$C = LU+MG_2 = LU+G_1G_2(PA-CH) = LU+PAG_1^1G_2-CHG_1G_2$$

$$C+CHG_1G_2 = LU+PAG_1G_2$$

$$C = \frac{LU}{1+HG_1G_2} + \frac{PAG_1G_2}{1+HG_1G_2}$$

Figure 7 - Block Diagram of a Closed Loop Automatic Control System

have the form $e^{r_n t}$ where r_n is a complex number such that

$$r_n = \gamma + i\beta.$$

If γ is positive then the value of C will constantly increase and the control system is unstable.

The problem of stability has now been reduced to the problem of determining whether the denominator of the closed loop transfer function has any real positive roots. Finding these roots by purely mathematical methods usually leads to difficulty, so simpler methods have been devised to determine if there are any real positive roots. One such method which is commonly used is the Nyquist plot method.

Nyquist Plot Method of Stability Analysis

"This plot is obtained by drawing a curve on polar co-ordinates where the vectorial angle for a frequency f is the open-loop phase angle, and the length of the radius vector is the open-loop magnitude ratio for the frequency f. The frequency is thus the parameter along the curve."[7] (The magnitude ratio of a system is defined as the ratio $\left|\frac{C}{M}\right|$ where M is the input to the system and C is the output of the system.)

"From complex variable theory involving the Nyquist stability criterion, the curves [Nyquist plots] must be

closed in a certain way (the closed curve is to be traversed once as one goes once, say, clockwise 'around' the right half of the S-plane) and the arcs for closing the curves can be taken to be circular arcs of very great radius..."[8] (See Figure 8.)

"The curve formed by the transfer locus, its conjugate, and closure arc will be called the 'closed transfer locus'....

"To get the net encirclement draw a vector from the point (1, -180 deg) to a point P on the transfer locus. Let P traverse the entire closed curve. The vector will rotate through an angle (360n) deg, where n is the number of times the locus encircles the point (1, - 180 deg).

"It is assumed that the closed-loop linear systems under discussion are stable if opened. For such systems Nyquist's famous stability criterion follows:

Nyquist Stability Criterion. Let S be a closed loop system that is stable when the loop is opened. The system S is stable if and only if in one traversal of the closed transfer locus the net encirclement of point (1, - 180 deg) is zero."[8]

Magnitude - Phase Method of Stability Analysis

"The magnitude-phase method of analysis may be employed to determine the performance and stability of an

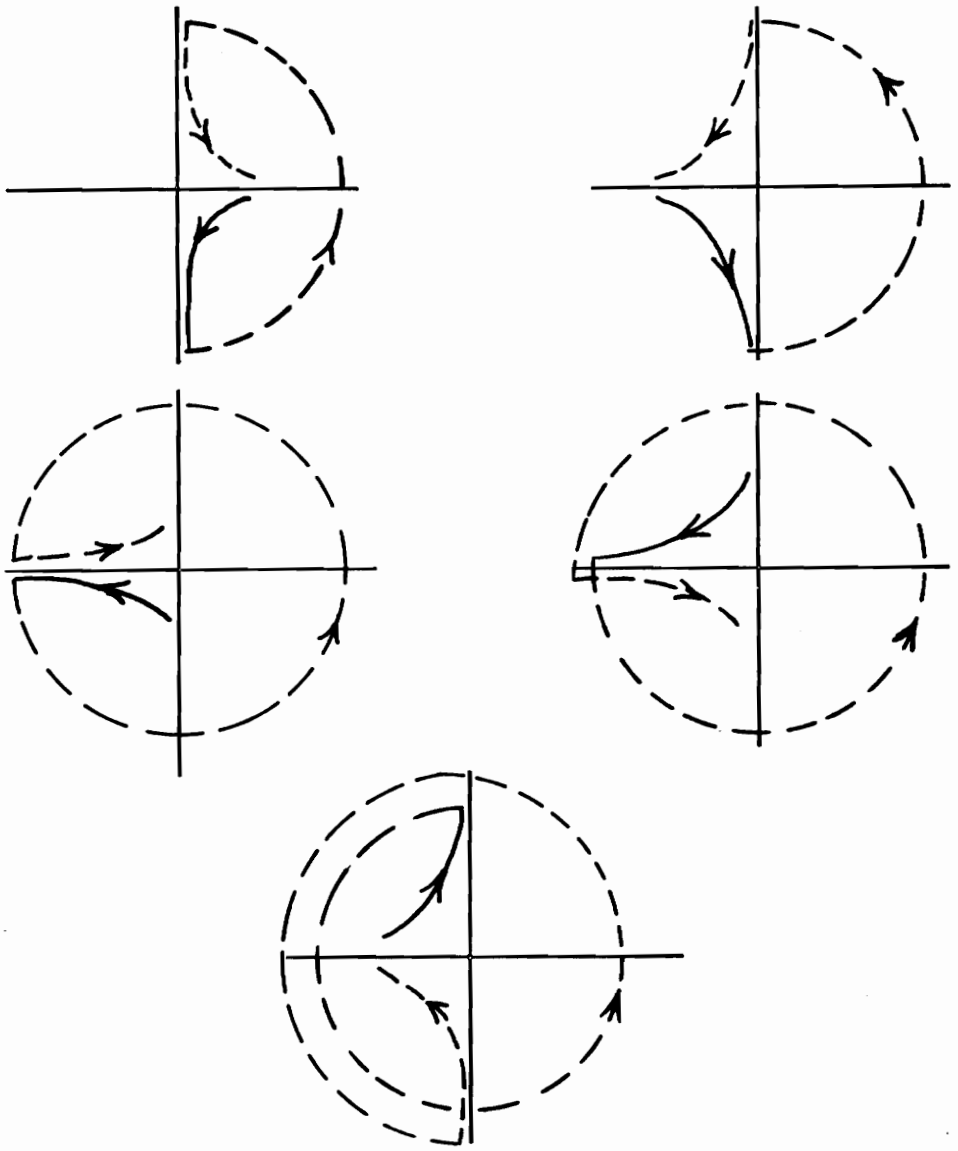

Figure 8 - Methods of Closing a Curve Formed by Transfer Locus and Its Conjugate

automatic control system. It is undoubtedly the most widely used method of analysis and synthesis of control systems. It is also one of the simplest methods.

"The Bode magnitude-phase method of analysis may be used for a wide range of problems, including the analysis of systems containing some nonlinear elements. Generally, however, it is more useful for systems having linear response."[9]

It has been found[9] that for a reasonable closed-loop response, the open loop phase angle should be about -135 deg at a frequency for which the magnitude ratio is one. It can be said, then, that a selection of open-loop phase will determine the closed-loop behavior for a system. This is the basis of the Bode magnitude-phase method.

The magnitude ratio is plotted on log-log coordinates against the frequency for values of magnitude ratio ranging from about 0.1 to 10. The phase is plotted separately on semi-log coordinates with frequency on the log coordinate and phase in degrees on the linear coordinate. For clarity the curves are usually plotted on the same set of coordinates with phase ranging linearly from 0° at a magnitude ratio of .1 to -360° at a magnitude ratio of 10.

"Stability and performance may be determined from the graphs by the following rules:

" 1. If the phase lag is less than 180 deg at the highest frequency for which the magnitude [ratio] is one, the closed-loop is stable. Conversely if the phase lag is greater than 180 deg, then the system is unstable.

" 2. If the phase lag is approximately 135 deg at the highest frequency for which the magnitude [ratio] is one, the closed loop response will be damped and slightly oscillatory in a 'satisfactory' manner. Sometimes the analysis may be made by employing the magnitude [ratio] - frequency diagram without reference to the phase lag. It is best however to use rule 3 as a check on the method listed above.

" 3. If the magnitude [ratio] - frequency curve does not change slope appreciably over two octaves of frequency near the highest frequency at which the magnitude [ratio] is one, and if the negative slope of the magnitude [ratio] - frequency curve is less than 2.0 (plotted on log co-ordinates), the system is probably stable.

" 4. If the magnitude [ratio] - frequency curve does not change slope appreciably over two octaves of frequency near the highest frequency at which the magnitude [ratio] is one, and if the negative slope is 1.5, the closed-loop system is probably stable. Furthermore, the closed-loop response will be damped and slightly oscillatory in a 'satisfactory' manner."[9]

The main disadvantage of the Nyquist plot method and the Bode magnitude-phase method of stability analysis is that they require extended testing of the actual machinery, resulting in increased cost and time. There is also the possibility that the equipment may be damaged during the frequency response tests. For this reason the electronic analog computer has become a common engineering tool for the analysis of automatic control systems.[10]

Analog Computer Method of Stability Analysis

"Experience has shown that the computing elements lend themselves very naturally to similation of closed or open-loop control systems. The proper application of a computer can save many hours of calculation in determining the proper range of coefficients to produce stability or an optimum response to a disturbing influence in a servo-mechanism system."[11]

The method which is used to perform a stability analysis of a control system by means of an analog computer will be given in detail in the investigation of this thesis.

From the above statements it appears that the easiest and most accurate method of determining the stability of a system is the use of an analog computer.

Adjustment of Controllers

"The quality of regulation obtained from automatic-control systems depends greatly on the adjustments made to their various control modes. To obtain the best control, a systematic adjustment method must be used; haphazard adjustments will rarely find the best settings. In general, the best settings are those which produce the desired stability....

"...Adjustments should be made under the most unstable conditions of load and set point that normally can occur. The three most widely used methods of adjusting controllers are:

1. Systematic trial methods.
2. Ultimate-sensitivity calculated method.*
3. Reaction-curve calculated method.* " [12]

Since this thesis is concerned with a proportional-integral controller combined with a torque sensing control, only the systematic trail method for the proportional-integral type of control will be considered.

"Step 1: With reset rate at zero [integral time set to infinity] (or its lowest value), ...[start with a large proportional band and narrow] the proportional band until

---

* Applicable only to proportional, reset, or rate-mode controllers.

a damping ratio of about 0.25 is obtained.... Then increase the band width slightly....

"Step 2: Allowing the proportional band to remain at this setting, begin with the slowest reset rate and increase the reset rate in small steps while creating set-point load changes until cyclic behavior begins to increase. Then reduce the reset rate slightly...."[13]

Improvement on Proportional-Integral-Derivative Controller As Applied To The Speed Control Of A Diesel-Alternator Set

There are two disadvantages to adding derivative control to a proportional-integral controller. One of the major disadvantages is its cost; another disadvantage is "that if the input to the governor includes unwanted speed changes of low amplitude but high frequency, then the derivative unit will tend to produce an unwanted output of high amplitude because of the high rate of change of the unwanted speed changes. If the original spurious errors are small enough to be ignored the addition of a derivative term would produce an output that could not be ignored. This disadvantage can be overcome by muting the derivative term at inputs of low amplitudes. It then becomes complicated."[14]

"The author considers that present-day designs are in the realm where no great improvement will be achieved unless a new approach to the subject is found. With the above reasoning in mind he has been developing such a governor, and attention has first been directed to the Diesel-alternator set. This has been done for two main reasons: (a) a demand exists for better governing of such sets; and (b) it is easy to measure electrical loads with simple robust equipments.

"For Diesel sets where the load is in the form of mechanical shaft horse-power and not electrical kilowatts, measuring the load is not cheap or simple, and the demand for better governing in that case is not so insistent. ...Simple electrical circuits are used to measure the electrical output and two signals are produced: (a) one proportional to kilowatts; and (b) one proportional to speed error.

"At this point it should be stressed that the second signal (speed error) is necessary because the load signal does not contain any indication of speed. These two signals are combined and amplified in order to produce a signal of the correct power level for effective use....

"...The action of this governor is as follows:——When the Diesel-alternator is running at its correct speed at a steady load, the amplifier is receiving signals which

indicate that: (a) the fuel bar should be in a position appropriate to the load, and (b) the speed is correct.

"When the load on the alternator increases, the amplifier receives electrical signals showing that: (a) the fuel bar should increase the fuel injected into the engine to a new value, and (b) should a speed change occur, that an error in speed exists.

"It is important to note that the positioning of the fuel bar to the new fuel setting is initiated before the engine has had time to change its speed, and any error in speed that does occur is mainly due to the slight inaccuracy in the fuel bar setting as a result of the load signal and the unavoidable small delay in getting this signal to the fuel bar.

"The signal showing an error in speed then trims the position of the fuel bar to its appropriate setting and brings the speed back to its correct value. A similar action takes place on a decrease in load, but with a decrease in fuel injected."[14]

Summary

Because of the high sensitivity demanded of speed controllers, it is necessary to use a combination of controllers to maintain stability. The simplest and most

stable type of speed controller is the proportional controller, but this type of controller has the disadvantage of offset. Integral control is added to proportional control in order to avoid offset, but the integral controller has a tendency to be unstable and cause the system to oscillate. Derivative control is added to proportional-integral control in order to reduce the maximum error and to stabilize the system, but derivative control is generally expensive, and it has the disadvantage of producing an unwanted output of high amplitude because of the high rate of change of relatively insignificant speed signal changes resulting from actual speed changes, or from "noise" in the speed signal.

From the above statements it would appear that a controller which could overcome the instability of integral control and the disadvantages of derivative control, while performing the operations of both, would be an improvement over the conventional proportional-integral-derivative controller.

Consider the operation of a torque sensing controller combined with a proportional-integral controller as applied to an internal combustion engine. If a load is suddenly applied to the engine, the torque will increase and cause the torque sensing controller to increase the throttle setting to a higher value. If the new throttle setting is

slightly in error the proportional-integral controller will correct for this error. Note that the torque sensing controller corrects for the change in load even before the speed has a chance to change. The proportional-integral controller is necessary only to correct small speed errors. Since the torque sensing governor sets the throttle to its proper position, and since the speed errors are relatively small, the magnitude of integral control is very small and derivative control is not necessary. The torque sensing controller overcomes the instability of integral control by causing the necessity for integral control to be greatly reduced, and at the same time completely does away with derivative control. From this it appears that a torque sensing governor would be an improvement over the conventional proportional-integral-derivative governor as applied to an internal combustion engine.

The direct mathematical stability analysis is seldom used because the system equations are seldom known accurately, and even when they are known they are very difficult to solve. The Nyquist plot and the magnitude-phase methods of stability analysis are easier to use than the mathematical method, but they both require actual testing of the control system. This takes time, and there is the danger that the equipment may be damaged during these tests. An electronic analog computer is relatively inexpensive to operate and

there is no danger of damage to the computer, even if a circuit is unstable. By simulation of the entire system on an analog computer, the stability analysis can be made before the controller is applied to the actual system.

III. INVESTIGATION

Object of Investigation

The object of this investigation was to present the design of a practical torque measuring device, and to show that the use of such a device with a constant speed governor will produce less error for less time than the conventional proportional-integral-derivative constant speed governor when used on an internal combustion engine.

Design of the Torque Sensing Device

The torque sensing device consisted of a shaft which twisted an amount which was directly proportional to the engine torque, a means of amplifying the shaft deflection, and a means of converting the amplified shaft deflection into an electric signal.

Since the engine used in this investigation was rated at 1/2 horsepower operating at a speed of 2100 rpm, the design torque was calculated to be 1 lb-ft. Using this value of torque it was calculated that the minimum shaft diameter could be about 0.2 in. for a mild steel shaft. It was also calculated that for a length of 2 in. a 0.2 in. diameter steel shaft will twist 0.95 deg under a 1 lb-ft torque. (Appendix A) A torque sensor shaft was designed

using these values, but it failed in the small diameter section (sensing section), so a shaft was designed using a diameter of 0.25 in. in the sensing section. (Figure 9)

The shaft was mounted in line with the crankshaft of the engine so the engine could be coupled to one end by means of a flexible coupling, and a load applied to the other end by means of a V-belt arrangement. The shaft deflection was amplified by two torque sensor disks. Torque sensor disk number one (Figure 10) was fastened to the engine end of the shaft by means of a tube (Figure 11) which was fixed to the engine end of the shaft and extended to the load side of the sensor section. The sensor disk number one was threaded on the load end of the tube and held by the lock nut shown in Figure 12A. Torque sensor disk number two (Figure 13) was threaded on the load end of the shaft and held by the lock nut shown in Figure 12B. A photograph of the torque sensor both assembled and disassembled, is shown in Figure 14. The torque sensor shaft was held in place by ball bearings which were pressed on the load end of the shaft, and held in place by the torque sensor holder shown in Figure 15. The engine end of the shaft was stabilized by means of a ball bearing which was pressed on the sensor disk holder retainer nut (Figure 16) and held in place by the bearing holder shown in Figure 17.

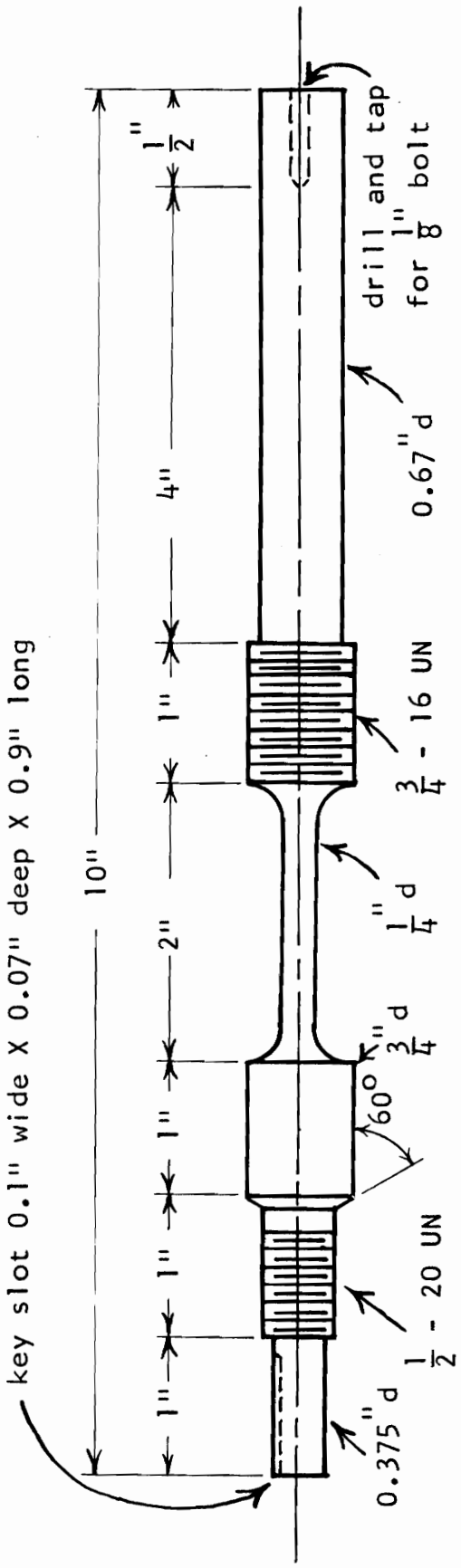

Figure 9 - Diagram of Torque Sensor Shaft

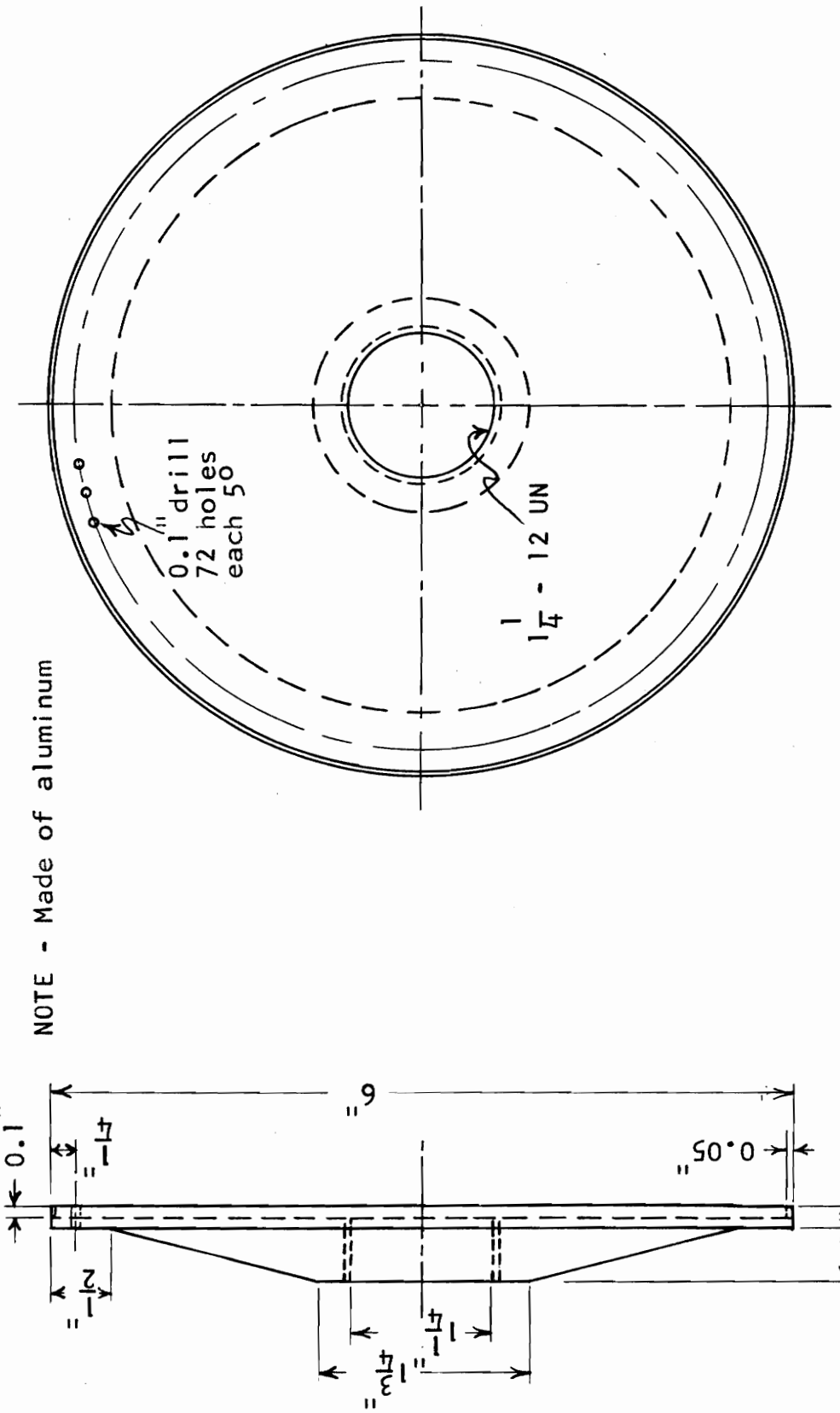

Figure 10 - Diagram of Torque Sensor Disk Number One

NOTE - Made of aluminum

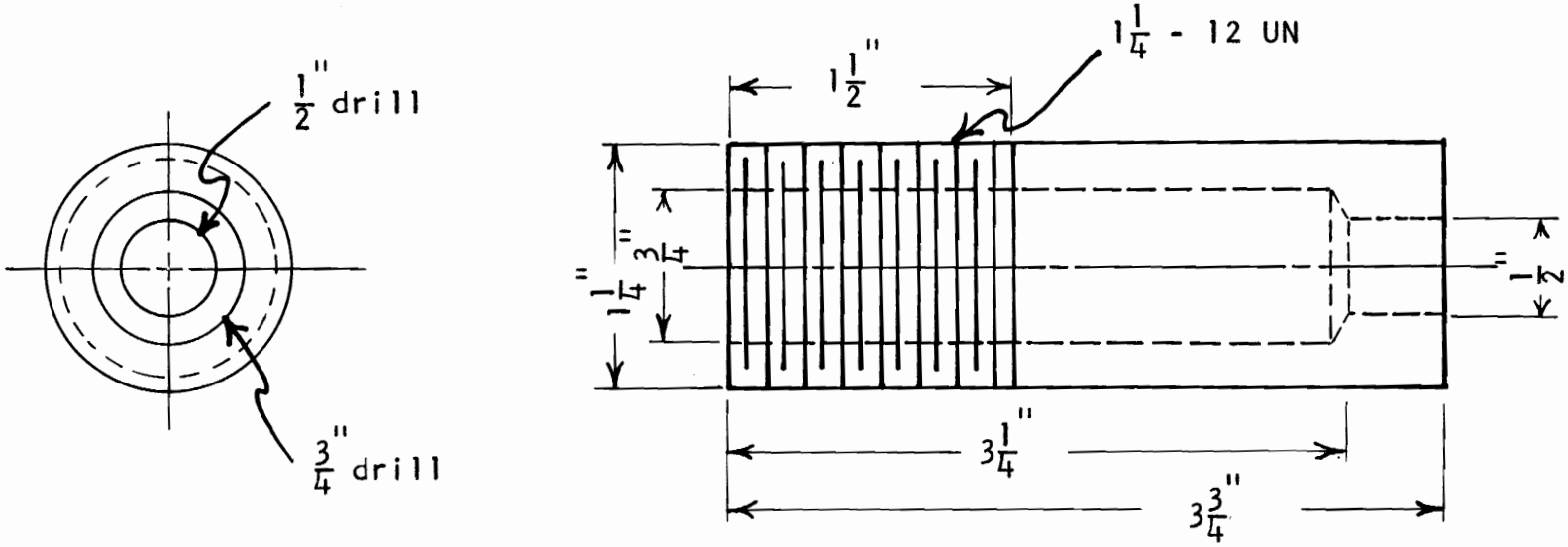

Figure 11 - Diagram of Sensor Disk Number One Holder Tube

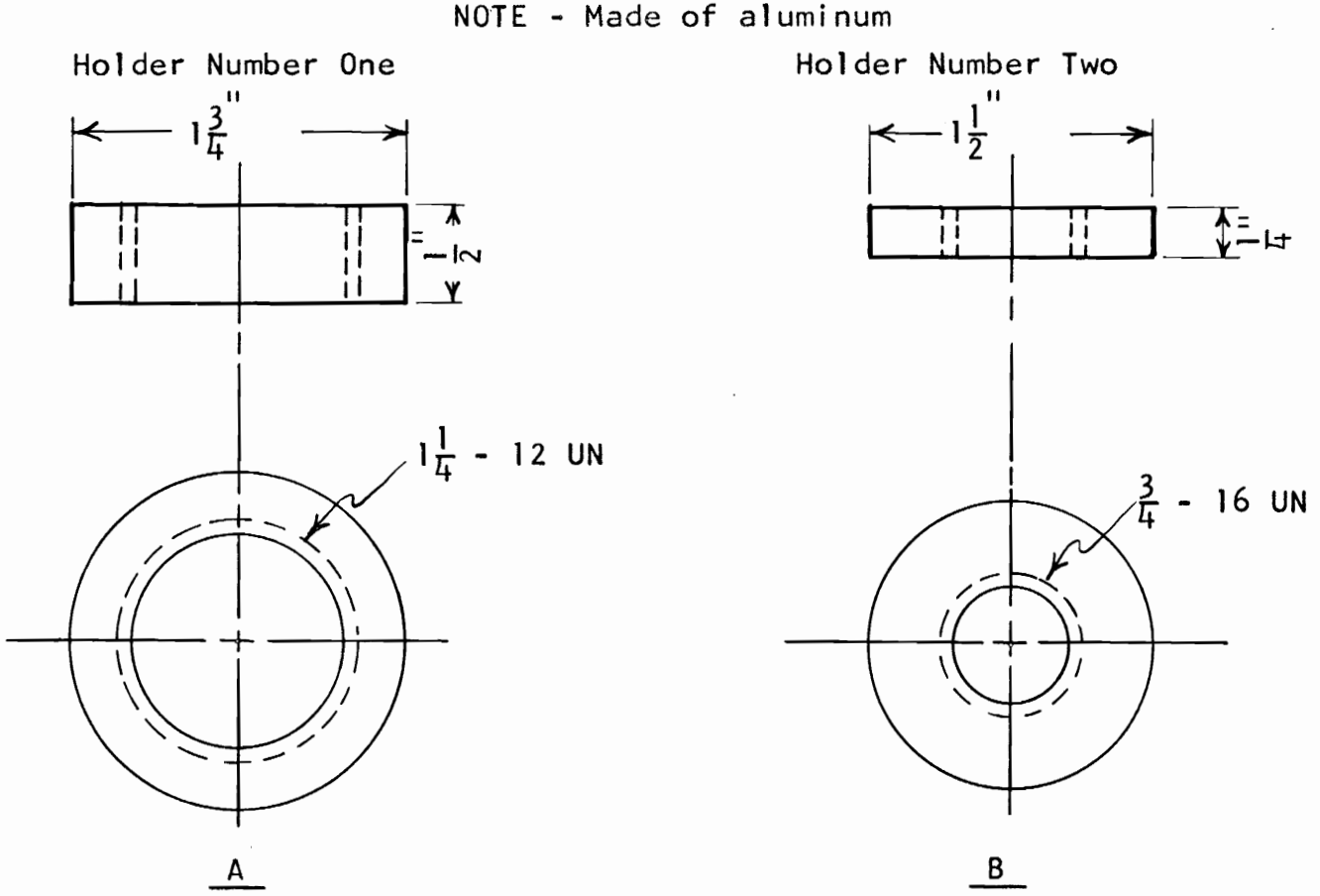

Figure 12 - Diagram of Sensor Disk Lock Nuts

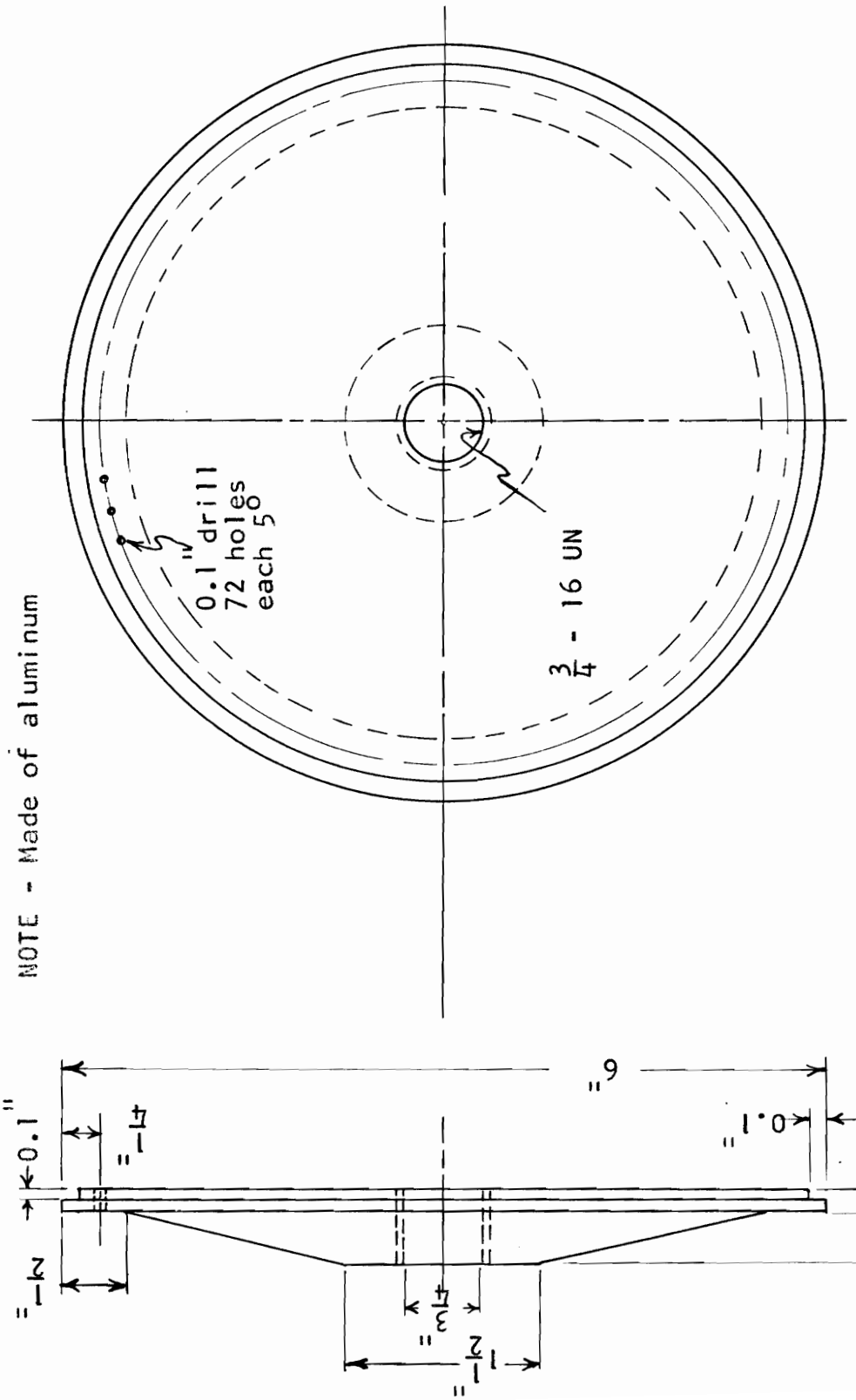

Figure 13 - Diagram of Torque Sensor Disk Number Two

Disassembled

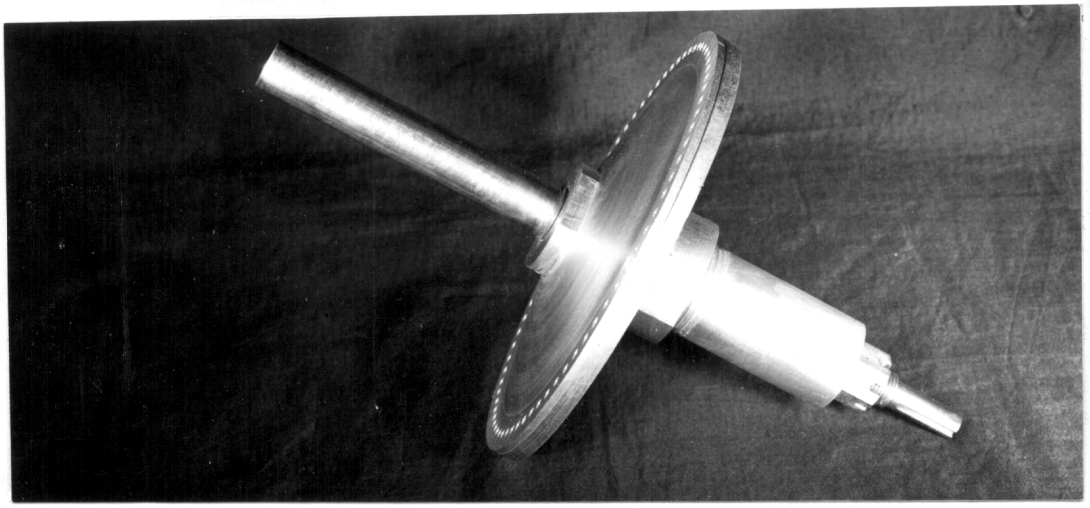

Assembled

Figure 14 - Photographs of Disassembled and Assembled Torque Sensor

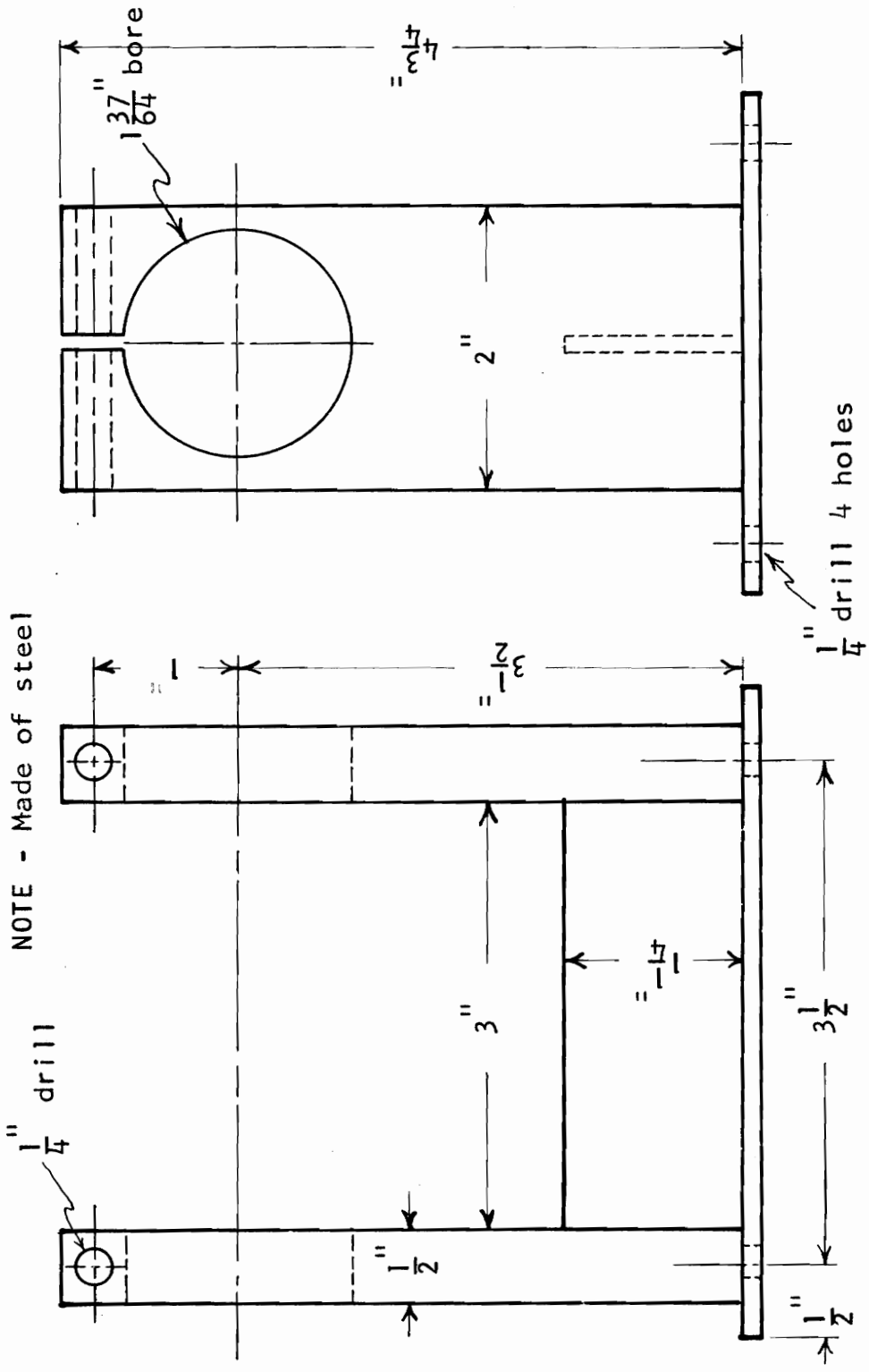

Figure 15 - Diagram of Torque Sensor Holder

NOTE - Made of steel

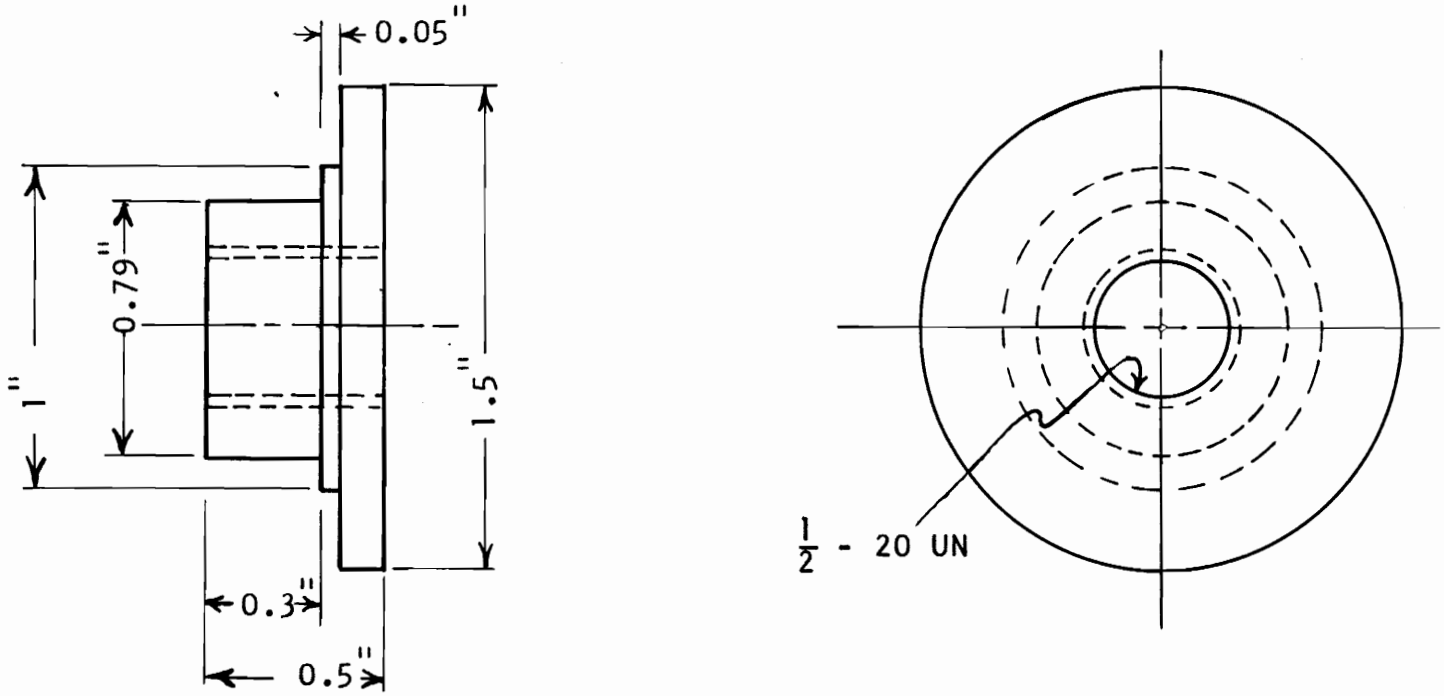

Figure 16 - Diagram of Sensor Disk Holder Retainer Nut

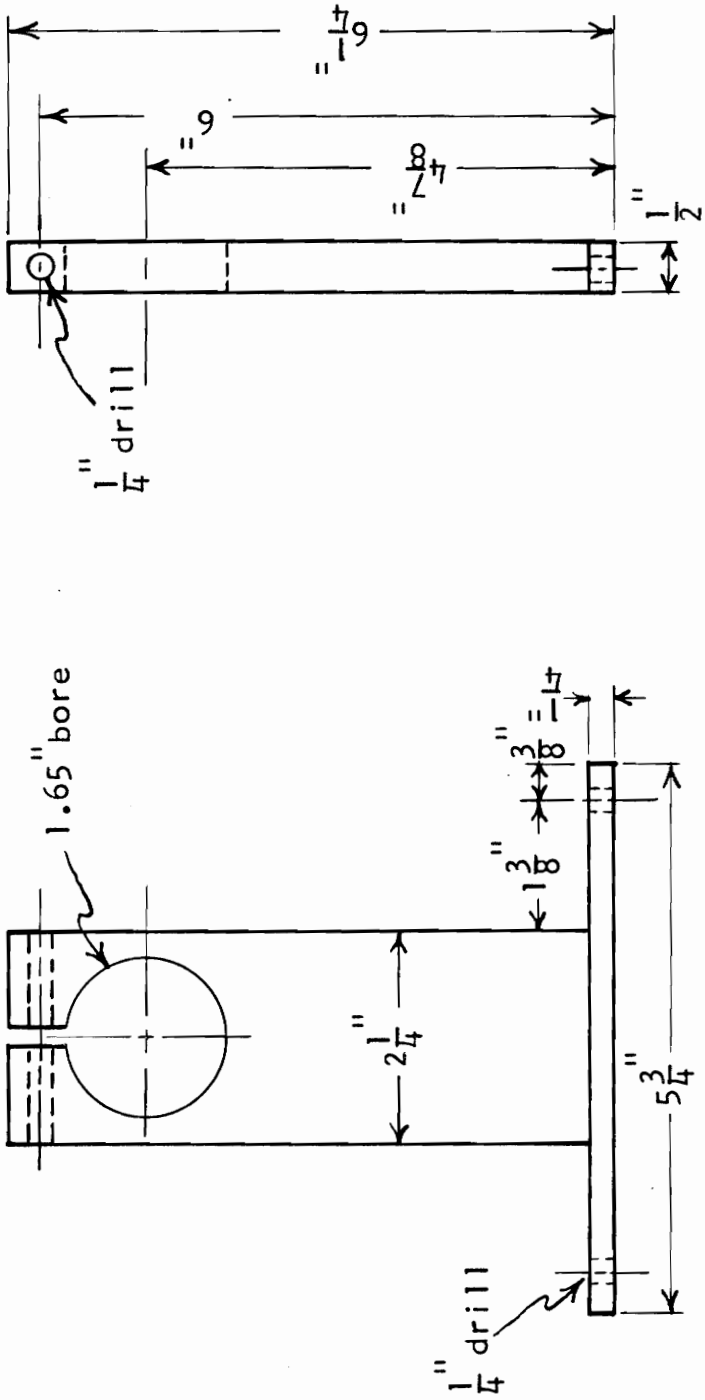

Figure 17 - Diagram of Bearing Holder Number Two

The amplified shaft deflection was converted into an electric signal by means of the 0.1 in. diameter holes in the torque sensor disks, an electric light bulb, and a photoconductive cell. The torque sensor disks were fastened to the torque sensor shaft in such a way that the holes in one disk were about halfway mismatched with the holes in the other disk when no torque was applied to the shaft. (Figure 18) A light bulb was placed on one side of the disks, and a photoconductive cell was placed on the other side of the disks, so that the photoconductive cell senses the light which passes through the holes in the disks. (Figure 19) When a torque was applied to the torque sensor shaft, the shaft deflected causing the holes in the disks to become more mismatched (Figure 18), which in turn caused the quantity of light sensed by the photoconductive cell to be reduced, thereby causing an increase in the resistance of the photoconductive cell. A voltage was obtained from the circuit shown in Figure 20. This voltage was a function of the torque applied to the torque sensor shaft. Figure 21 is a photograph of the mounted torque sensing device.

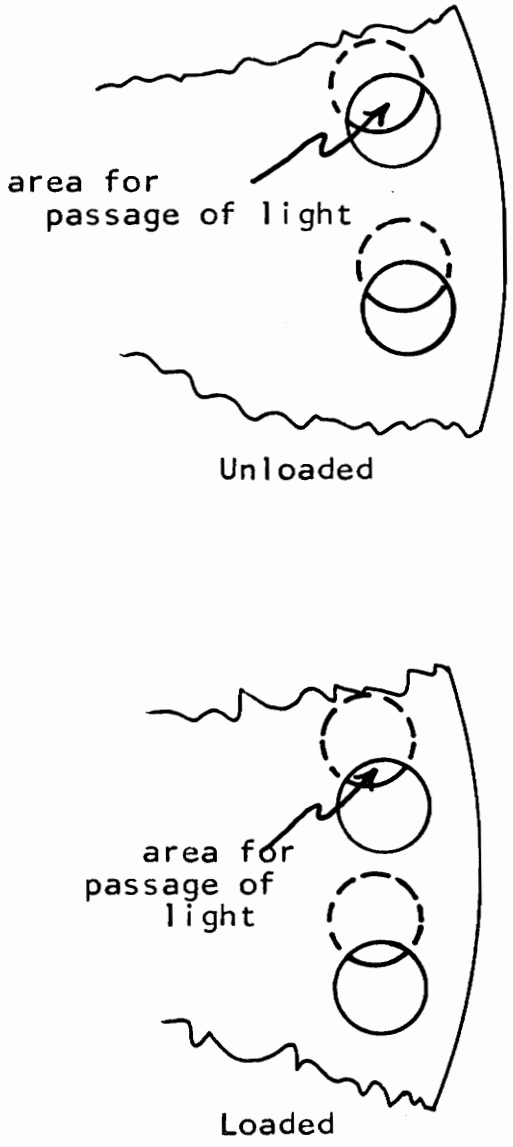

Figure 18 - Detail of Torque Sensor Disk Holes

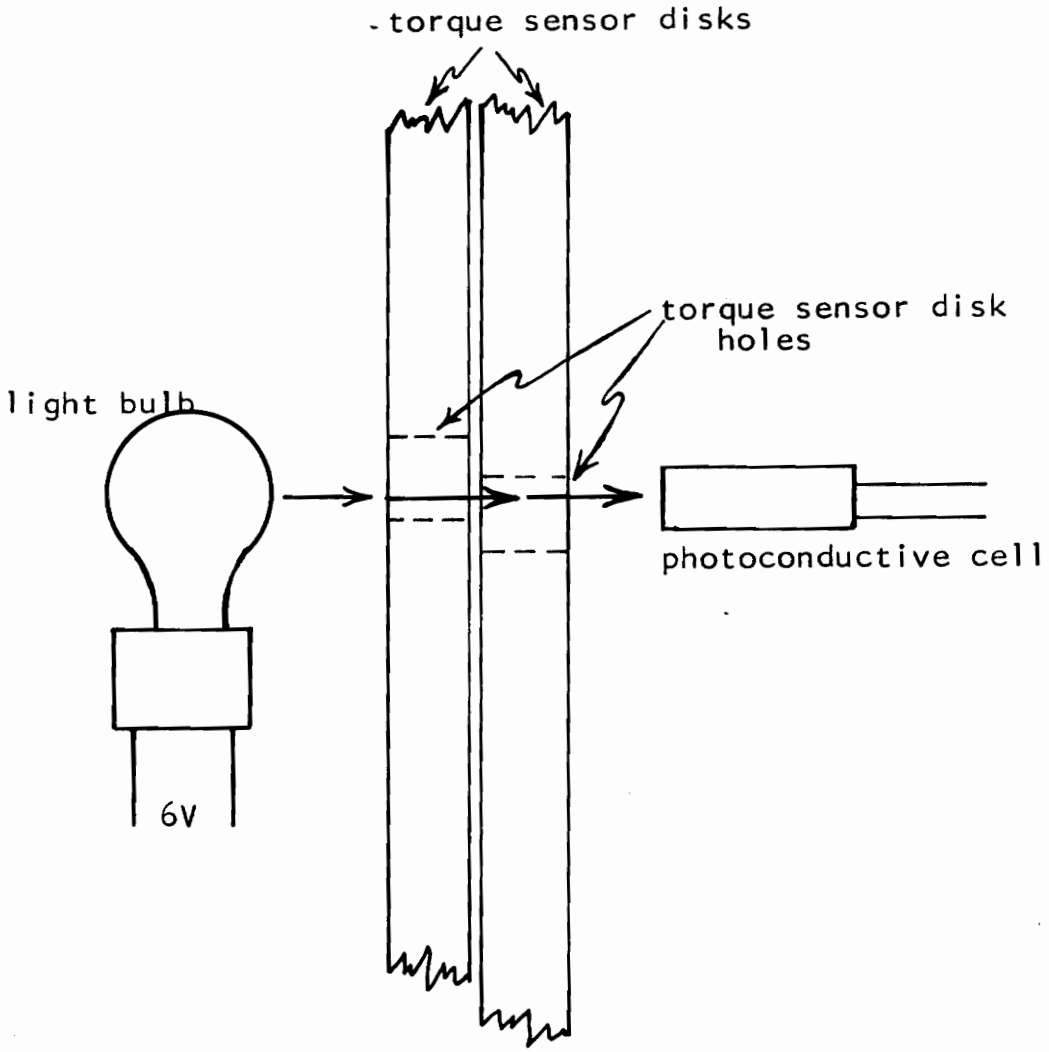

Figure 19 - Detail of Light Sensing Arrangement

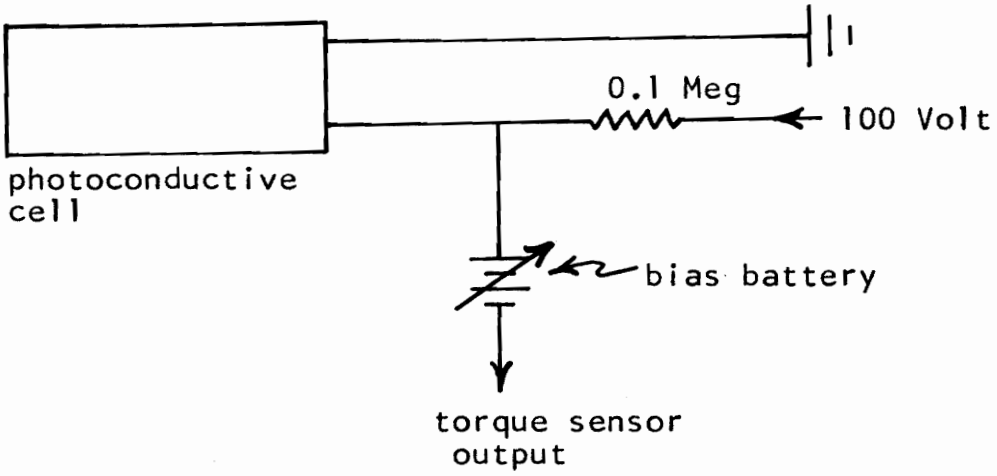

Figure 20 - Schematic Diagram of Circuit Used to Obtain Voltage Output as a Function of Photoconductive Cell Resistance

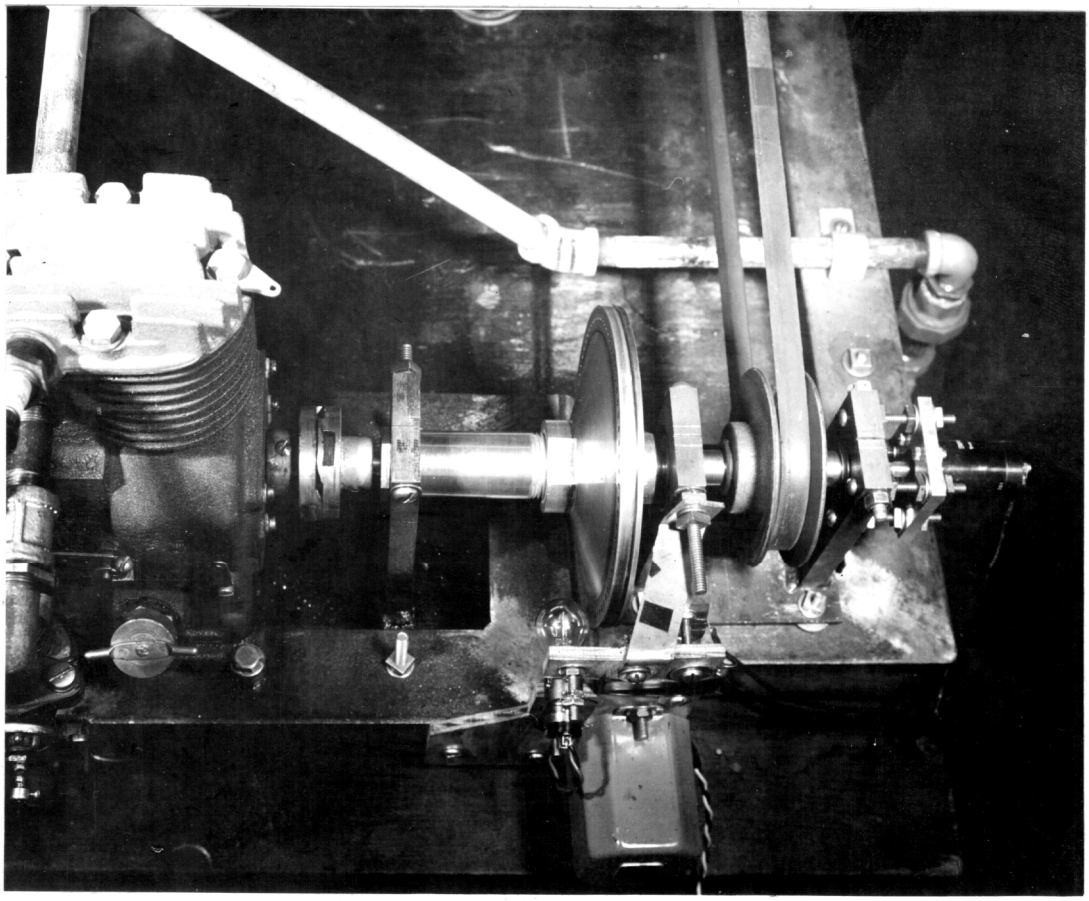

Figure 21 - Photograph of the Mounted Torque Sensor

Throttle Control Mechanism

A Minneapolis-Honeywell millivolt recorder was used to operate the engine throttle. A crank mechanism was attached to the cable drum shaft (Figure 22) so that the throttle setting would be a function of the angle of rotation of the drum. Since the drum rotation is directly proportional to the input voltage to the recorder, the throttle setting will be a function of the voltage input to the recorder.

The crank mechanism was designed in such a way that full throttle movement could be obtained by using only 20% of the recorder range. Since the time required for full range movement of the recorder was 1 second, this gave full throttle movement in 0.2 seconds.

An external voltage divider was used to divide the throttle signal from the control circuit by 334. This made it possible to use a throttle signal of 0 to 2.5 volts rather than 0 to 0.0075 volts (20% of the full range of the recorder used). Figure 23 shows the external voltage divider circuit.

Figure 24 is a photograph showing the throttle control mechanism, the engine, and the torque sensor.

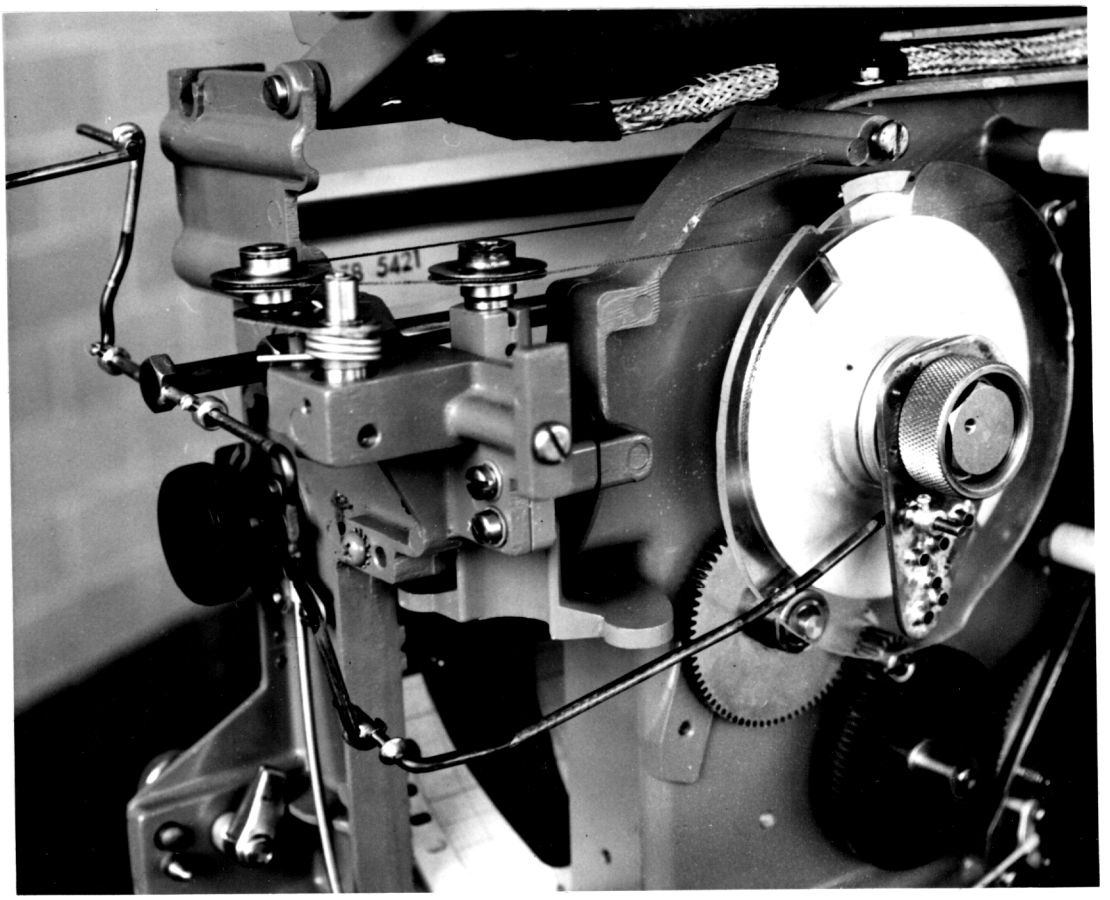

Figure 22 - Photograph of the Throttle Control Linkage Attached to the Recorder

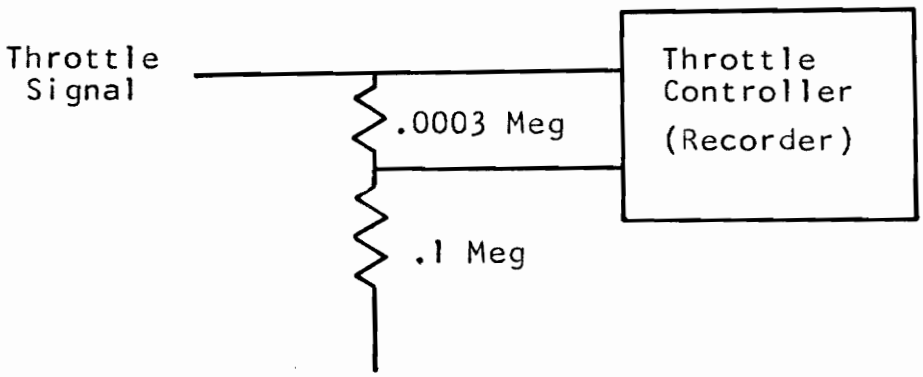

Figure 23 - Schematic Diagram of the Voltage Divider Used to Reduce the Input Signal to the Throttle Controller

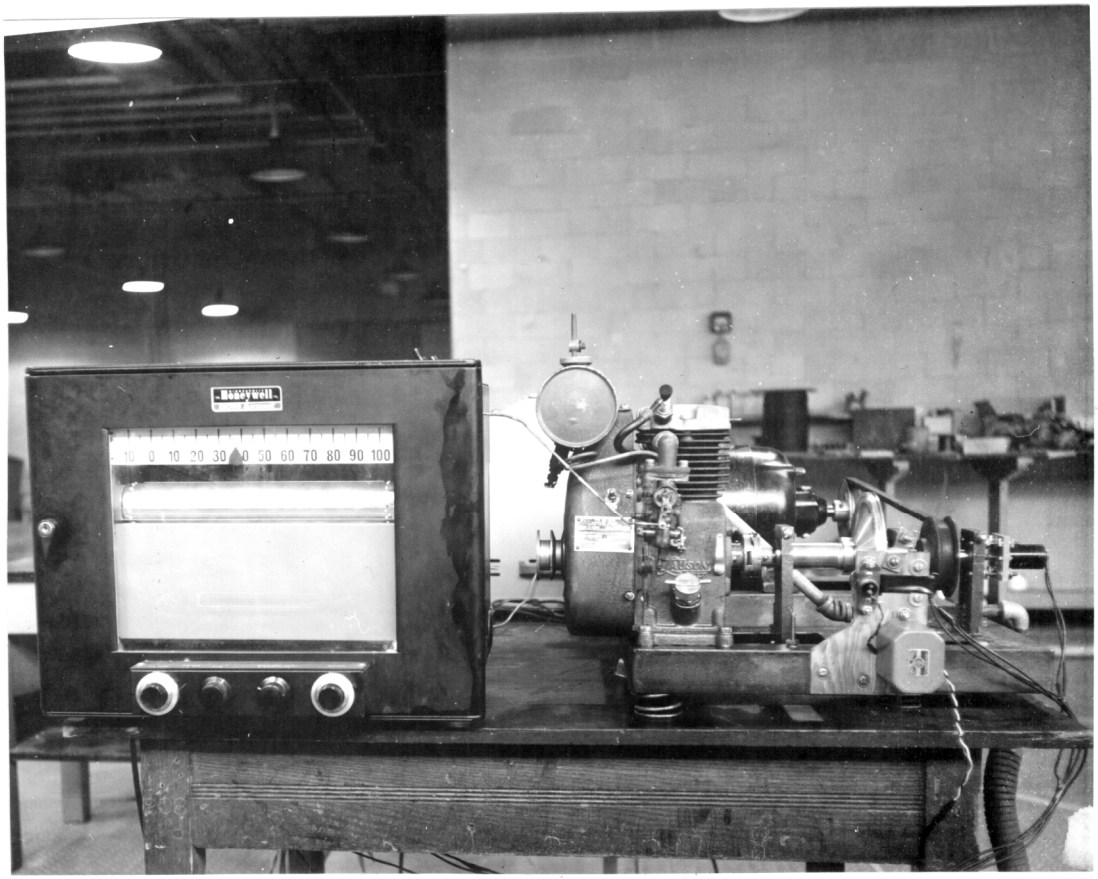

Figure 24 - Photograph of the Throttle Controller Connected to the Engine

Load Control

The engine was loaded by a 0.5 KW D. C. generator which was driven by means of a V-belt arrangement. The load was controlled by a rheostat in the field circuit, and by a switch in the load circuit. (Figure 25)

Speed Measurement

A tachometer generator was used to obtain a D. C. voltage which was proportional to the engine speed. The tachometer was mounted on the load end of the torque sensor shaft. (Figure 21) The tachometer generator was calibrated against a Strobotac type 631-B tachometer. It was found that the tachometer generator output was 7 volts per 1000 rpm.

Determination of System Characteristics

The system characteristics were determined so that the system could be simulated by the electric analog computer.

The no load speed characteristics of the engine were obtained by opening the load switch of the generator and reducing the field voltage to its lowest value, then giving various steady voltage signals to the throttle control

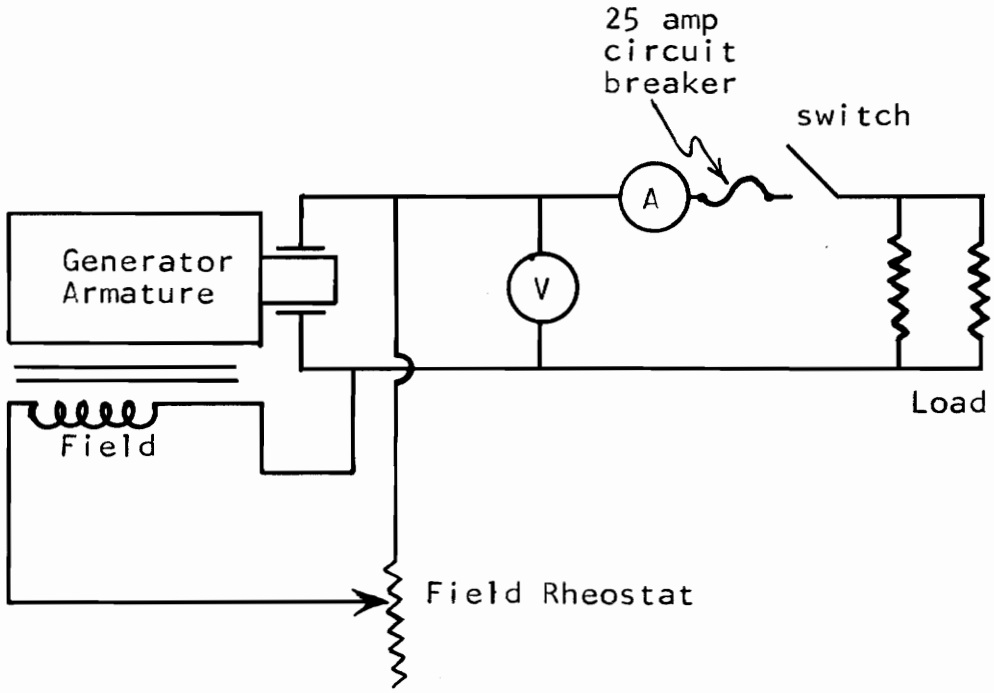

Figure 25 - Schematic Diagram of the Load Control Circuit

mechanism and recording the resulting steady state engine speeds. Figure 26 shows the steady state no load engine speed corresponding to various throttle signals.

The steady state torque sensor output values were obtained by applying a constant throttle signal to the engine and varying the load on the engine. Figure 27 shows the steady state torque sensor output as a function of engine speed and throttle signal.

The effects of inertia on changes in engine speed were determined in two ways. The engine was allowed to run at a steady speed under no load, and the throttle was suddenly opened. A cathode-ray oscilloscope was connected to the system in such a way that it would start its sweep at the same time that the throttle was opened. The speed signal was fed to the vertical deflection of the oscilloscope and a time exposure photograph was taken of the oscilloscope face. This procedure was repeated for several different initial and final speeds, and the results measured from the photographs. Figure 28 shows the no load speed changes of the engine resulting from sudden increases in throttle setting. A similar set of curves was obtained by the same procedure, but using a sudden reduction in load rather than a sudden increase in throttle setting. Figure 29 shows the constant throttle speed changes of the engine resulting from sudden decreases in load.

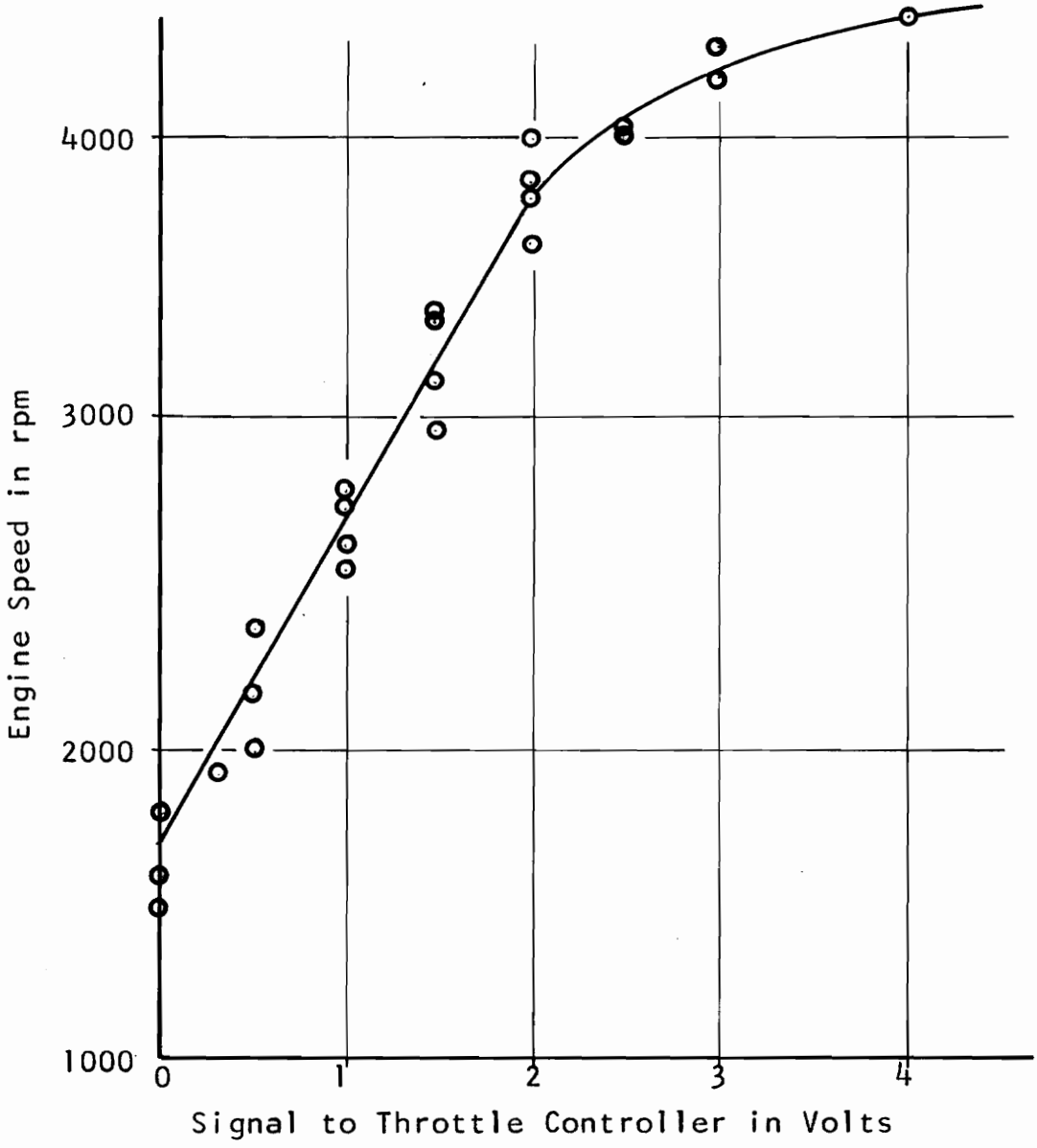

Figure 26 - Steady State No Load Engine Speed as a Function of Throttle Input Signal

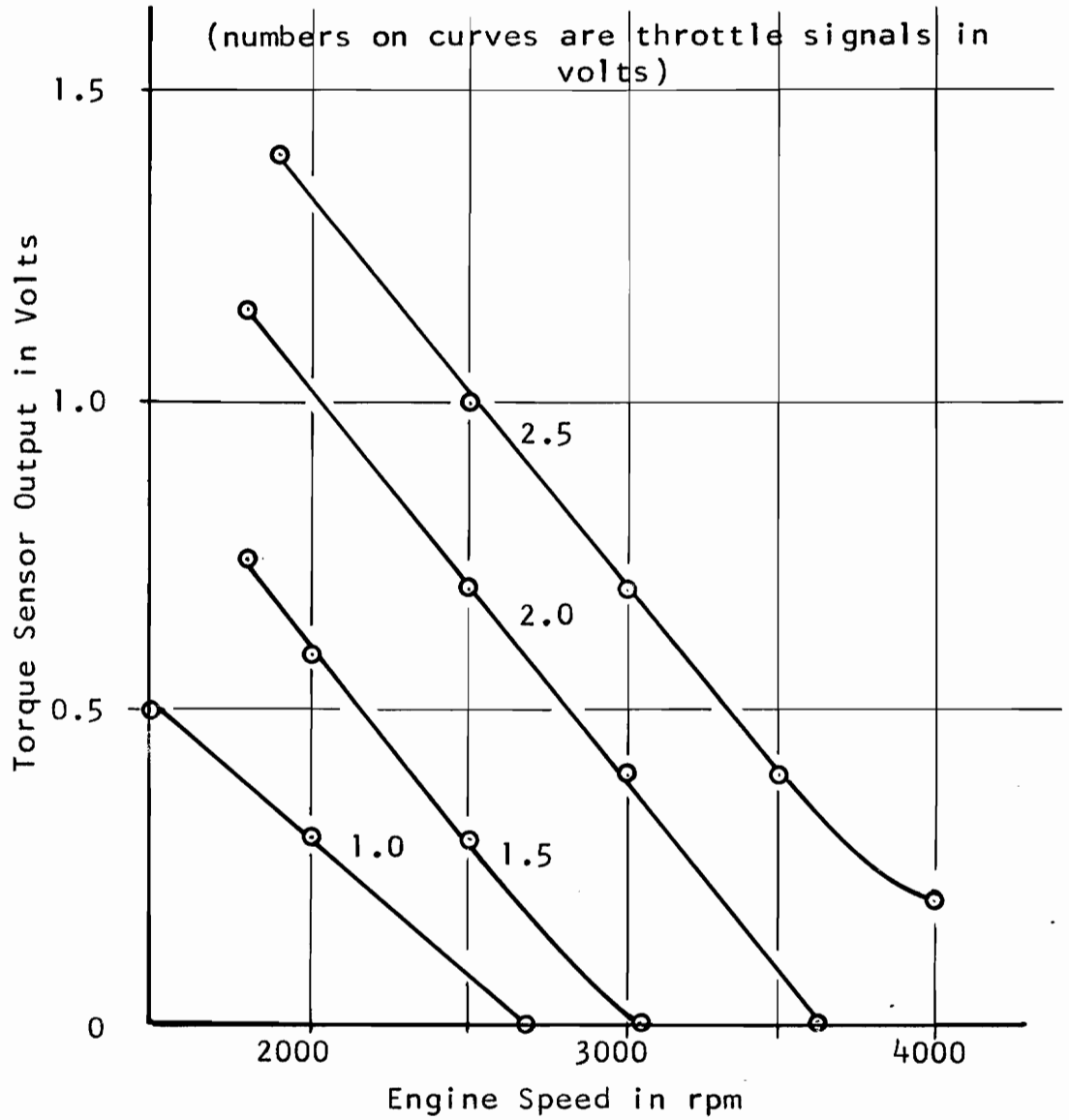

Figure 27 - Steady State Torque Sensor Output as a Function of Engine Speed for Various Constant Throttle Signals

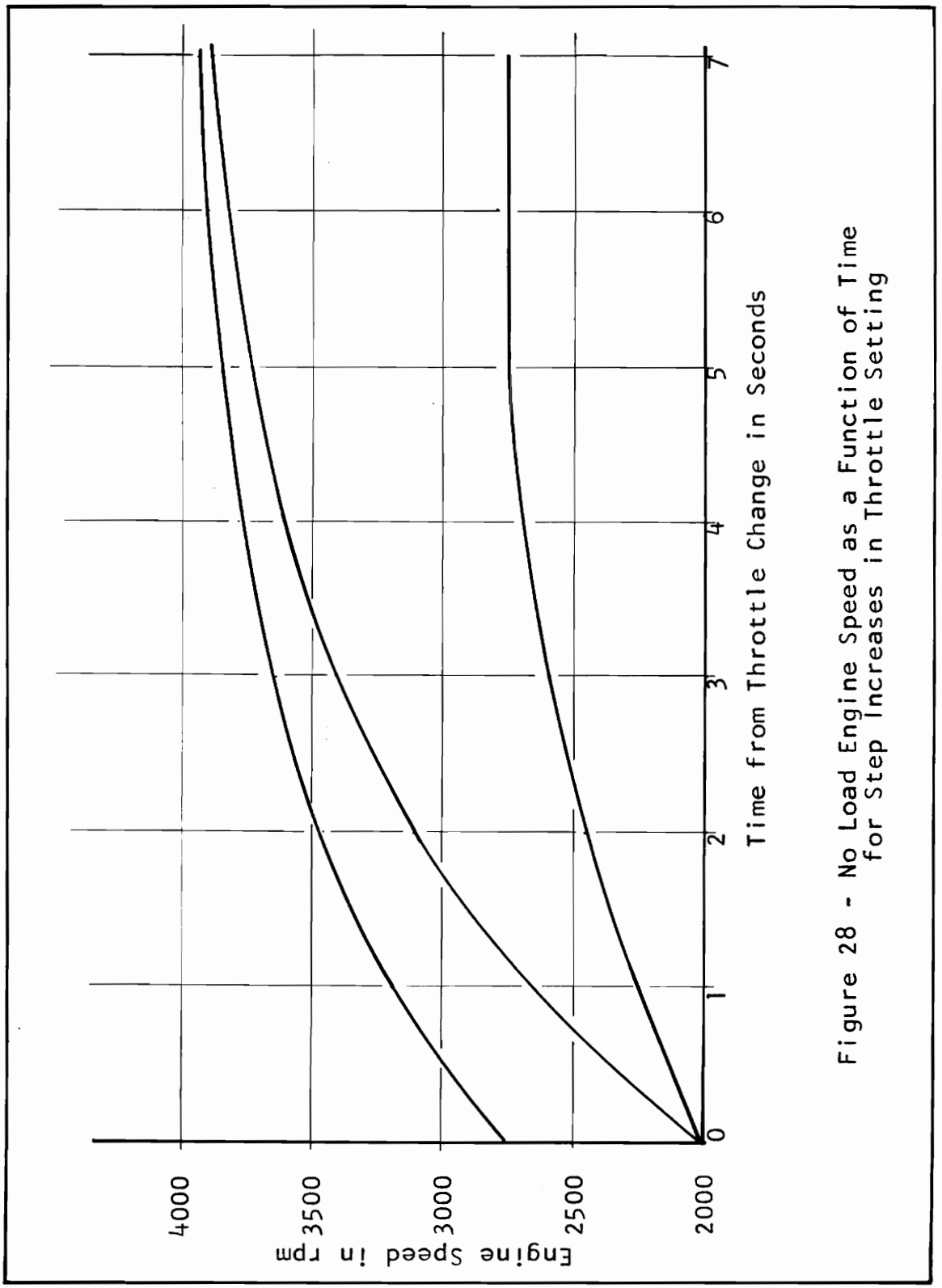

Figure 28 - No Load Engine Speed as a Function of Time for Step Increases in Throttle Setting

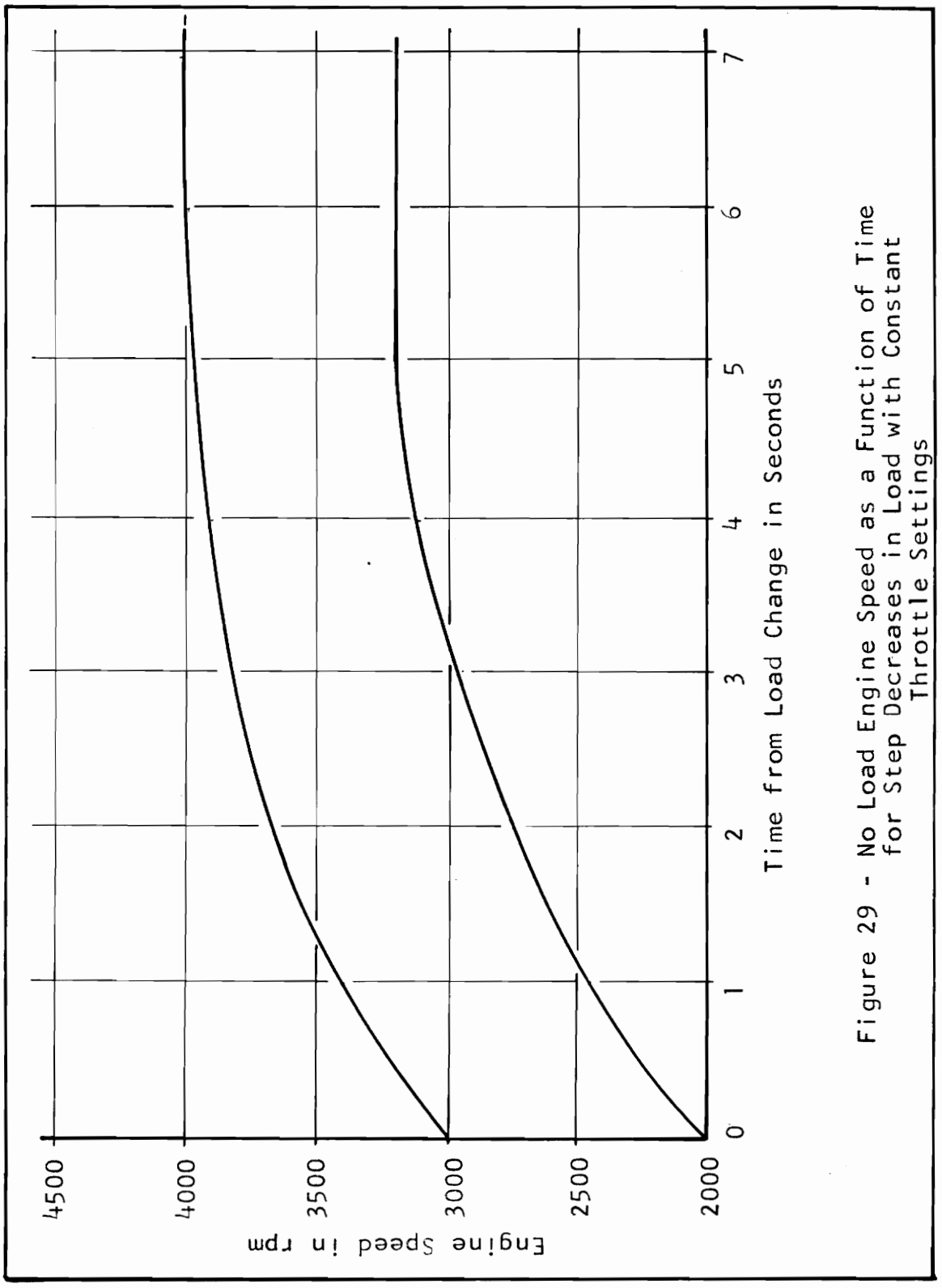

Figure 29 - No Load Engine Speed as a Function of Time for Step Decreases in Load with Constant Throttle Settings

In order to obtain the effects of inertia on the torque sensor output the engine was operated at 2000 rpm, and the throttle suddenly opened to 2 volts. The speed variation was recorded by means of a camera and oscilloscope as before. The same operation was repeated and the torque sensor output was recorded by photographing the oscilloscope. Figure 30 shows the speed change and torque sensor output as found by the above procedure. The acceleration of the engine at various times in Figure 30 was determined by measuring the slope of the speed curve. The torque sensor output at these same times was read from Figure 30, and a curve of dynamic torque sensor output was plotted as a function of engine acceleration. (Figure 31) Since the speed and throttle setting were known at every point on the curve in Figure 31, the static torque sensor output was found experimentally as a function of the engine acceleration for the given conditions of Figure 31. The difference between the static and dynamic torque sensor outputs was the decrease in torque sensor output due to engine acceleration. Figure 32 is a graph of decrease in torque sensor output due to engine acceleration as a function of engine acceleration.

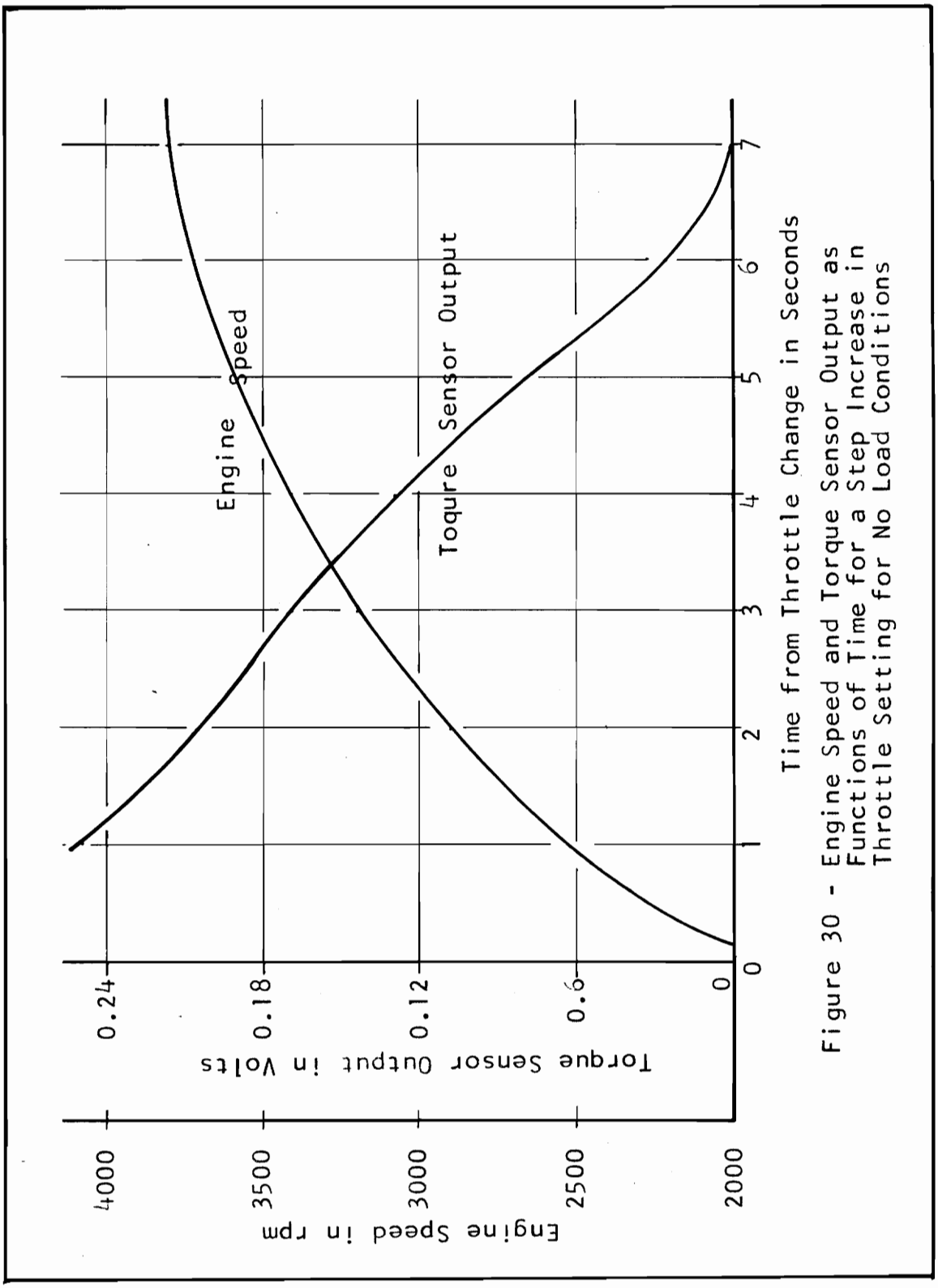

Figure 30 - Engine Speed and Torque Sensor Output as Functions of Time for a Step Increase in Throttle Setting for No Load Conditions

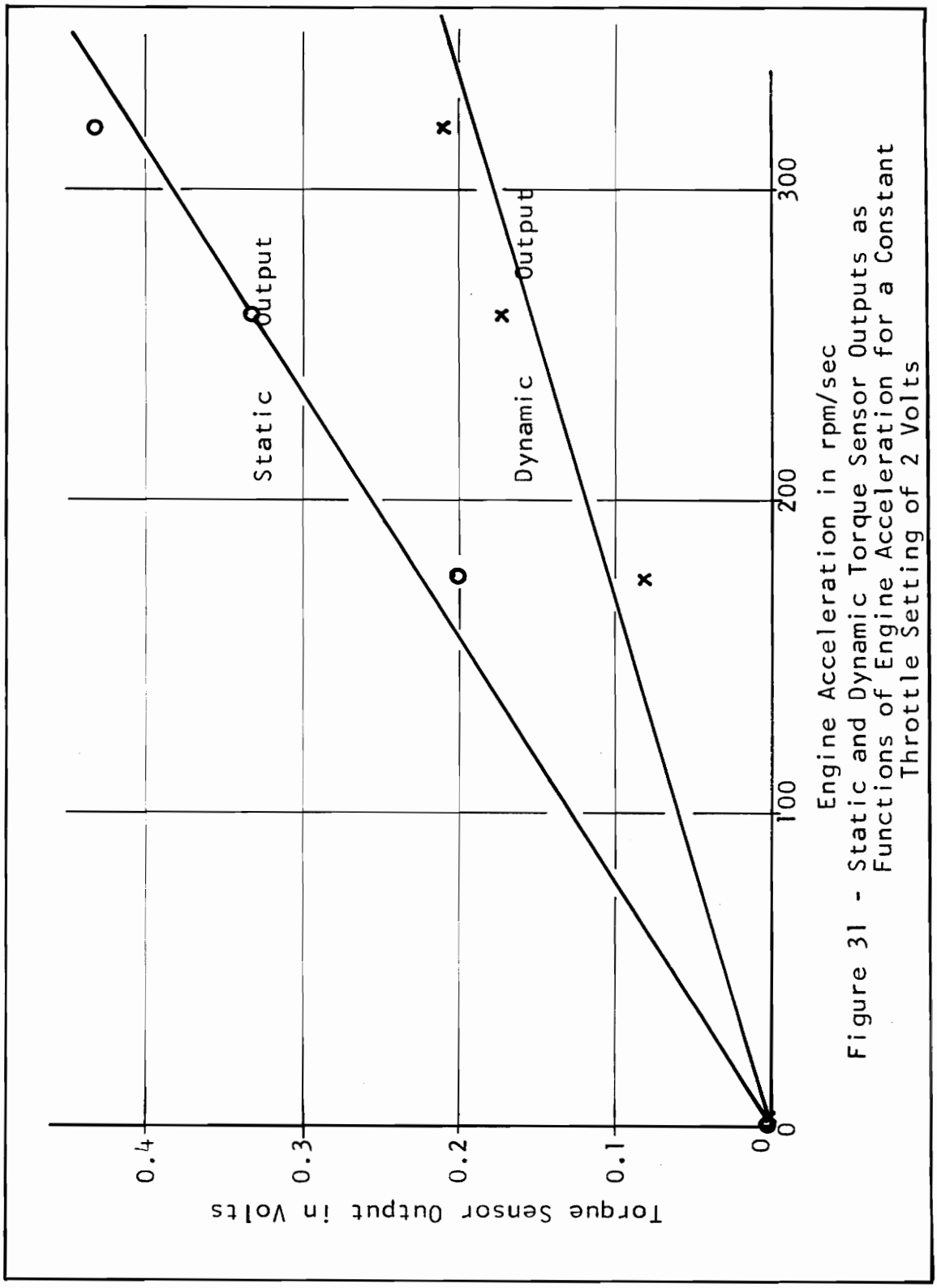

Figure 31 - Static and Dynamic Torque Sensor Outputs as Functions of Engine Acceleration for a Constant Throttle Setting of 2 Volts

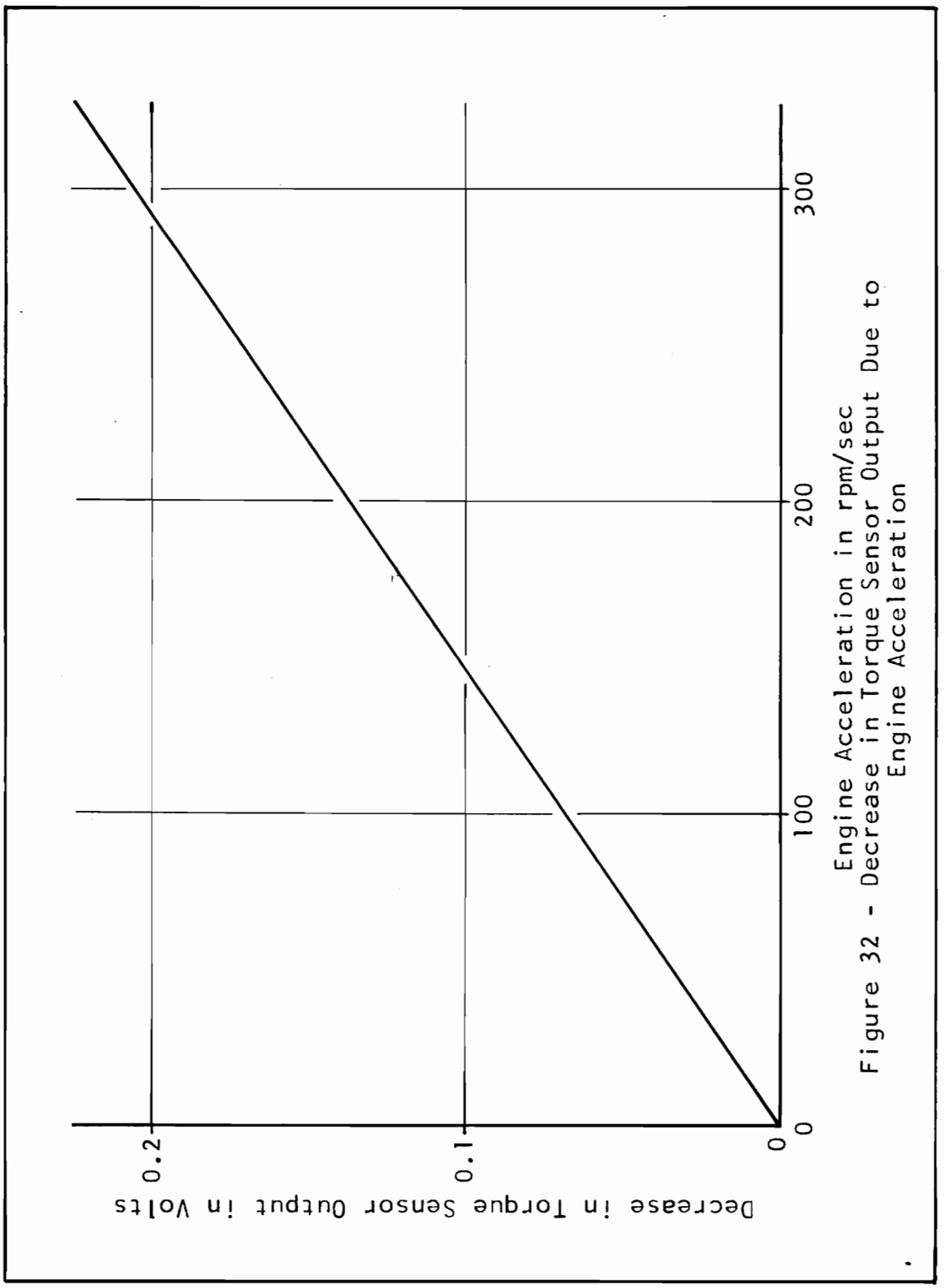

Figure 32 - Decrease in Torque Sensor Output Due to Engine Acceleration

Computer Simulator Circuits

In order to simulate the system with an analog computer, the system characteristics were reduced to equations which could be used on the computer. The system was simulated in real time, and the scale was ten volts equals one unit.

The curve of no load engine speed as a function of the throttle signal was approximated by a straight line having the equation

$$N_{nl} \times 10^{-3} = 1.7 + 1.05V$$

where N_{nl} was the no load engine speed in rpm corresponding to the throttle signal V. The throttle signal was limited to values between 0 and 2.5 real volts.

In order to obtain an equation for the effect of inertia on changes in engine speed, the analog computer was used as a curve fitting device. The curves of Figure 28 were drawn on the face of an oscilloscope and a circuit was set up on the computer and varied until the computer output matched the given curves for the same input conditions. The equation found was

$$N = 0.451 \int (N_{nl} - N)dt$$

where N was the engine speed at any time t.

The preceding two engine speed equations were combined to obtain an equation for the engine speed at any time as a function of the throttle signal. The resulting equation was

$$N \times 10^{-3} = 0.451 \int [1.7 + 1.05V - N \times 10^{-3}]dt.$$

The computer circuit which was used to simulate this equation is shown in Figure 33.

The steady state torque sensor output curves of Figure 27 were approximated by a series of straight lines having the equation

$$T.\ S. = (3.625 - N \times 10^{-3})\ (0.627) + 0.73(V - 2)$$

where T. S. was the steady state torque sensor output.

The curve of decrease in torque sensor output due to engine acceleration (Figure 32) was approximated by a straight line having the equation

$$Ta = 0.685\ (\propto \times 10^{-3})$$

where Ta was the decrease in torque sensor output due to engine acceleration, and $\propto$ was the engine acceleration in rpm/sec.

The equation of torque sensor output at any time was obtained by combining the above two equations. The resulting equation was

NOTE - 1volt =.1 unit

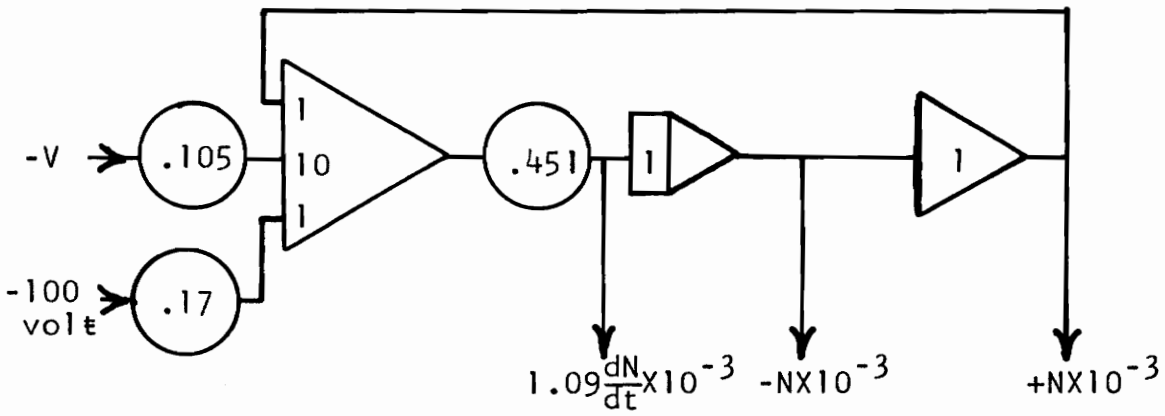

Figure 33 - Schematic Diagram of the Computer Circuit Which Simulates the Engine

$$T = 0.627(3.625 - N \times 10^{-3}) + 0.73(V-2) - 0.685(\alpha \times 10^{-3})$$

where T was the torque sensor output at any time. The computer circuit which was used to simulate the above equation is shown in Figure 34.

The recorder which was used as the throttle control mechanism was simulated by the circuit shown in Figure 35. This circuit also includes the time delay in the engine due to the absence of an acceleration pump. This circuit was determined by using the computer as a curve fitting device in the following manner. The engine was operated at 3000 rpm, and a sine wave input throttle signal supplied to the recorder. The variations in engine speed were recorded for various frequencies of input at a given amplitude. A circuit was then placed on the computer to simulate the recorder and connected to the simulated engine. A sine wave input of the same amplitude as before was given to the simulated recorder and the circuit parameters were varied until the output of the simulated engine matched the output of the real engine for the same input frequencies.

The complete engine-torque sensor-recorder simulator circuit is shown in Figure 36. A photograph of the analog computer programmed to simulate the complete engine-torque sensor-recorder system is shown in Figure 37.

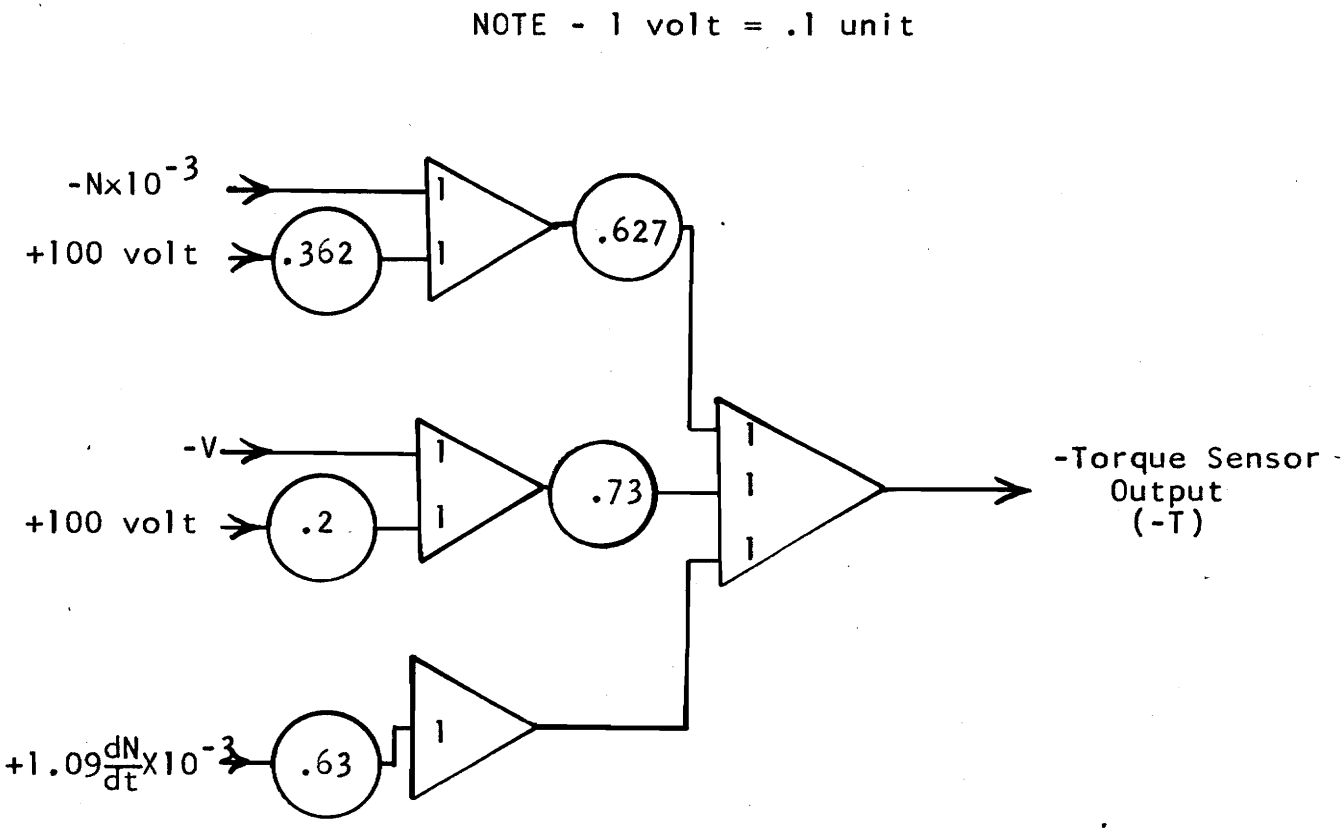

Figure 34 - Schematic Diagram of the Computer Circuit Which Simulates the Torque Sensor

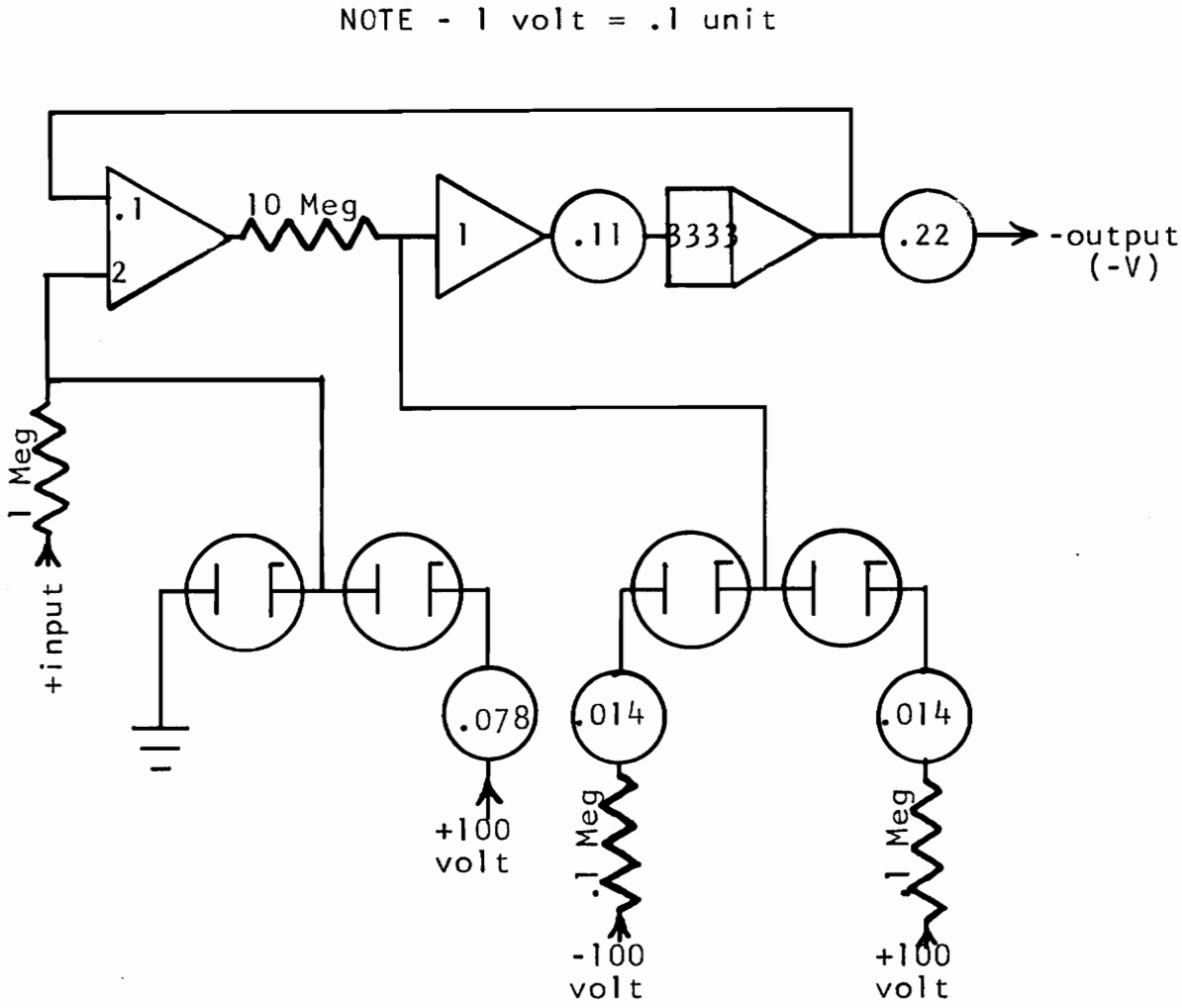

Figure 35 - Schematic Diagram of the Computer Circuit Which Simulates the Throttle Controller and the Time Delay in Engine Response to Throttle Change

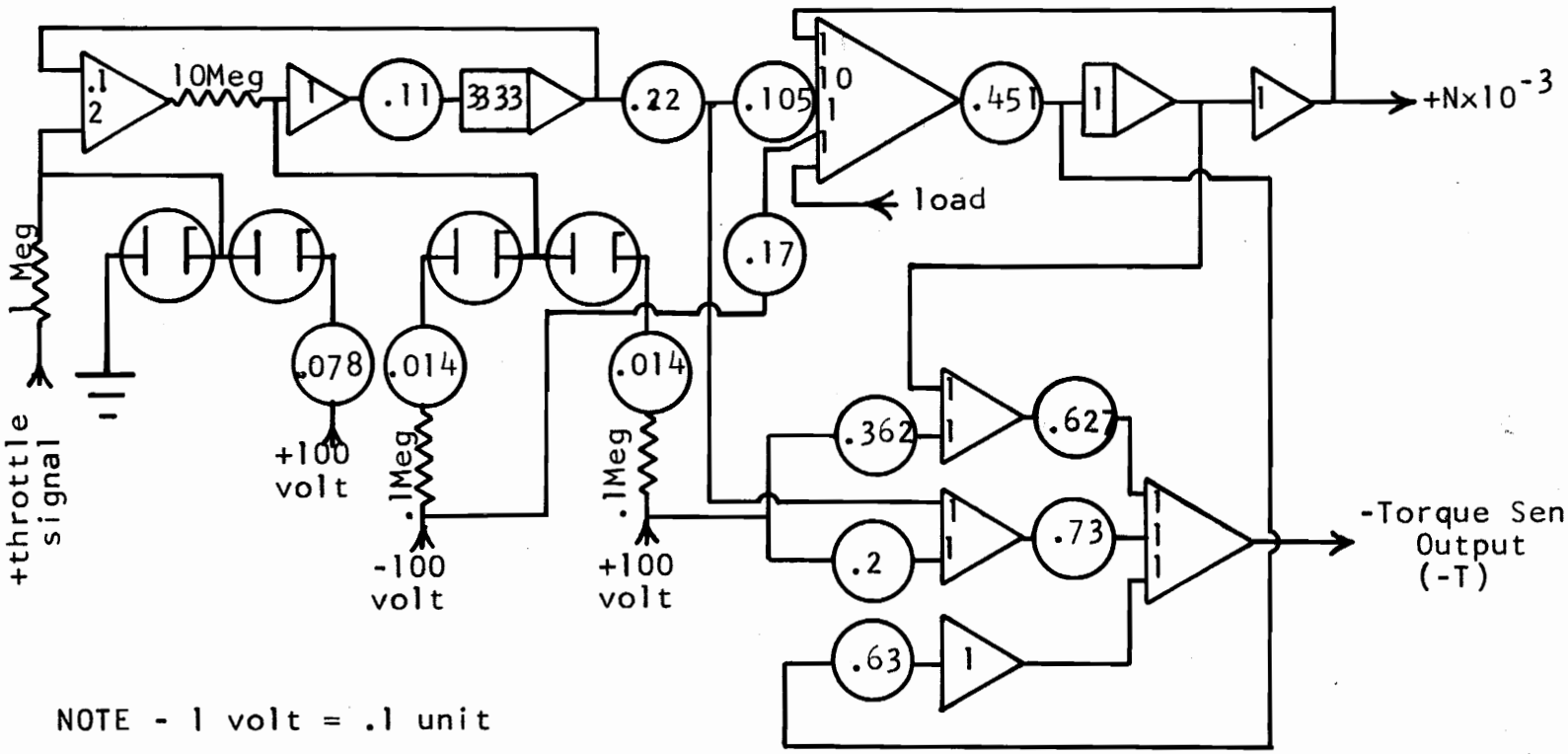

Figure 36 - Schematic Diagram of the Complete Engine-Torque Sensor-Recorder Simulator Circuit

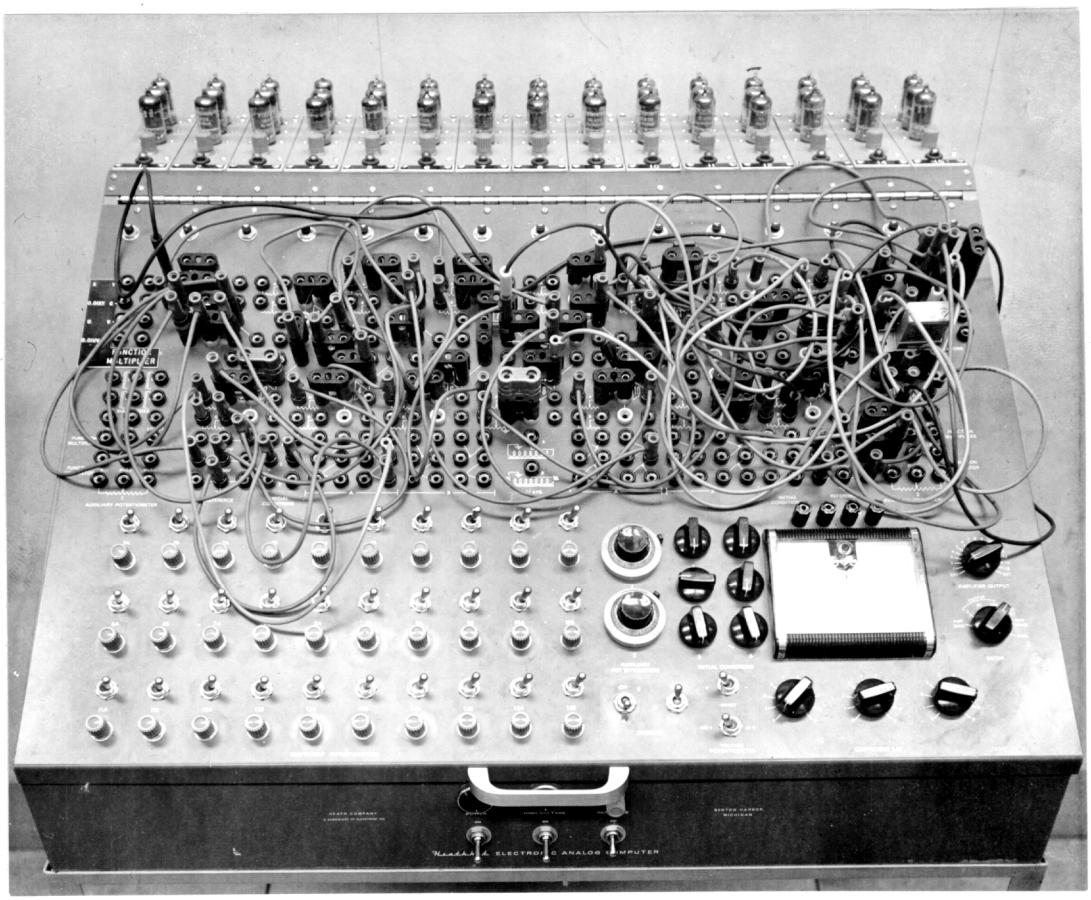

Figure 37 - Photograph of the Analog Computer with the Complete Simulator Circuit and Torque Sensing Governor Plugged in

Torque Sensing Governor Circuit for the Simulated System

The transfer function of the torque sensing governor was designed to be

$$M = k_t T + k_c E + \frac{1}{T_i} \int E dt$$

where k_t was the torque sensor sensitivity. Written in terms of engine speed, set point, and throttle signal, the equation was

$$V = k_t T + k_c (R - N) + \frac{1}{T_i} \int (R - N) dt$$

where R was the set point in revolutions per minute.

The computer circuit which was used to simulate this equation is shown in Figure 38. This circuit was used as a torque sensing governor for the simulated system.

The optimum values of k_t, k_c, and $\frac{1}{T_i}$ were determined by a systematic trial method. The values of k_t, k_c, and $\frac{1}{T_i}$ were set as nearly as possible to zero and the value of k_t was increased slightly. A step increase in load was applied to the engine, and after equilibrium had been reached a step decrease in load was applied. The above procedure was repeated, increasing k_t slightly before each load increase, until the system began to become unstable. The value of k_t was then decreased slightly. The value of k_c was found in the same manner, but small adjustments were

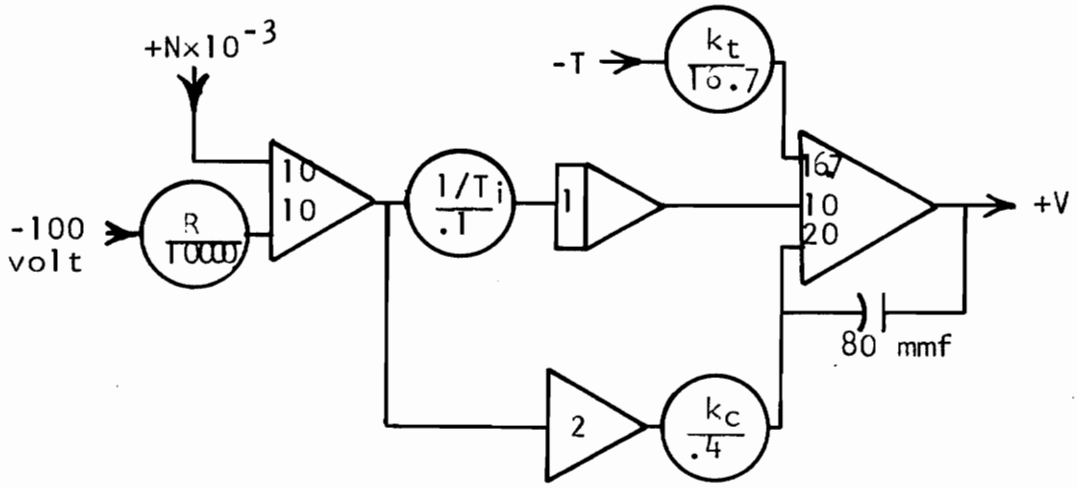

NOTE - 1 volt = .1 unit

Figure 38 - Schematic Diagram of the Torque Sensing Governor Circuit Used with the Simulated System

made in k_t during the process. The process was again repeated in order to find the optimum value of $\frac{1}{T_i}$, and the values of k_t and k_c had to be slightly altered during the process to maintain optimum conditions. The optimum values of k_t, k_c, and $\frac{1}{T_i}$ are listed in the Results.

Proportional-Integral-Derivative Governor Circuit for the Simulated System

The transfer function of the proportional-integral-derivative governor was

$$V = k_c(R - N) + \frac{1}{T_i}\int (R - N)dt + T_d \frac{d(R - N)}{dt} .$$

The computer circuit which was used to simulate this equation is shown in Figure 39. This circuit was used to govern the simulated system, and optimum values of k_c, $\frac{1}{T_i}$, and T_d were found by the same process which was used to find the optimum values of k_t, k_c, and $\frac{1}{T_i}$ for the torque sensing governor. The optimum values of k_c, $\frac{1}{T_i}$, and T_d are listed in the Results.

Control Response of the Simulated System

To obtain a comparison of the two governors as applied to the simulated system, a step change in load was applied to the simulated engine in the same manner for each

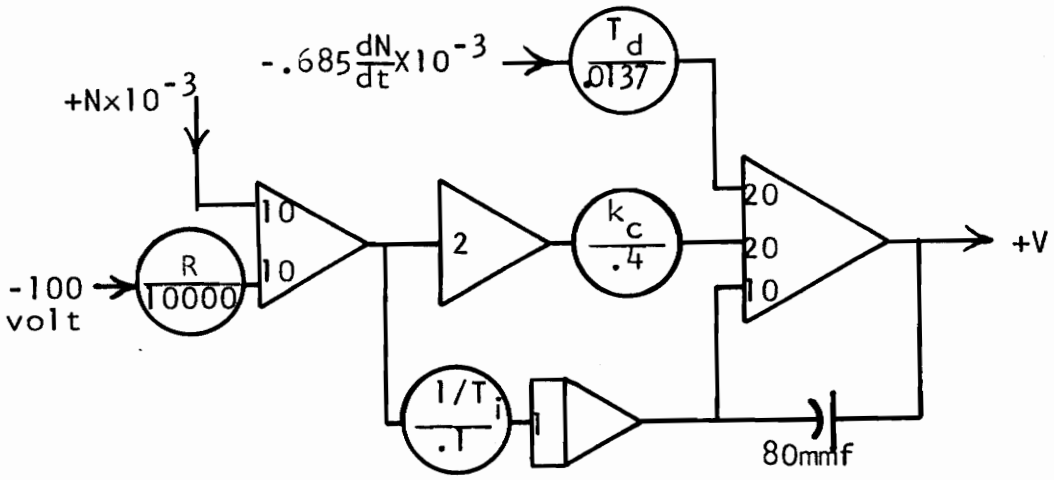

NOTE - 1volt = .1 unit

Figure 39 - Schematic Diagram of the Proportional-Integral-Derivative Governor Circuit Used with the Simulated System

governor, and the resulting speed changes recorded. The control responses of the simulated systems are presented in the Data and Results section of this thesis.

Torque Sensing Governor Circuit for the Real System

The transfer function used was the same as for the simulated system, that is

$$V = k_t T + k_c(R - N) + \frac{1}{T_i} \int (R - N)dt$$

The circuit which was used to simulate this equation for use with the real system is shown in Figure 40. The values of k_t, k_c, and $\frac{1}{T_i}$ were initially set to the optimum values indicated by the simulated system, then the system was optimized by making small changes in k_t, k_c, and $\frac{1}{T_i}$. The optimum values of k_t, k_c, and $\frac{1}{T_i}$ are listed in the Results.

Proportional-Integral-Derivative Governor Circuit for the Real System

The transfer function used was the same as for the simulated system.

$$V = k_c (R - N) + \frac{1}{T_i} \int (R - N)dt + T_d \frac{d(R - N)}{dt}$$

The computer circuit which was used to simulate this equation is shown in Figure 41. It was necessary to use a

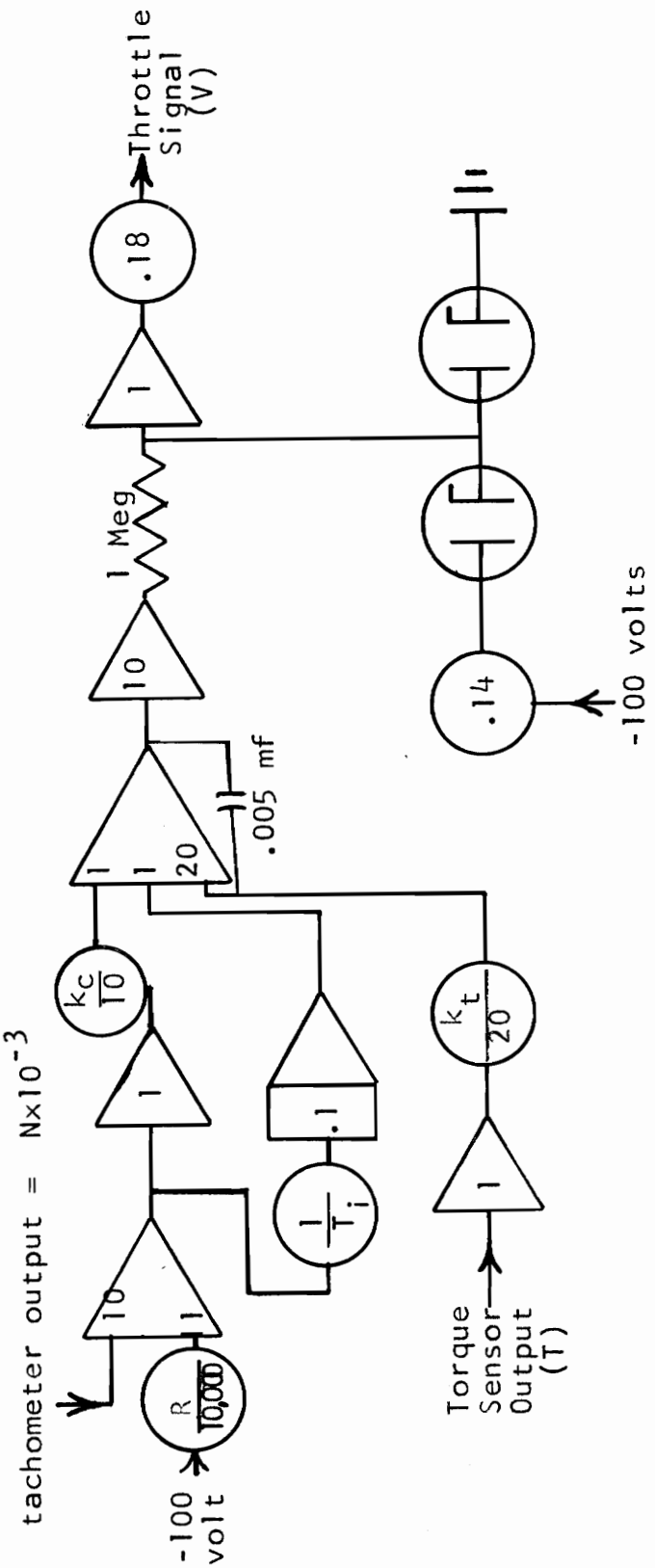

NOTE - 1 volt = 1 unit

Figure 40 - Schematic Diagram of the Torque Sensing Governor Circuit Used with the Real System

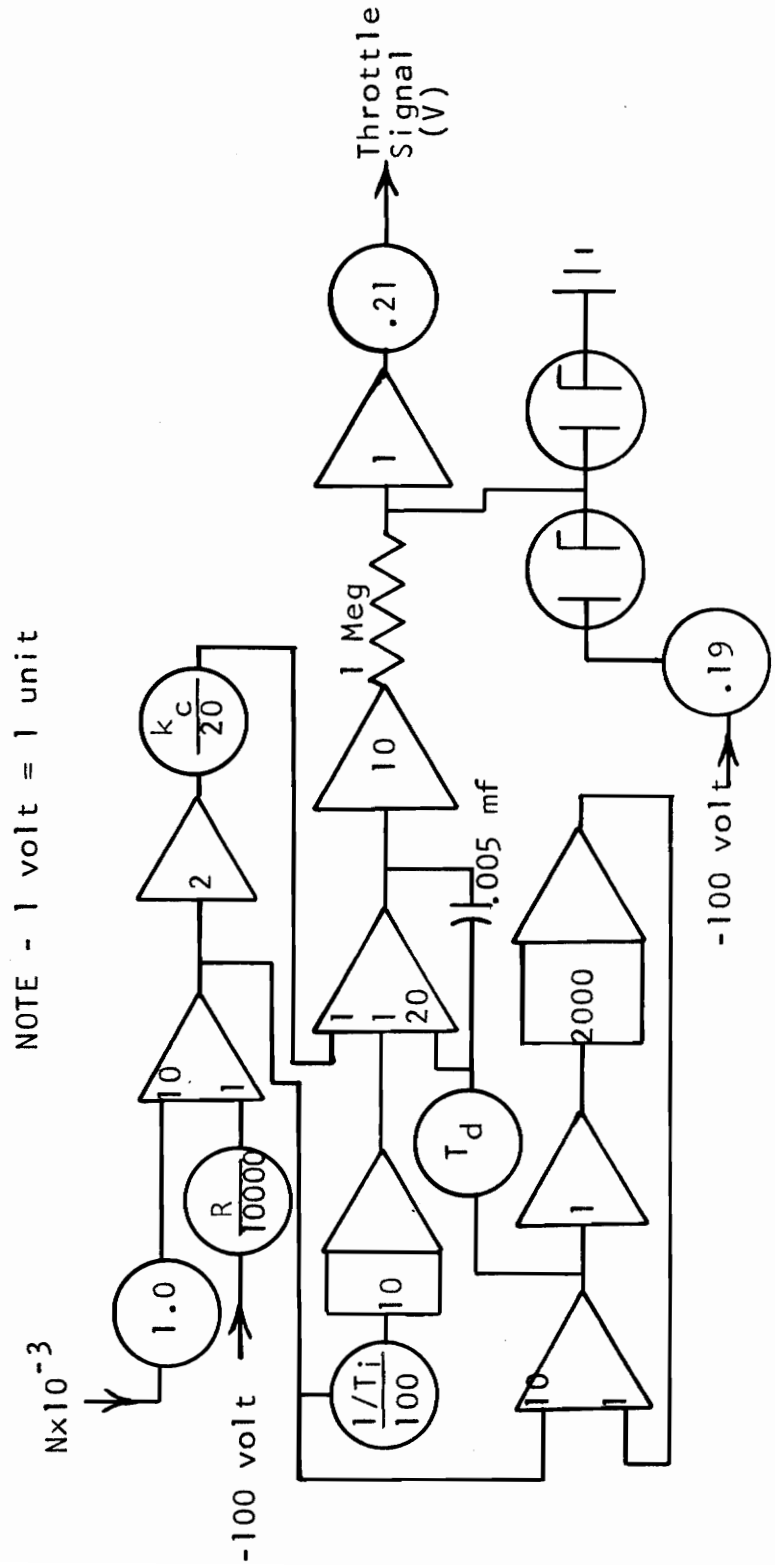

Figure 41 - Schematic Diagram of the Proportional-Integral-Derivative Governor Circuit Used with the Real System

derivative circuit for the real system because the derivative of R − N with respect to time was not available from the system itself. The optimum values of k_c, $\frac{1}{T_i}$, and T_d were found in the same manner as the optimum parameters of the torque sensing governor. These optimum values are listed in the Results.

Control Response of the Real System

For purposes of comparison a step change in load was applied to the system in the same manner for each governor, and the resulting speed changes recorded. The control responses of the real system are presented in the Data and Results section of this thesis.

Open-loop frequency response characteristics were determined for each system so that Nyquist plots could be made for each system. The loop was opened between the throttle signal and the throttle control mechanism. (Figure 42) A sine wave input signal was given to the throttle control mechanism by means of the variable frequency sine wave generator circuit shown in Figure 43. The input signal to the throttle control mechanism and the output throttle signal from the governor circuit were both fed to a dual channel oscilloscope so that the output signal resulting from a given input signal could be photographed.

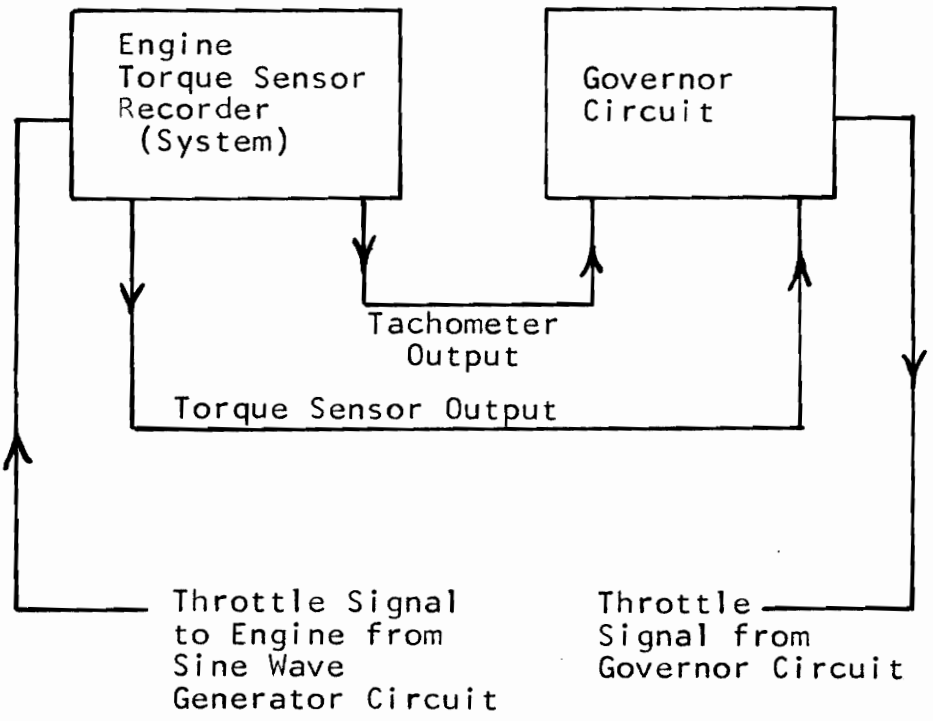

Figure 42 - Block Diagram of the Open Loop Real System

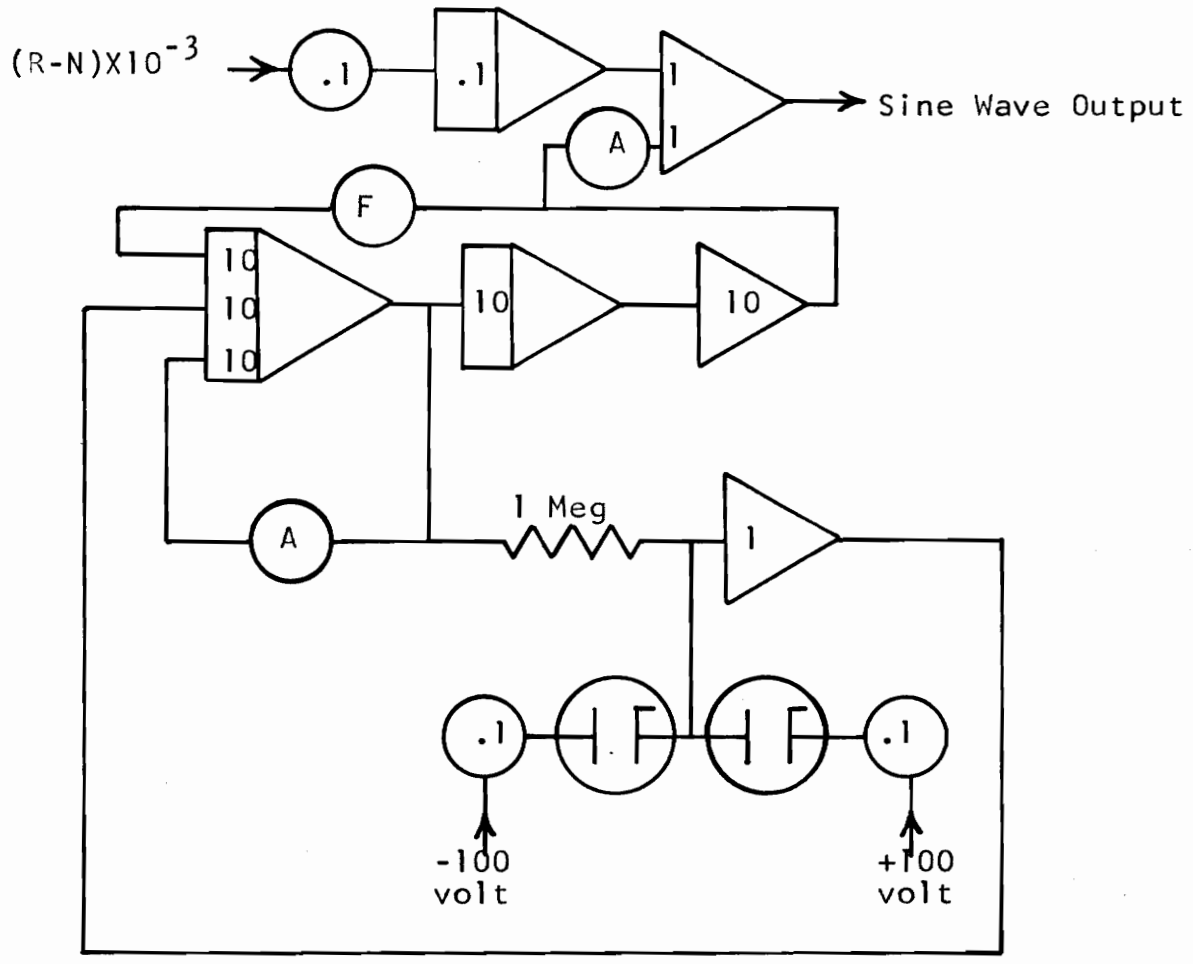

NOTE - The amplitude is determined by A.
The frequency is determined by F.

Figure 43 - Schematic Diagram of the Variable Frequency Sine Wave Generator Circuit Used in the Frequency Response Analysis of the Real System

The magnitude ratio and phase lag for different frequencies were obtained by measuring the amplitudes and phase differences from the photographs, then calculating the desired quantities. (Appendix B) The values obtained from these photographs are given in the Data. The Nyquist plots resulting from the frequency response characteristics are shown in the Data and Results section of this thesis.

List of Equipment

1. Tachometer Generator built by Servo-Tek Products Co., Inc., Hawthorne, New Jersey, Model No. SB-740A-2, flange mounting, 8.5 gm-cm^2 inertia, 7 volts/1000 rpm, maximum speed of 12,000 rpm. Used to measure engine speed.

2. Internal Combustion Engine built by the Lauson Company, New Holstein, Wisconsin, Model RLA2091, single cylinder, 1/2 hp at 2100 rpm, serial no. 3A1522. This engine was governed by the computer circuit.

3. Recorder built by Minneapolis-Honeywell Reg. Co., Brown Instruments Div., Philadelphia, Pa., Model No. Y153X17(VA)-X-30DNG, Serial No. 830845, range 0-1 to 0-51 MV, 115V, 60 cycle. This recorder was used as a servo to position the throttle linkage.

4. D. C. Generator built by General Electric Co., Schenectady, N. Y., Model No. 32646, type SD, 18V, 0.5 KW, 27.8 AMP, 1725 rpm, shunt wound, self excited. Used to load the engine.

5. Analog Computer. Heath Co., Group C analog computer consisting of 15 D. C. operational amplifiers each having a gain of approximately 50,000.

6. Oscilloscope built by Hewlett Packard Co., Palo Alto, Calif., Model 122AR, dual channel.

7. Oscillograph-Record Camera built by Allen B. DuMont Laboratories, Inc., Clifton, N. J., type 297. This camera was used to photograph the oscilloscope face.

8. X-Y Recorder built by Houston Instrument Corp., Houston, Texas, Model HR-95. This recorder was used to record engine speed as a function of time.

IV. DATA AND RESULTS

The data and results obtained during this investigation are presented in Tables 1, 2, 3, and 4, and in Figures 44, 45, 46, 47, 48, 49, 50, and 51.

The phase lags and magnitude ratios obtained from the open-loop frequency response tests on the real system are listed in Table 1 for the torque sensing governor and for the proportional-integral-derivative governor.

The speed changes resulting from a step change in load on the engine are shown graphically in Figures 44, 45, 46, 47, 48, and 49 for both the real and simulated systems using each type of governor.

The optimum control parameters for both the real and simulated systems using each type of governor are shown in Table 2.

Pertinent values which were read from Figures 44, 45, 46, 47, 48, and 49 are listed in Tables 3 and 4 for the purpose of comparison.

The Nyquist plots resulting from the open-loop frequency response tests on the real system are shown for each type of governor in Figures 50 and 51.

Table I

Open-Loop Frequency Response Data for the Real System Using Each Governor

A) Torque Sensing Governor

Phase Lag Deg	Magnitude Ratio
139	0.350
175	0.279
184	0.167
226	0.175
226	0.151
249	0.111
303	0.093
372	0.033

B) Proportional-Integral-Derivative Governor

Phase Lag Deg	Magnitude Ratio
121	1.15
155	0.119
177	0.066
201	0.025
304	

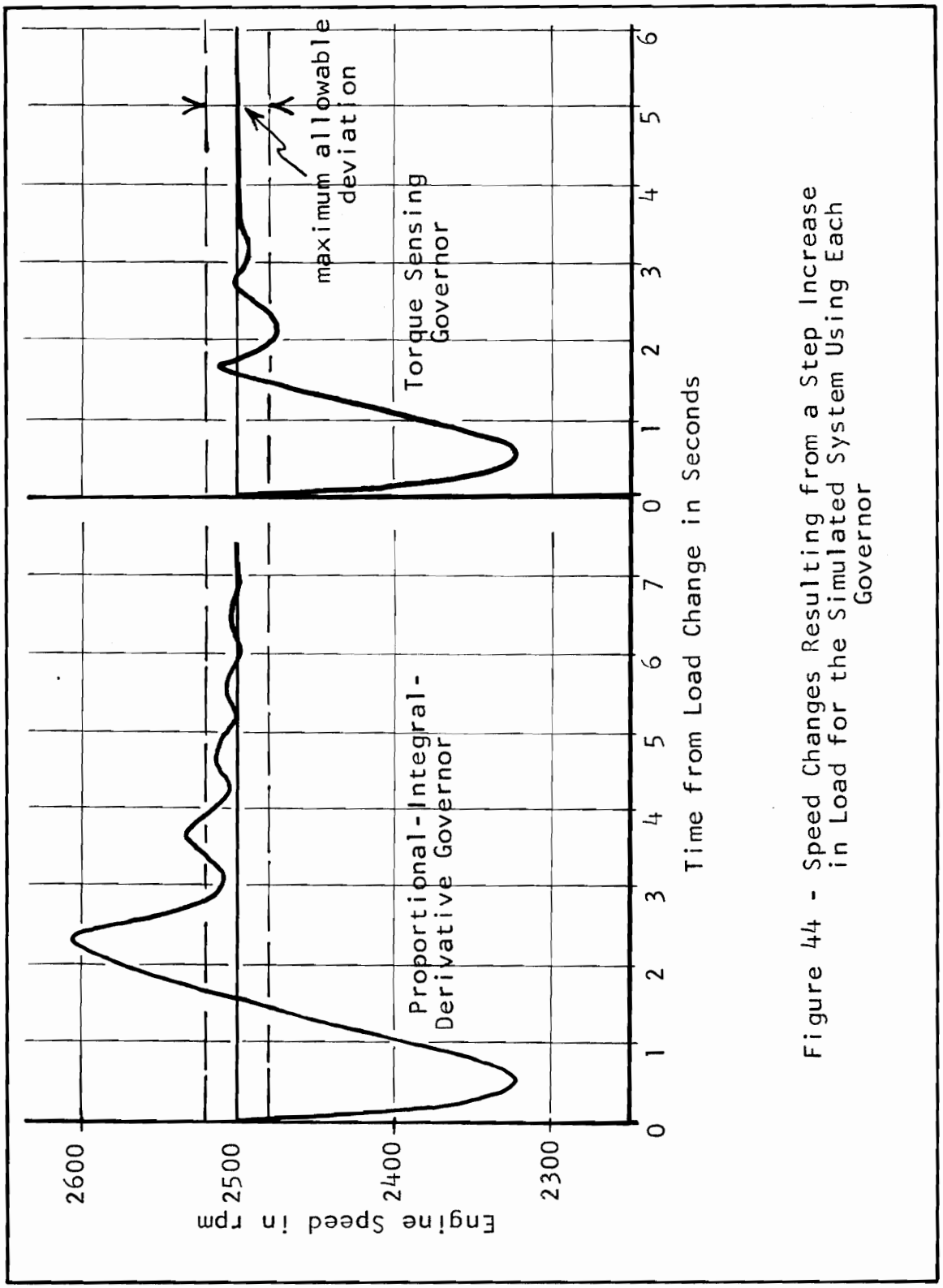

Figure 44 - Speed Changes Resulting from a Step Increase in Load for the Simulated System Using Each Governor

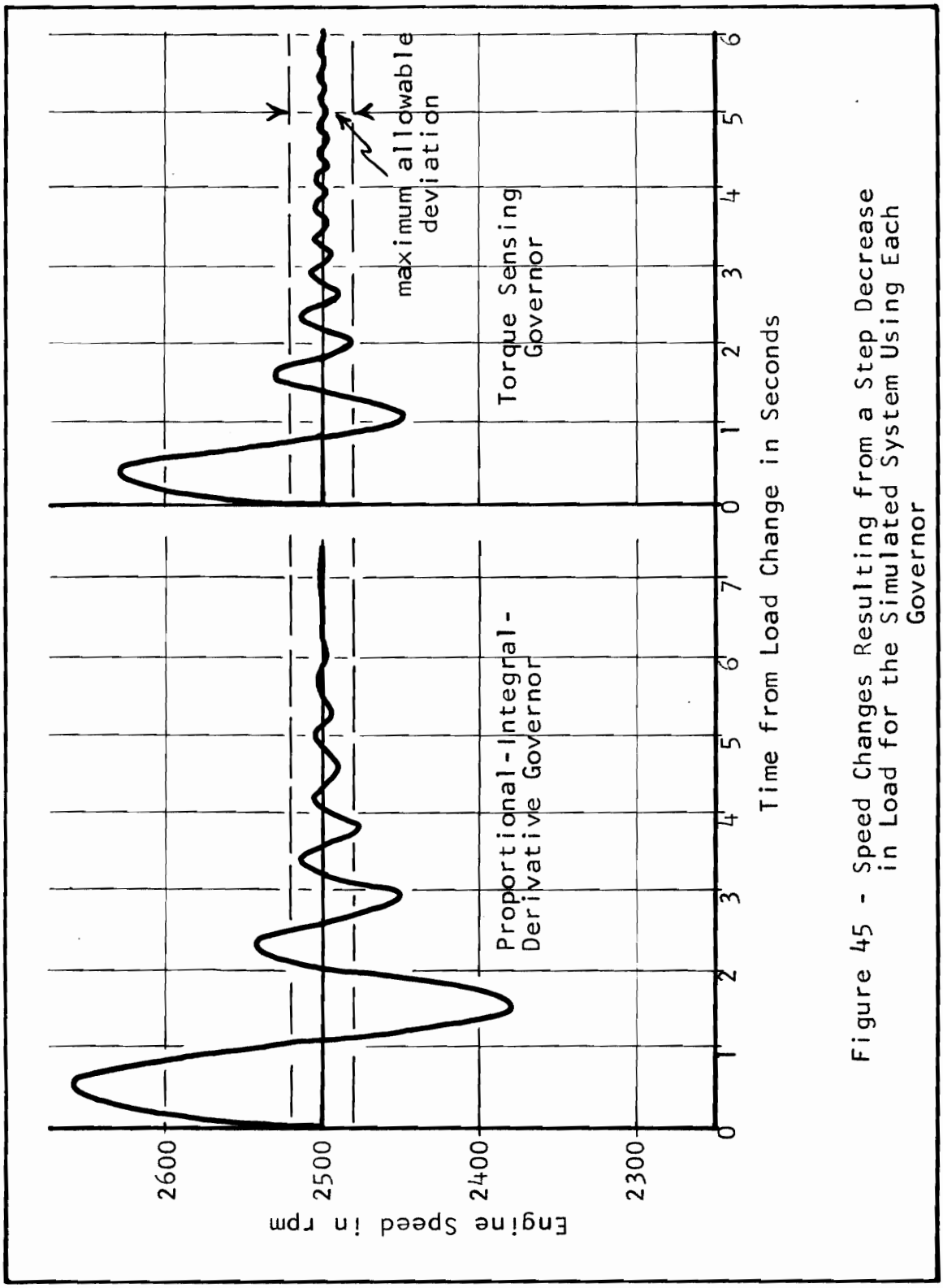

Figure 45 - Speed Changes Resulting from a Step Decrease in Load for the Simulated System Using Each Governor

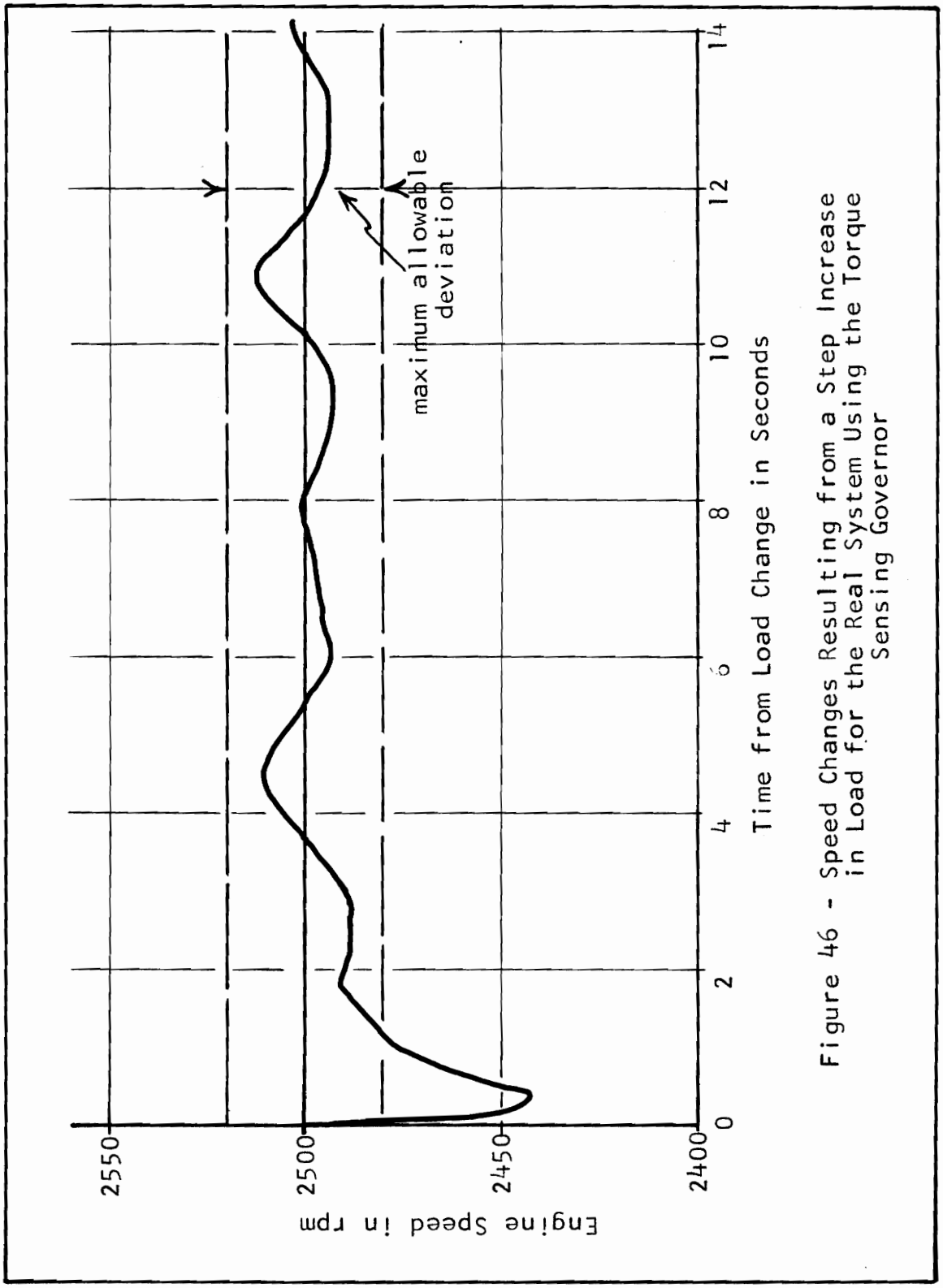

Figure 46 - Speed Changes Resulting from a Step Increase in Load for the Real System Using the Torque Sensing Governor

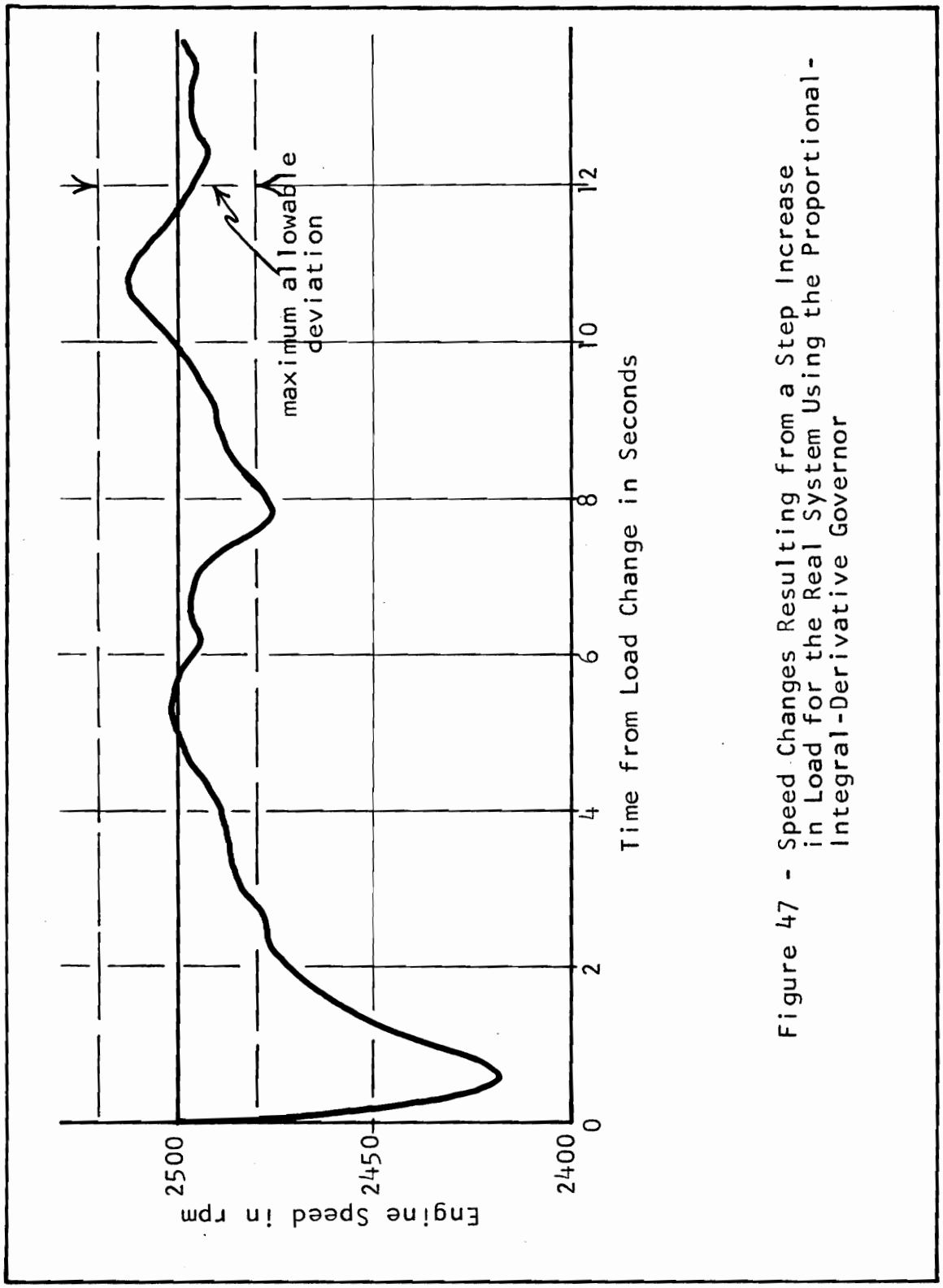

Figure 47 - Speed Changes Resulting from a Step Increase in Load for the Real System Using the Proportional-Integral-Derivative Governor

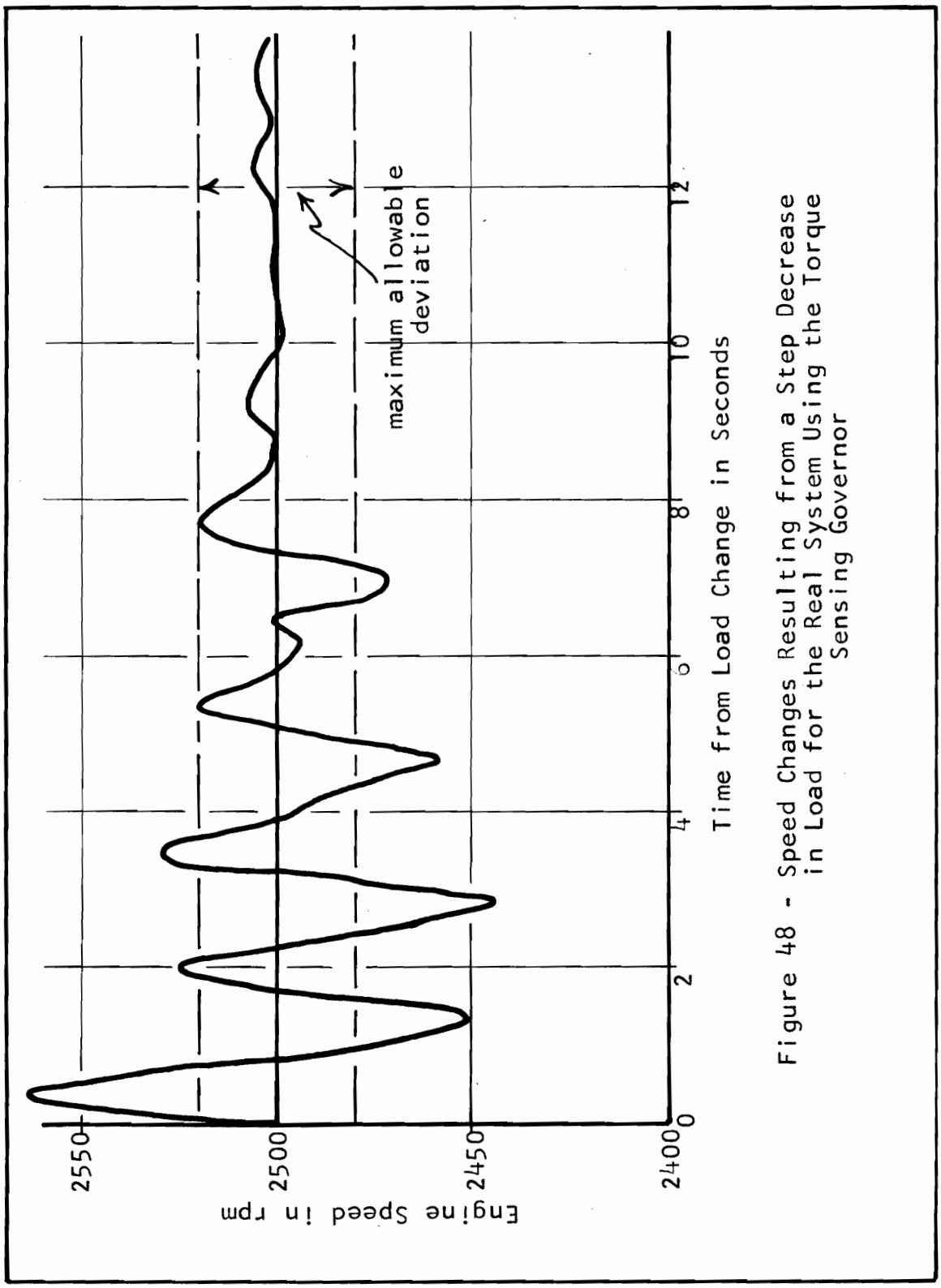

Figure 48 - Speed Changes Resulting from a Step Decrease in Load for the Real System Using the Torque Sensing Governor

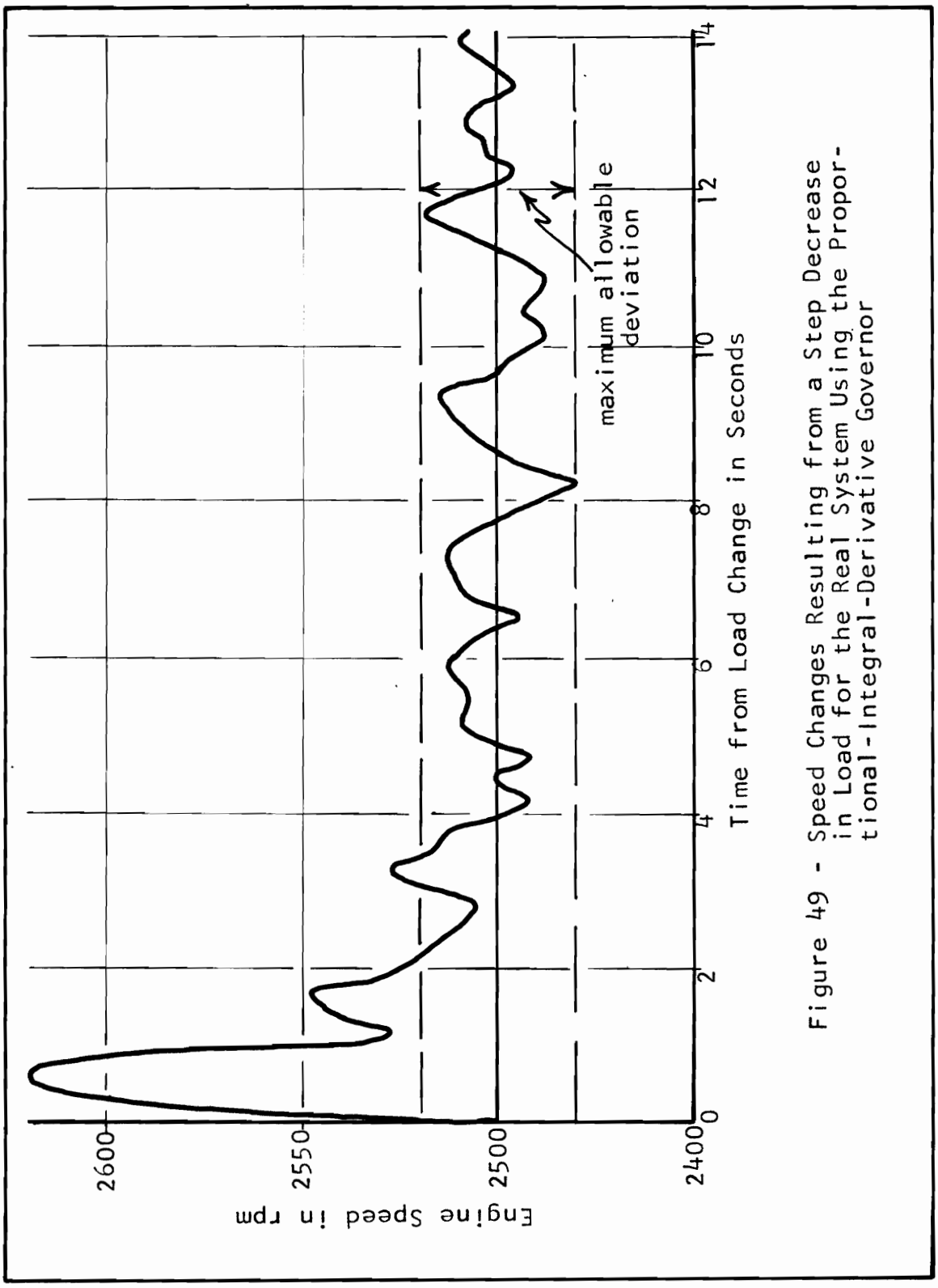

Figure 49 - Speed Changes Resulting from a Step Decrease in Load for the Real System Using the Proportional-Integral-Derivative Governor

Table 2

Optimum Control Parameters

A) Torque Sensing Governor	
Simulated System	Real System
$k_t = 1.97$ $k_c = 51 \times 10^{-3}$ $\frac{1}{T_i} = 1.45 \times 10^{-3}$	$k_t = 1.4$ $k_c = 38 \times 10^{-3}$ $\frac{1}{T_i} = 1 \times 10^{-3}$
B) Proportional-Integral-Derivative Governor	
Simulated System	Real System
$k_c = 93 \times 10^{-3}$ $\frac{1}{T_i} = 21.8 \times 10^{-3}$ $T_d = 2.8 \times 10^{-3}$	$k_c = 80 \times 10^{-3}$ $\frac{1}{T_i} = 14 \times 10^{-3}$ $T_d = 0.97 \times 10^{-3}$

Table 3

Response of the Simulated System to a Step Change in Load

	Torque Sensing Governor	Proportional-Integral-Derivative Governor
A) Step Increase in Load		
Steady State Throttle Setting Before Load Change	0.8 volt	0.8 volt
Steady State Throttle Setting After Load Change	1.8 volt	1.8 volt
Set Point	2500 rpm	2500 rpm
Maximum Speed Deviation	177 rpm	177 rpm
Stabilization Time*	2.4 sec	3.9 sec
Error-Time Value**	148 rpm-sec	214 rpm-sec
B) Step Decrease in Load		
Steady State Throttle Setting Before Load Change	1.8 volt	1.8 volt
Steady State Throttle Setting After Load Change	0.8 volt	0.8 volt
Set Point	2500 rpm	2500 rpm
Maximum Speed Deviation	130 rpm	160 rpm
Stabilization Time*	1.75 sec	3.9 sec
Error-Time Value**	76 rpm-sec	172 rpm-sec

* Time required for the speed to go within the allowable limits for the last time.
**The error-time value was obtained by measuring the area enclosed by the engine speed and maximum allowable deviation lines at the locations where the engine speed was outside of the allowable deviation lines, by means of a planimeter, and multiplying this area by the rpm per inch on the speed scale and the seconds per inch on the time scale.

Table 4

Response of the Real System to a Step Change in Load

	Torque Sensing Governor	Proportional-Integral-Derivative Governor
A) Step Increase in Load		
Steady State Throttle Setting Before Load Change	0.8 volt	0.8 volt
Steady State Throttle Setting After Load Change	1.8 volt	1.8 volt
Set Point	2500 rpm	2500 rpm
Maximum Speed Deviation	58 rpm	82 rpm
Stabilization Time*	1.1 sec	2.8 sec
Error-Time Value**	20 rpm-sec	79.2 rpm-sec
B) Step Decrease in Load		
Steady State Throttle Setting Before Load Change	1.8 volt	1.8 volt
Steady State Throttle Setting After Load Change	0.8 volt	0.8 volt
Set Point	2500 rpm	2500 rpm
Maximum Speed Deviation	64 rpm	120 rpm
Stabilization Time*	4.9 sec	3.4 sec
Error-Time Value**	63.2 rpm-sec	88 rpm-sec

* Time required for the speed to go within the allowable limits for the last time.
**The error-time value was obtained by measuring the area enclosed by the engine speed and maximum allowable deviation lines at the locations where the engine speed was outside of the allowable deviation lines, by means of a planimeter, and multiplying this area by the rpm per inch on the speed scale and the seconds per inch on the time scale.

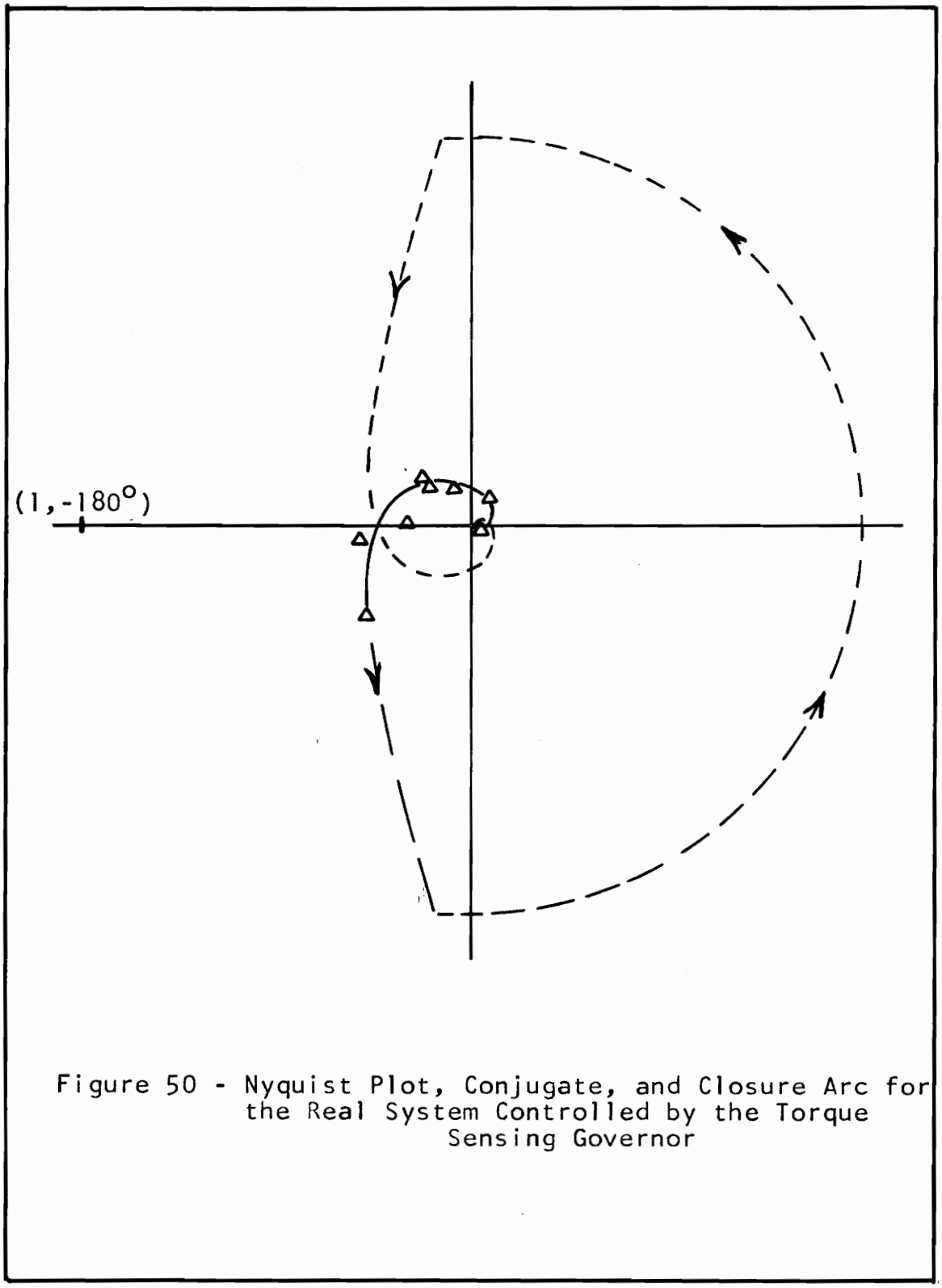

Figure 50 - Nyquist Plot, Conjugate, and Closure Arc for the Real System Controlled by the Torque Sensing Governor

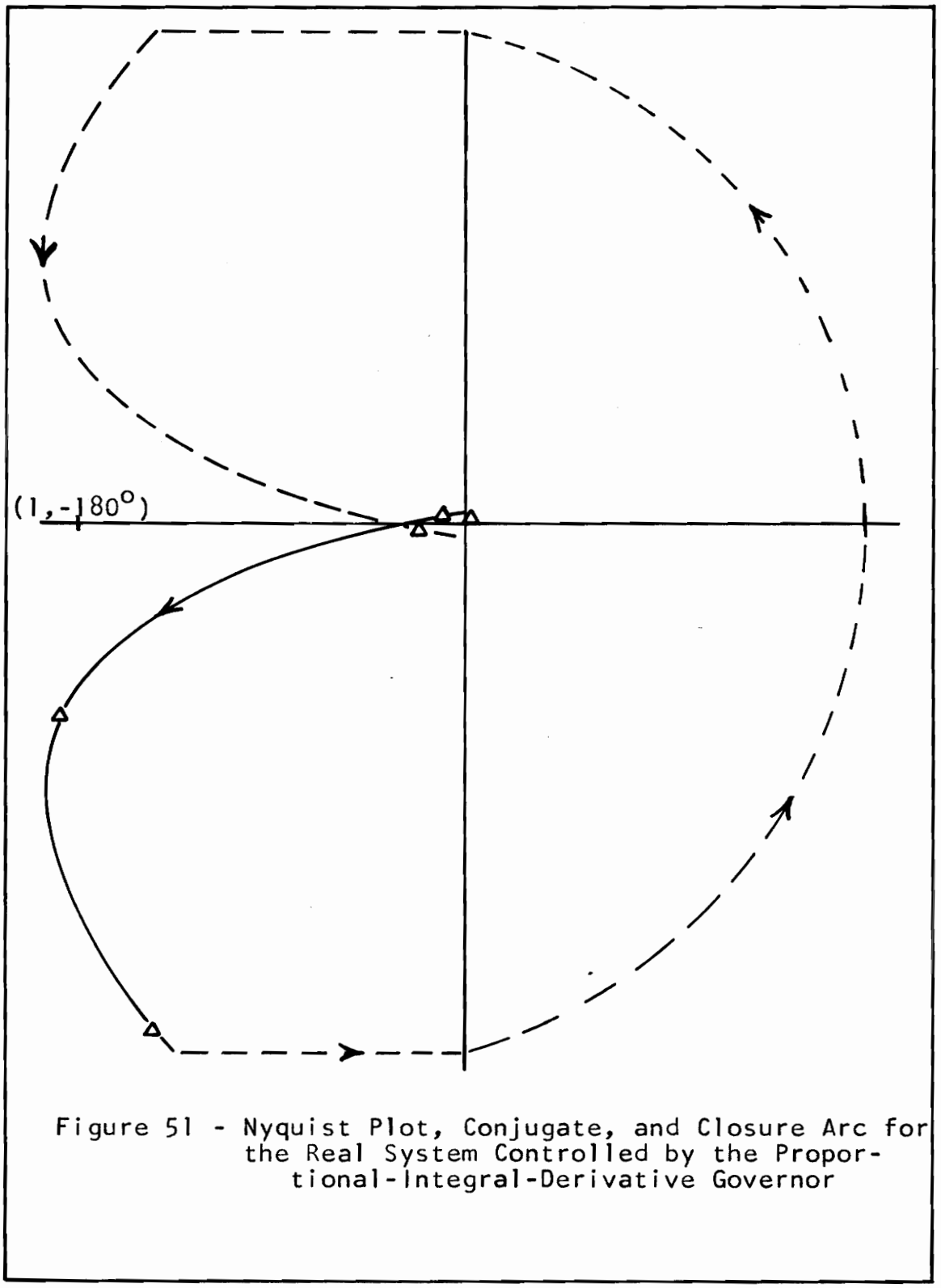

Figure 51 - Nyquist Plot, Conjugate, and Closure Arc for the Real System Controlled by the Proportional-Integral-Derivative Governor

V. DISCUSSION OF RESULTS

Similarity of Real and Simulated Systems

The real and simulated systems did not produce the same results quantitatively, but the results were similar from a qualitative point of view. The similarity between the real and simulated systems can best be shown by comparing the torque sensing governor to the proportional-integral-derivative governor using the simulated system and then making the same comparison using the real system.

For a step increase in load on the simulated system the same maximum speed deviation of 177 rpm occurred with each governor. The torque sensing governor returned the system to an allowable speed (2500 $\pm$ 20 rpm) in 2.4 seconds, but the proportional-integral-derivative governor required 3.9 seconds to return the system to an allowable speed. Figure 44 indicates that the torque sensing governor was more stable than the proportional-integral-derivative governor.

For the same step increase in load on the real system the torque sensing governor allowed a maximum speed deviation of 58 rpm as compared to 82 rpm for the proportional-integral-derivative governor. The torque sensing governor returned the system to an allowable speed in 1.1 seconds

as compared to 2.8 seconds for the proportional-integral-derivative governor. A comparison of Figures 46 and 47 indicates that the torque sensing governor was the more stable of the two.

A step decrease in load on the simulated system caused a maximum speed deviation of 130 rpm with the torque sensing governor, and a maximum speed deviation of 160 rpm with the proportional-integral-derivative governor. The torque sensing governor returned the system to an allowable speed in 1.75 seconds as compared to 3.9 seconds for the proportional-integral-derivative governor. As can be seen in Figure 45 there was a tendency toward sustained small amplitude oscillation in the system using the torque sensing governor.

For the same step decrease in load on the real system the maximum speed deviation allowed by the torque sensing governor was 64 rpm. The maximum speed deviation allowed by the proportional-integral-derivative governor was 120 rpm. Because of the tendency toward sustained small amplitude oscillation in the system using the torque sensing governor, the torque sensing governor required 4.9 seconds to return the system to an allowable speed as compared to 3.4 seconds for the proportional-integral-derivative governor.

Comparison of Optimum Control Parameters

It can be seen from Table 2 that the optimum control parameters for the real system are about three fourths as large as the optimum control parameters of the simulated system with the exception of derivative time (T_d). The cause of this fairly consistent difference between the real and simulated systems was not determined, but it was probably due to an error in the simulation of the time delay in the engine response to a throttle change. Even with this error the optimum control parameters obtained from the simulated system were good approximate values for use with the real system.

The reason for the large difference between the derivative time for the real and simulated systems is that the real system had a large amount of "noise" in the speed signal which caused the derivative circuit to produce significant throttle signals even when there was no speed change in the engine.

Stability of the Real Systems As Indicated by the Nyquist Plots

The Nyquist plots (Figures 50 and 51) indicate that both of the real systems are stable because the net encirclement of the point $(1, -180^{o})$ is zero for one traversal

of the closed transfer locus. From the shape of the Nyquist plots it appears that the phase lag is much less and the magnitude ratio much greater for the torque sensing governor than for the proportional-integral-derivative governor. This indicates that the torque sensor has done a much better job of reducing the phase lag than the derivative controller, thereby allowing the torque sensing governor to use higher gains than the proportional-integral-derivative governor.

VI. CONCLUSIONS

The following conclusions were drawn from this investigation:

1. The torque sensing device which was used is practical in that it is easy to build, gives dependable results, and may be used with any type of load.

2. The methods used to simulate the systems are sufficiently accurate for use in the design of control systems.

3. The torque sensing governor produces less speed error for less time than a conventional proportional-integral-derivative governor as applied to an internal combustion engine.

VII. SUMMARY

The purpose of this investigation was to present the design of a practical torque sensing device which can be used with any type of load, and to show that the use of such a device with a constant speed governor would produce less speed error for less time than a conventional proportional-integral-derivative constant speed governor when used on an internal combustion engine.

The system characteristics were determined so that the system could be simulated by an analog computer. The simulated system was governed by the torque sensing governor and optimized, then the same procedure was followed using the proportional-integral-derivative governor. The real system was then governed by each governor using the optimum values of governor parameters obtained from the simulated system as approximate optimum values for the real system. The real system was then optimized for each type of governor. The optimum values of governor parameters for the real and simulated systems using both governors are listed in the Results.

The control responses of the real and simulated systems using both governors were determined by applying a step change in load and recording the speed changes. From these response curves it was determined that for both the

real and simulated systems the torque sensing governor produced less speed error for less time than the proportional-integral-derivative governor.

Open-loop frequency response data were taken for the real system using each governor so that Nyquist plots could be made. According to the Nyquist stability criterion the real system was stable when either governor was used.

VIII. RECOMMENDATIONS

1. It is recommended that this investigation be repeated using an engine which is smoother running and has better carburetion than the engine used, such as an automotive engine, or using a turbine.

2. It is also recommended that an investigation be made of the usefulness of the torque sensing device in parallel operation of constant speed prime movers.

3. It is finally recommended that an investigation be made of the torque sensing governor with derivative control added to the torque sensing circuit to obtain a transfer function such as

$$V = k_t T - T_{dt} \frac{dT}{dt} + k_c(R - N) + \frac{1}{T_i} \int (R - N)dt.$$

IX. ACKNOWLEDGMENTS

The author wishes to acknowledge the valuable assistance of Professor C. E. Trent and Professor H. P. Marshall, who were members of his thesis committee. The author wishes to express special gratitude to Dr. H. L. Wood, the head of his thesis committee, for his assistance, encouragement, and criticism during this investigation.

To Professor J. B. Jones, Head of the Mechanical Engineering Department, the author expresses his sincere appreciation for making his graduate study possible.

To his wife, Ann, the author dedicates this thesis as an expression of gratitude for her assistance and support during his course of study. She typed both the rough and final drafts of this thesis.

X. BIBLIOGRAPHY

1. Eckman, Donald P., "Automatic Process Control," John Wiley and Sons, Inc., New York, 1958, p. 6.

2. Ibid., p. 2.

3. Ibid., pp. 59-102.

4. Ibid., pp. 102-104.

5. Considine, Douglas M., ed., "Process Instruments and Controls Handbook," McGraw-Hill Book Company, Inc., New York, 1957, pp. 11-27, 11-28.

6. Op. Cit., Eckman, pp. 303-304.

7. Oldenburger, Rufus, "Frequency-Response Data Presentation Standards and Design Criteria," Paper No. 53-A-11, "Frequency Response Symposium," presented at the ASME Annual Meeting, New York City, Dec. 12, 1953, p. 9.

8. Ibid., p. 10.

9. Op. Cit., Eckman, pp. 317-320.

10. Ibid., p. 337.

11. Johnson, Clarence L., "Analog Computer Techniques," McGraw-Hill Book Company, Inc., New York, 1956, p. 45.

12. Op. Cit., Considine, pp. 11-35.

13. Ibid., pp. 11-37.

14. Abstract in Oil Engine and Gas Turbine, v25, n296, April, 1958, pp. 446-447, Fuller, R. A., "Governing of Diesel Engines," Diesel Engineers and Users Assn., Paper No. S260, July, 1958, pp. 1-13.

15. Black, Paul H., "Machine Design," McGraw-Hill Book Company, Inc., New York, 1955, p. 185.

16. Ibid., p. 81.

17. Ibid., p. 190.

18. "Kent's Mechanical Engineers' Handbook," Design and Production Volume, John Wiley and Sons, Inc., New York, 1958, pp. 11-18.

XI. VITA

The author was born in Vicksburg, Mississippi on December 28, 1936, the son of Mr. and Mrs. Francis M. Donovan, Sr. He attended St. Aloysius High School in Vicksburg and was graduated in 1955. He entered Hinds Junior College that fall, transferred to Mississippi State University in September of 1956, and was graduated in 1959, with a Bachelor of Science Degree in Mechanical Engineering. After working for the General Electric Company for a year and a half, he entered the Graduate School of Virginia Polytechnic Institute to work toward a Master of Science Degree in Mechanical Engineering. During his graduate study he has been employed as an instructor in the Mechanical Engineering Department.

The author was married to Miss Margaret Ann Johnson of Morton, Mississippi in May 1959.

Francis M Donovan jr.

XII. APPENDICES

Appendix A

1. Calculation of size of torque sensor shaft

The shaft was to be made of mild steel so the design calculations were made on the basis of SAE 1050 steel. The size of the sensor section was calculated by using the equation[15]

$$\frac{\pi d^3}{16} = \frac{T}{S_{sa}}$$

where d is the shaft diameter in inches, T is the torque applied to the shaft in inch-pounds, and S_{sa} is the maximum allowable shear stress in pounds per square inch. If the above equation is solved for d

$$d = \left[\frac{16T}{\pi S_{sa}}\right]^{1/3}$$

and combined with the equation for engine horsepower

$$hp = \frac{2\pi TN}{(33000)(12)} \quad \text{or} \quad T = \frac{198000}{\pi N} hp$$

where N is the engine speed in revolutions per minute, the result is

$$d = \left[\frac{(16)(198000)(hp)}{\pi^2 N S_{sa}}\right]^{1/3}.$$

The engine horsepower was 1/2 at a speed of 2100 rpm, and the value of S_{sa} was taken to be 32,200 psi.[16] If the above substitutions are made in the equation the result is

$$d = \left[\frac{(16)(198000)(1/2)}{\pi^2(2100)(32200)}\right]^{1/3}$$

$$d = (.00238)^{1/3}$$

$$d = 0.14 \text{ in.}$$

Since this is the minimum diameter allowable, the shaft was designed with a diameter of 0.2 in., and was later increased to 0.25 in. because of failure of the 0.2 in. shaft.

2. Calculation of shaft deflection

The following calculations are based on a 2 in. sensor length and a 0.2 in. shaft diameter. The shaft deflection was calculated by means of the following equation,[17]

$$\theta = \frac{584LT}{Gd^4} \quad \text{or} \quad \theta = \frac{(584)(198000)hpL}{Gd^4\pi N}$$

where θ is the shaft deflection in degrees, L is the length of the test section in inches, and G is the torsional modulus of elasticity in pounds per square inch (11.5×10^6 for steel).[18] When the proper substitutions are made the result is

$$\theta = \frac{(548)(198000)(1/2)(2)}{(11500000)(0.2)^4(\pi)(2100)}$$

$$\theta = 0.95 \text{ deg}$$

Since the above calculation was for a shaft diameter of 0.2 in., the deflection is not accurate for the final 0.25 in. diameter shaft. The correct deflection is

$$\theta' = \theta \left(\frac{0.2}{0.25}\right)^4 = 0.41\theta$$

where θ' is the deflection of the 0.25 in. shaft. The true deflection is

$$\theta' = (0.41)(0.95)$$

$$\theta' = 0.39 \text{ deg}$$

Appendix B

Determination of phase lag and magnitude ratio from a photograph of the open-loop input and output signals.

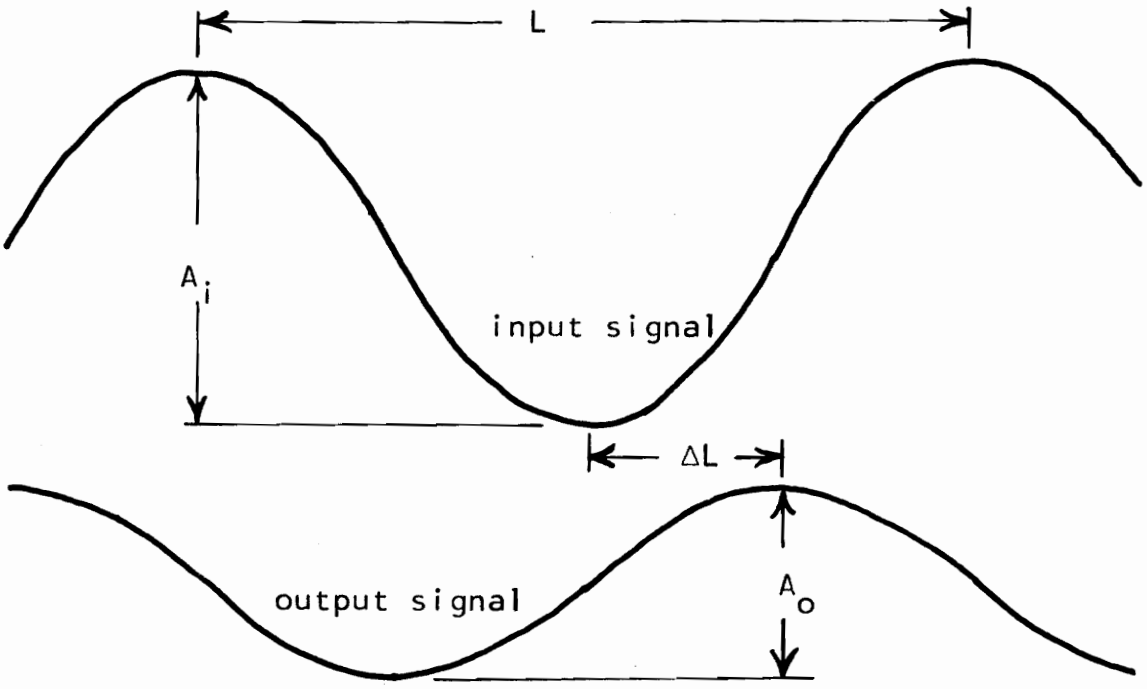

$$\text{Magnitude Ratio } (M) = \frac{A_o}{A_i}$$

$$\text{Phase Lag } (\phi) = 360\frac{\Delta L}{L}\text{deg}$$

ABSTRACT

The design of a practical torque sensing governor which can be used with any type of prime mover and load was accomplished. An investigation was performed to determine the advantages of such a governor as applied to a small internal combustion engine.

The characteristics of the engine, torque sensor, and load were determined in order that the system composed of the aforementioned elements could be simulated on an analog computer. The simulated system was governed by a simulated torque sensing governor and optimized, then the same procedure was followed with a simulated proportional-integral-derivative governor. The real system was then governed by each type of governor using the optimum values of governor parameters obtained from the simulated system.

The control response curves of the real and simulated systems using both governors were obtained by application of a step change in load. From these response curves it was determined that for both the real and simulated systems the torque sensing governor produced less speed error for less time than the porportional-integral-derivative governor.

Open-loop frequency response data were taken for the real system using each governor and the Nyquist stability

criteria applied. The Nyquist criteria showed the system to be stable when either governor was used. The Nyquist plots showed that the torque sensor reduced phase lag more than the derivative component of conventional control.